

ANL-HEP-PR-94-24

FERMILAB-PUB-94-073-T

NUHEP-TH-94-5

July 1994

Revised January 1997

**Rigorous QCD Analysis
of Inclusive Annihilation and Production
of Heavy Quarkonium**

Geoffrey T. Bodwin

High Energy Physics Division, Argonne National Laboratory, Argonne, IL 60439

Eric Braaten*

Theory Group, Fermilab, Batavia, IL 60510

G. Peter Lepage

Newman Laboratory of Nuclear Studies, Cornell University, Ithaca, NY 14853

Abstract

A rigorous QCD analysis of the inclusive annihilation decay rates of heavy quarkonium states is presented. The effective-field-theory framework of non-relativistic QCD is used to separate the short-distance scale of annihilation, which is set by the heavy quark mass M , from the longer-distance scales asso-

*On leave from Dept. of Physics and Astronomy, Northwestern University, Evanston, IL 60208.

ciated with quarkonium structure. The annihilation decay rates are expressed in terms of nonperturbative matrix elements of 4-fermion operators in non-relativistic QCD, with coefficients that can be computed using perturbation theory in the coupling constant $\alpha_s(M)$. The matrix elements are organized into a hierarchy according to their scaling with v , the typical velocity of the heavy quark. An analogous factorization formalism is developed for the production cross sections of heavy quarkonium in processes involving momentum transfers of order M or larger. The factorization formulas are applied to the annihilation decay rates and production cross sections of S-wave states, up to corrections of relative order v^3 , and of P-wave states, up to corrections of relative order v^2 .

I. INTRODUCTION

Calculations of the decay rates of heavy quarkonium states into light hadrons and into photons and lepton pairs are among the earliest applications of perturbative quantum chromodynamics (QCD) [1,2,3,4]. In these early analyses, it was assumed that the decay rate of the meson factored into a short-distance part that is related to the annihilation rate of the heavy quark and antiquark, and a long-distance factor containing all the nonperturbative effects of QCD. The short-distance factor was calculated in terms of the running coupling constant $\alpha_s(M)$ of QCD, evaluated at the scale of the heavy-quark mass M , while the long-distance factor was expressed in terms of the meson's nonrelativistic wavefunction, or its derivatives, evaluated at the origin. In the case of S-waves [5,6] and in the case of P-wave decays into photons [7], the factorization assumption was supported by explicit calculations at next-to-leading order in α_s . However, no general argument was advanced for its validity in higher orders of perturbation theory. In the case of P-wave decays into light hadrons, the factorization is spoiled by logarithmic infrared divergences that appear in the $Q\bar{Q}$ annihilation rates at order α_s^3 [7,8]. Logarithmic infrared divergences also appear in relativistic corrections to the annihilation decays of S-wave states [8]. These divergences cast a shadow over applications of perturbative QCD to the calculation of annihilation rates of heavy quarkonium states.

In this paper, we present a rigorous QCD analysis of the annihilation decays of heavy quarkonium. We derive a general factorization formula for the annihilation rates of S-wave, P-wave, and higher orbital-angular-momentum states, which includes not only perturbative corrections to all orders in α_s , but relativistic corrections as well. Factorization occurs in the annihilation decay rates because the heavy quark and antiquark can annihilate only when they are within a distance of order $1/M$, where M is the heavy-quark mass. Since, in the meson rest frame, the heavy quark and antiquark are nonrelativistic, with typical velocities $v \ll 1$, this distance is much smaller than the size of the meson, which is of order $1/(Mv)$. Factorization involves separating the relativistic physics of annihilation (which

involves momenta $p \sim M$) from the nonrelativistic physics of quarkonium structure (which involves $p \sim Mv$). A particularly elegant approach for separating relativistic from nonrelativistic scales is to recast the analysis in terms of nonrelativistic quantum chromodynamics (NRQCD) [9], an effective field theory designed precisely for this purpose. NRQCD consists of a nonrelativistic Schrödinger field theory for the heavy quark and antiquark that is coupled to the usual relativistic field theory for light quarks and gluons. The theory is made precisely equivalent to full QCD through the addition of local interactions that systematically incorporate relativistic corrections through any given order in the heavy-quark velocity v . It is an effective field theory, with a finite ultraviolet cutoff of order M that excludes relativistic states — states that are poorly described by nonrelativistic dynamics. A heavy quark in the meson can fluctuate into a relativistic state, but these fluctuations are necessarily short-lived. This means that the effects of the excluded relativistic states can be mimicked by local interactions and can, therefore, be incorporated into NRQCD through renormalizations of its infinitely many coupling constants. Thus, nonrelativistic physics is correctly described by the nonperturbative dynamics of NRQCD, while all relativistic effects are absorbed into coupling constants that can be computed as perturbation series in $\alpha_s(M)$.

The main advantage offered by NRQCD over ordinary QCD in this context is that it is easier to separate contributions of different orders in v in NRQCD. Thus, we are able not only to organize calculations to all orders in α_s , but also to elaborate systematically the relativistic corrections to the conventional formulas. Furthermore, we provide nonperturbative definitions of the long-distance factors in terms of matrix elements of NRQCD, making it possible to evaluate them in numerical lattice calculations. Analyzing S-wave decays within this framework, we recover, up to corrections of relative order v^2 , the standard factorization formulas, which contain a single nonperturbative parameter. At relative order v^2 , the decay rates satisfy a more general factorization formula, which contains two additional independent nonperturbative matrix elements. Our results for P-wave decays into light hadrons are even more striking, as we have discussed in Ref. [10]. Up to corrections of relative order v^2 , the factorization formula for these decay rates is the sum of two terms. In addition to the

conventional term, which takes into account the annihilation of the $Q\bar{Q}$ pair from a color-singlet P-wave state, there is a second term that involves annihilation from a color-octet S-wave state. The infrared divergences encountered in previous calculations are absorbed into the matrix element of the color-octet term.

Our presentation is organized as follows. In Section II, we first review NRQCD in general, emphasizing the velocity-scaling rules, which are used in separating contributions of different orders in v . We then discuss the space-time structure of the annihilation of heavy quarks and antiquarks and explain how the effects of annihilation can be taken into account in NRQCD by adding local 4-fermion operators to the effective lagrangian. In Section III, we analyze the matrix elements of the 4-fermion operators. We discuss their scaling with v , the constraints on them that follow from heavy-quark spin symmetry, their relations to Coulomb-gauge wavefunctions, and their dependences on the factorization scale. In Section IV, we apply our formalism to the annihilation decays of S-wave quarkonium states, up to corrections of relative order v^3 , and to P-wave decays, up to corrections of relative order v^2 . In Section V, we sketch the derivation of our results in a more conventional perturbative approach to factorization. In Section VI, we develop an analogous factorization formalism for calculating the production cross sections of heavy quarkonium. In the concluding section, we compare our formalism with previous approaches to the annihilation and production of heavy quarkonium, and we summarize the current status of calculations of annihilation and production rates.

II. NRQCD

We begin this section with a brief discussion of the various momentum scales involved in heavy quarkonia. Nonrelativistic QCD (NRQCD) [9] is our major tool for resolving the different momentum scales involved in their annihilation decays. We review this effective field theory and its application to heavy-quarkonium physics. Then we discuss the space-time structure of the $Q\bar{Q}$ annihilation process and develop a general factorization formula for the annihilation decay rates of heavy quarkonia in terms of matrix elements of NRQCD.

A. Energy Scales in Heavy Quarkonium

In a meson containing a heavy quark and antiquark, there are several different momentum scales that play important roles in the dynamics. The most important scales are the mass M of the heavy quark, its typical 3-momentum Mv (in the meson rest frame), and its typical kinetic energy Mv^2 . The heavy-quark mass M sets the overall scale of the rest energy of the bound state and also provides the short-distance scale for annihilation processes. The size of the bound state is the inverse of the momentum Mv , while Mv^2 is the scale of the energy splittings between radial excitations and between orbital-angular-momentum excitations. Spin splittings within a given radial and orbital-angular-momentum excitation are of order Mv^4 , but this scale plays no significant role in the dynamics.

The typical velocity v of the heavy quark decreases as the mass M increases. If M is large enough, v is proportional to the running coupling constant $\alpha_s(M)$, and it therefore decreases asymptotically like $1/\log(M)$. Thus, if M is sufficiently large, the heavy quark and antiquark are nonrelativistic, with typical velocities $v \ll 1$. We assume in this paper that the mass M is heavy enough that the momentum scales M , Mv and Mv^2 are well-separated: $(Mv^2)^2 \ll (Mv)^2 \ll M^2$. Quark potential model calculations indicate that the average value of v^2 is about 0.3 for charmonium and about 0.1 for bottomonium [11], and these estimates are confirmed by lattice QCD simulations. Thus, the assumption $(Mv^2)^2 \ll (Mv)^2 \ll M^2$

is very good for bottomonium, and reasonably good even for charmonium. For lighter quarkonium states, such as the $s\bar{s}$ system, our analysis does not apply.

Another momentum scale that plays a role in the physics of heavy quarkonium is Λ_{QCD} , the scale associated with nonperturbative effects involving gluons and light quarks. It determines, for example, the long-range behavior of the potential between the heavy quark and antiquark, which is approximately linear, with a coefficient of $(450 \text{ MeV})^2$ [11]. We can use this coefficient as an estimate for the nonperturbative scale: $\Lambda_{QCD} \approx 450 \text{ MeV}$. For both charmonium and bottomonium, the first radial excitation and the first orbital-angular-momentum excitation are both about 500 MeV above the ground state. Taking this value as an estimate for the scale Mv^2 , we see that Λ_{QCD} and Mv^2 are comparable for both charmonium and bottomonium.

Our analysis of heavy quarkonium annihilation is based on separating the effects at the momentum scale M from those at the lower momentum scales Mv , Mv^2 and Λ_{QCD} . The effects at the scale M are taken into account through the coupling constants of 4-fermion operators in the lagrangian for NRQCD. We assume that $\alpha_s(M) \ll 1$, so that these coupling constants can be calculated using perturbation theory in $\alpha_s(M)$. The assumption that $\alpha_s(M) \ll 1$ is well-satisfied for bottomonium, for which $\alpha_s(M) \approx 0.18$, and reasonably well-satisfied for charmonium, for which $\alpha_s(M) \approx 0.24$.

The effects of the lower momentum scales Mv , Mv^2 , and Λ_{QCD} are factored into matrix elements that can be calculated using nonperturbative methods, such as lattice-QCD simulations. These matrix elements are organized into a hierarchy in terms of their dependence on v . Our final expression for the annihilation rate therefore takes the form of a double expansion in $\alpha_s(M)$ and v . These expansion parameters are not independent for quarkonium. The typical velocity v of the heavy quark is determined by a nonperturbative balance between its kinetic energy $Mv^2/2$ and the potential energy, which, for sufficiently large M , is dominated by a color-Coulomb term proportional to $\alpha_s(1/r)/r$. Setting $r \sim 1/(Mv)$ in the potential and equating it with the kinetic energy, we obtain the identification

$$v \sim \alpha_s(Mv). \tag{2.1}$$

This equation can be solved self-consistently to obtain an approximate value for the typical velocity v . The identification (2.1) has a simple, but important, implication for calculations of annihilation rates. Since the running coupling constant in QCD decreases with the momentum scale, v is greater than or of order $\alpha_s(M)$. Thus relativistic corrections of order $(v^2)^n$ can be expected to be more important than perturbative corrections of order $\alpha_s^{2n}(M)$. In particular, there is little to be gained by calculating perturbative corrections at next-to-next-to-leading order in $\alpha_s(M)$, unless relativistic corrections through relative order v^2 are included as well.

B. The NRQCD Lagrangian

The most important energy scales for the structure and spectrum of a heavy quarkonium system are Mv and Mv^2 , where M is the mass of the heavy quark Q and $v \ll 1$ is its average velocity in the meson rest frame. Momenta of order M play only a minor role in the complex binding dynamics of the system. We can take advantage of this fact in our analysis of heavy-quark mesons by modifying QCD in two steps.

We start with full QCD, in which the heavy quarks are described by 4-component Dirac spinor fields. In the first step, we introduce an ultraviolet momentum cutoff Λ that is of order M . This cutoff explicitly excludes relativistic heavy quarks from the theory, as well as gluons and light quarks with momenta of order M . It is appropriate to our analysis of heavy quarkonium, since the important nonperturbative physics involves momenta of order Mv or less. Of course, the relativistic states we are discarding do have some effect on the low-energy physics of the theory. However, any interaction involving relativistic intermediate states is approximately local, since the intermediate states are necessarily highly virtual and so cannot propagate over long distances. Thus, generalizing standard renormalization procedures, we systematically compensate for the removal of relativistic states by adding new local interactions to the lagrangian. To leading order in $1/\Lambda$ or, equivalently, $1/M$, these

new interactions are identical in form to interactions already present in the theory, and so the net effect is simply to shift bare masses and charges. Beyond leading order in $1/M$, one must extend the lagrangian to include nonrenormalizable interactions that correct the low-energy dynamics order-by-order in $1/M$. In this cutoff formulation of QCD, all effects that arise from relativistic states, and only these effects, are incorporated into renormalizations of the coupling constants of the extended lagrangian. Thus, in the cutoff theory, relativistic and nonrelativistic contributions are automatically separated. This separation is the basis for our analysis of the annihilation decays of heavy quarkonia.

The utility of the cutoff theory is greatly enhanced if, as a second step, a Foldy-Wouthuysen-Tani transformation [12] is used to block-diagonalize the Dirac theory so as to decouple the heavy quark and antiquark degrees of freedom. Such a decoupling of particle and antiparticle is a familiar characteristic of nonrelativistic dynamics and is quite useful in our study of heavy quarkonium. The net effect is that the usual relativistic field theory of four-component Dirac spinor fields is replaced by a nonrelativistic Schrödinger field theory, with separate two-component Pauli spinor fields for the heavy quarks and for the heavy antiquarks. This field theory is NRQCD [9]. The lagrangian for NRQCD is

$$\mathcal{L}_{\text{NRQCD}} = \mathcal{L}_{\text{light}} + \mathcal{L}_{\text{heavy}} + \delta\mathcal{L}. \quad (2.2)$$

The gluons and the n_f flavors of light quarks are described by the fully relativistic lagrangian

$$\mathcal{L}_{\text{light}} = -\frac{1}{2}\text{tr} G_{\mu\nu}G^{\mu\nu} + \sum \bar{q} i\not{D}q, \quad (2.3)$$

where $G_{\mu\nu}$ is the gluon field-strength tensor expressed in the form of an $\text{SU}(3)$ matrix, and q is the Dirac spinor field for a light quark. The gauge-covariant derivative is $D^\mu = \partial^\mu + igA^\mu$, where $A^\mu = (\phi, \mathbf{A})$ is the $\text{SU}(3)$ matrix-valued gauge field and g is the QCD coupling constant. The sum in (2.3) is over the n_f flavors of light quarks. The heavy quarks and antiquarks are described by the term

$$\mathcal{L}_{\text{heavy}} = \psi^\dagger \left(iD_t + \frac{\mathbf{D}^2}{2M} \right) \psi + \chi^\dagger \left(iD_t - \frac{\mathbf{D}^2}{2M} \right) \chi, \quad (2.4)$$

where ψ is the Pauli spinor field that annihilates a heavy quark, χ is the Pauli spinor field that creates a heavy antiquark, and D_t and \mathbf{D} are the time and space components of the gauge-covariant derivative D^μ . Color and spin indices on the fields ψ and χ have been suppressed. The lagrangian $\mathcal{L}_{\text{light}} + \mathcal{L}_{\text{heavy}}$ describes ordinary QCD coupled to a Schrödinger field theory for the heavy quarks and antiquarks. The relativistic effects of full QCD are reproduced through the correction term $\delta\mathcal{L}$ in the lagrangian (2.2).

The correction terms in the effective lagrangian for NRQCD that are most important for heavy quarkonium are bilinear in the quark field or the antiquark field:

$$\begin{aligned}
\delta\mathcal{L}_{\text{bilinear}} = & \frac{c_1}{8M^3} \left(\psi^\dagger (\mathbf{D}^2)^2 \psi - \chi^\dagger (\mathbf{D}^2)^2 \chi \right) \\
& + \frac{c_2}{8M^2} \left(\psi^\dagger (\mathbf{D} \cdot g\mathbf{E} - g\mathbf{E} \cdot \mathbf{D}) \psi + \chi^\dagger (\mathbf{D} \cdot g\mathbf{E} - g\mathbf{E} \cdot \mathbf{D}) \chi \right) \\
& + \frac{c_3}{8M^2} \left(\psi^\dagger (i\mathbf{D} \times g\mathbf{E} - g\mathbf{E} \times i\mathbf{D}) \cdot \boldsymbol{\sigma} \psi + \chi^\dagger (i\mathbf{D} \times g\mathbf{E} - g\mathbf{E} \times i\mathbf{D}) \cdot \boldsymbol{\sigma} \chi \right) \\
& + \frac{c_4}{2M} \left(\psi^\dagger (g\mathbf{B} \cdot \boldsymbol{\sigma}) \psi - \chi^\dagger (g\mathbf{B} \cdot \boldsymbol{\sigma}) \chi \right), \tag{2.5}
\end{aligned}$$

where $E^i = G^{0i}$ and $B^i = \frac{1}{2}\epsilon^{ijk}G^{jk}$ are the electric and magnetic components of the gluon field strength tensor $G^{\mu\nu}$. By charge conjugation symmetry, for every term in (2.5) involving ψ , there is a corresponding term involving the antiquark field χ , with the same coefficient c_i , up to a sign. The operators in (2.5) must be regularized, and they therefore depend on the ultraviolet cutoff or renormalization scale Λ of NRQCD. The coefficients $c_i(\Lambda)$ also depend on Λ in such a way as to cancel the Λ -dependence of the operators. Renormalization theory tells us that NRQCD can be made to reproduce QCD results as accurately as desired by adding correction terms to the lagrangian like those in (2.5) and tuning the couplings to appropriate values [13].

Mixed 2-fermion operators involving χ^\dagger and ψ (or ψ^\dagger and χ) correspond to the annihilation (or the creation) of a $Q\bar{Q}$ pair. Such terms are excluded from the lagrangian as part of the definition of NRQCD. If such an operator annihilates a $Q\bar{Q}$ pair, it would, by energy conservation, have to create gluons (or light quarks) with energies of order M . The amplitude for annihilation of a $Q\bar{Q}$ pair into such high energy gluons cannot be described accurately in a nonrelativistic theory such as NRQCD. Nevertheless, as is discussed in Section II E, the

effects of such annihilation processes on low energy amplitudes can be reproduced by adding 4-fermion operators such as $\psi^\dagger \chi \chi^\dagger \psi$ to the effective lagrangian.

Operators containing higher-order time derivatives, such as $\psi^\dagger D_t^2 \psi$, are also omitted from the effective lagrangian as part of the definition of NRQCD. These operators can be eliminated by field redefinitions that vanish upon use of the equations of motion. Because of these field redefinitions, the off-shell Green's functions of NRQCD need not agree with those of full QCD, but the two theories are equivalent for on-shell physical quantities.

The coefficients c_i in (2.5) must be tuned as functions of the coupling constant α_s , the heavy-quark mass parameter in full QCD, and the ultraviolet cutoff Λ of NRQCD, so that physical observables are the same as in full QCD. The coefficients are conveniently determined by matching low-energy scattering amplitudes of heavy quarks and antiquarks in NRQCD, calculated in perturbation theory in α_s and to a given precision in v , with the corresponding perturbative scattering amplitudes in full QCD. It is necessary to use on-shell scattering amplitudes for this purpose, because the equations of motion have been used to simplify the effective lagrangian for NRQCD by eliminating terms with more than one power of D_t . The scattering amplitudes can be calculated using perturbation theory in α_s , since the radiative corrections to the coefficients in the NRQCD lagrangian are dominated by relativistic momenta. These coefficients therefore have perturbative expansions in powers of $\alpha_s(M)$ [9,14]. The coefficients in (2.5) are defined so that $c_i = 1 + O(\alpha_s)$.

The explicit factors of M in (2.5) were introduced in order that the coefficients c_i be dimensionless. These coefficients therefore depend on the definition of the heavy-quark mass parameter M . Our definition of M is specified by the lagrangian (2.4): $1/(2M)$ is the coefficient of the operator $\psi^\dagger \mathbf{D}^2 \psi$. If a different prescription is adopted for M , then all the c_i 's must be changed accordingly. The simplest way to determine the mass parameter M is to match the location of the pole in the perturbative propagator for a heavy quark in NRQCD with that in full QCD. In both NRQCD and full QCD, the kinetic energy for a heavy quark of momentum p in perturbation theory has the form $E = p^2/(2M_{\text{pole}}) - p^4/(8M_{\text{pole}}^3) + \dots$, where M_{pole} is the perturbative pole mass. In Appendix B 1, the self-energy of the heavy quark

is calculated in NRQCD to order α_s and to leading order in v . If we use a regularization scheme in which power divergences are subtracted, then the energy-momentum relation gives $M = M_{\text{pole}}(1 + O(\alpha_s^2))$. The corresponding calculation using a lattice regularization has been carried out by Morningstar [15]. The perturbative pole mass can be related to any other definition of the heavy-quark mass by a calculation in full QCD.

C. Velocity-scaling Rules

In principle, infinitely many terms are required in the NRQCD lagrangian in order to reproduce full QCD, but in practice only a finite number of these is needed for precision to any given order in the typical heavy-quark velocity v . We can assess the relative importance of various terms by using velocity-scaling rules that were derived in Ref. [14] and are summarized in Table I. This table lists the fields and operators from which terms in the NRQCD action are built, together with the approximate magnitude of each for matrix elements between heavy quarkonium states that are localized in space. The scaling rules were derived in Ref. [14] by analyzing the equations of motion for the quantum field operators of NRQCD. The typical heavy-quark velocity v is determined dynamically by a balance between the kinetic and potential terms in the equation of motion for the heavy-quark field, and v can be used as an expansion parameter in order to analyze the importance of other terms. The scaling rules are certainly correct within perturbation theory in α_s , but, since they are based on the self-consistency of the field equations, they should also be valid in the presence of nonperturbative effects.

There is an important *caveat* to the velocity-scaling rules that involves ultraviolet-divergent loop corrections. Loop corrections to an operator give rise to power ultraviolet divergences, as well as to logarithmic divergences. The logarithmic divergences modify the scaling rules by factors of $\log(\Lambda/Mv)$. The power divergences can contribute factors of $1/v^n$, and the scaling rules apply only after such $1/v^n$ divergences have been subtracted. The subtracted expression is the relevant one for the following reason. The power-divergent con-

tributions to a given operator \mathcal{O} that yield factors of $1/v^n$ have the form of renormalizations of lower-dimension operators. When the coefficients of NRQCD are tuned so as to reproduce full QCD, the coefficients of the lower-dimension operators are adjusted so that their contributions to physical quantities cancel the contributions of the $1/v^n$ power-divergent loop corrections to the operator \mathcal{O} . Consequently, the inclusion of a given operator in the NRQCD lagrangian yields a net correction to any physical quantity that is in accordance with the velocity-scaling rules, up to logarithmic corrections.

The estimates for the magnitudes of $g\phi$ and $g\mathbf{A}$ in Table I hold in Coulomb gauge. Coulomb gauge is a natural gauge for analyzing heavy quarkonium, because it avoids spurious retardation effects that are present in covariant gauges, but cancel out in physical quantities [16]. Coulomb gauge is also a physical gauge, that is, a gauge with no negative norm states. Thus, it allows a sensible Fock-state expansion for the meson. The dominant Fock state is of course $|Q\bar{Q}\rangle$, but the meson also contains the Fock state $|Q\bar{Q}g\rangle$, which includes a dynamical gluon, and higher Fock states as well.

The estimates in Table I were derived assuming that one can do perturbation theory in the typical heavy-quark velocity. This perturbation theory relies on the fact that soft gluons have a weak coupling to heavy quarks, not because the coupling constant α_s is small, but because the interaction is proportional to the heavy-quark velocity v . In the derivation of the magnitude of $g\mathbf{A}$ in Ref. [14], dynamical gluons were assumed to have typical momenta of order Mv , which is the inverse size of the quarkonium. The perturbative estimate for the magnitude of the operator $g\mathbf{A}$ is $\alpha_s(k)vk$ for a dynamical gluon of momentum k . For k of order Mv , we can set $\alpha_s \sim v$ and recover the estimate Mv^3 given in Table I. For k of order Mv^2 , we can set $\alpha_s \sim 1$, and we again obtain the estimate Mv^3 . This estimate relies on perturbation theory, which may be suspect because of the strong coupling between gluons with momenta on the order of Mv^2 . However such gluons necessarily have wavelengths of order $1/(Mv^2)$ or larger, which is much larger than the typical size $1/(Mv)$ of the quarkonium. For such long-wavelength gluons, the multipole expansion, whose validity transcends that of perturbation theory in the coupling constant, can be used to justify the estimate for

$g\mathbf{A}$ in Table I [17].

The velocity-scaling rules in Table I show that the terms in $\delta\mathcal{L}_{\text{bilinear}}$ in (2.5) all give contributions that are suppressed by $O(v^2)$ relative to those from the leading lagrangian $\mathcal{L}_{\text{heavy}}$. Recalling that mixed 2-fermion operators, such as $\psi^\dagger(\mathbf{D}^2)^2\chi$, and operators involving higher time derivatives, such as $\psi^\dagger D_t^2\psi$, are omitted as part of the definition of NRQCD, we see that $\delta\mathcal{L}_{\text{bilinear}}$ contains all the 2-fermion NRQCD operators of relative order v^2 . The lagrangian $\mathcal{L}_{\text{light}} + \mathcal{L}_{\text{heavy}} + \delta\mathcal{L}_{\text{bilinear}}$ can therefore be used to calculate NRQCD matrix elements between heavy-quarkonium states with an error of order v^4 . If an error of order v^2 is sufficiently accurate, then the matrix elements can be calculated by using the lagrangian $\mathcal{L}_{\text{light}} + \mathcal{L}_{\text{heavy}}$.

It is instructive to contrast the relative magnitudes of the NRQCD operators in the case of a heavy quarkonium with the relative magnitudes of the same operators in the case of a heavy-light meson. (In the meson rest frame, the lagrangian for NRQCD is identical to that for Heavy Quark Effective Theory, which is the standard formalism for treating heavy-light mesons [18].) In a heavy-light meson, the typical 3-momentum of the heavy quark is of order Λ_{QCD} , and is independent of the heavy-quark mass. The binding energy is also of order Λ_{QCD} , and is much larger than the heavy-quark kinetic energy, which is of order Λ_{QCD}^2/M . Thus, in a heavy-light meson, the 3-momentum and the energy of the heavy-quark are both of order Λ_{QCD} , in contrast with the situation in a heavy quarkonium, in which the 3-momentum is of order Mv and the energy is of order Mv^2 . Consequently, in a heavy-light meson, the effects of operators of dimension d are of order $(\Lambda_{QCD}/M)^{d-4}$ relative to the effects of the dimension-4 operator $\psi^\dagger iD_t\psi$. The leading term $\psi^\dagger iD_t\psi$ describes a static heavy quark acting as a source of gluon fields. All effects of relative order Λ_{QCD}/M can be taken into account by adding the dimension-5 operators $\psi^\dagger \mathbf{D}^2\psi$ and $\psi^\dagger g\mathbf{B} \cdot \boldsymbol{\sigma}\psi$.

D. Quarkonium in NRQCD

Several qualitative features of heavy quarkonium can be inferred directly from the NRQCD lagrangian by exploiting the heavy-quark velocity v as an expansion parameter.

Expansions in powers of v are possible in ordinary QCD, but they are complicated by the need to make a nonrelativistic expansion of each individual Lorentz-invariant operator in order to separate the various powers of v . Relativistic effects have been unraveled to a large extent in NRQCD, with the leading v -dependence of each operator being specified by the velocity-scaling rules in Table I.

The most distinctive phenomenological feature of heavy quarkonium is that, for many purposes, it is accurately described by the quark potential model, in which the heavy quark and antiquark are bound by an instantaneous potential. This model is a tuned phenomenology, rather than a theory, but it is far simpler than a full field-theoretic description based on NRQCD or QCD. Its validity rests upon two essential ingredients of heavy-quarkonium physics. The first is that the dominant effect of the exchange of gluons between the heavy quark and antiquark is to produce an instantaneous interaction. The reason for this is that the most important gluons have momenta of order Mv and energies of order Mv^2 . Such gluons are off their energy shells by amounts of order Mv , which are much greater than the typical kinetic energy Mv^2 of the heavy quark. Consequently, the interaction times of the gluons are shorter by a factor of $1/v$ than the time scale associated with the motion of the heavy quarks, and the gluons' interactions are, therefore, instantaneous as far as the heavy quarks are concerned.

The second essential ingredient underlying the quark potential model is that the probability of finding dynamical gluons (those that are not part of the potential) in the meson is small. This is important because dynamical gluons with very low energy produce effects that are not instantaneous and are not readily incorporated into the quark potential model. In particular, gluons with energies of order Mv^2 have interaction times comparable to that of the heavy quarks, and their exchange therefore leads to significant retardation effects. The probability for the Fock state $|Q\bar{Q}g\rangle$ of the meson can be estimated by considering the energy shift of a quarkonium state $|H\rangle$ that is due to the presence of a Fock-state component $|Q\bar{Q}g\rangle$. In Coulomb gauge, the only terms that connect the dominant Fock state $|Q\bar{Q}\rangle$ to the Fock state $|Q\bar{Q}g\rangle$ are terms that involve the vector potential \mathbf{A} . At leading order in v ,

the contributions to the energy shift come from the term $ig\mathbf{A} \cdot \psi^\dagger \nabla \psi / M$ in $\mathcal{L}_{\text{heavy}}$:

$$\Delta E = -\frac{1}{M} \langle H | \int d^3x ig\mathbf{A} \cdot \psi^\dagger \nabla \psi | H \rangle. \quad (2.6)$$

Using the velocity-scaling rules in Table I and taking into account the relevant integration volume $1/(Mv)^3$, we obtain the estimate $\Delta E \sim Mv^4$. This energy shift can be written in a different way — as the product of the probability $P_{Q\bar{Q}g}$ for the $Q\bar{Q}g$ state multiplied by the energy $E_{Q\bar{Q}g}$ of that state. For gluons with momenta k of order Mv , the energy of the $Q\bar{Q}g$ state is dominated by the energy of the gluon, and we find that $P_{Q\bar{Q}g} \sim v^3$. For dynamical gluons with very low energies of order Mv^2 or less, the energy of the $Q\bar{Q}g$ state is of order Mv^2 and we obtain the estimate $P_{Q\bar{Q}g} \sim v^2$. For heavy quarkonium, $Q\bar{Q}g$ states are therefore suppressed relative to the dominant $Q\bar{Q}$ state by a factor of order v^2 in the probability. Hence, for most quantities, effects due to Fock states like $|Q\bar{Q}g\rangle$ that contain dynamical gluons are suppressed by powers of v . This might be expected from the phenomenological successes of the quark potential model. However, there are quantities, such as the decay rates of P-wave states into light hadrons [10], for which the effects of the Fock state $|Q\bar{Q}g\rangle$ are of leading order in v and the quark potential model fails completely.

The above estimates for the probabilities of $|Q\bar{Q}g\rangle$ Fock states apply if the spin state of the $Q\bar{Q}$ pair is the same as in the dominant $|Q\bar{Q}\rangle$ Fock state. If the spin state is different, we must replace $g\mathbf{A} \cdot \nabla$ in (2.6) with $g\mathbf{B} \cdot \boldsymbol{\sigma}$ to obtain a nonzero matrix element. Using the velocity-scaling rules of Table I, we again obtain an estimate $\Delta E \sim Mv^4$ for the energy shift, implying that the probability for a $|Q\bar{Q}g\rangle$ state containing a gluon with momentum on the order of Mv is $P_{Q\bar{Q}g} \sim v^3$. However, in the derivation of the velocity-scaling rules in Ref. [14], it was assumed that dynamical gluons have momenta of order Mv . If the gluon has a much smaller momentum k , then the estimate M^2v^4 for the operator $g\mathbf{B}$ in Table I should be replaced with k^2v^2 . Using this to estimate the energy shift from a $|Q\bar{Q}g\rangle$ Fock state containing a gluon with momentum of order Mv^2 , we obtain $\Delta E \sim Mv^6$ and $P_{Q\bar{Q}g} \sim v^4$. Thus, gluons with very low momenta exhibit the suppression that is characteristic of the multipole expansion. We conclude that a $|Q\bar{Q}g\rangle$ Fock state that can be reached from the

dominant $|Q\bar{Q}\rangle$ Fock state by a spin-flip transition is dominated by dynamical gluons with momenta of order Mv and that the probability of such a Fock state is $P_{Q\bar{Q}g} \sim v^3$.

Another important feature of quarkonium structure is its approximate independence of the heavy-quark spin. This feature follows immediately from the structure of the NRQCD lagrangian, which exhibits an approximate heavy-quark spin symmetry. The leading term $\mathcal{L}_{\text{heavy}}$ is completely independent of the heavy-quark spin. With just this term, states that differ only in the spins of the heavy quark and antiquark have identical properties; heavy-quark spin is conserved and can be used to label the energy eigenstates. Spin-dependence enters first through the bilinear terms in (2.5) that contain Pauli matrices, and they give corrections that are of relative order v^2 .¹ Thus, spin splittings for quarkonia should be smaller than splittings between radial and orbital-angular-momentum excitations, with the ratios of these splittings scaling roughly as v^2 . This familiar feature of the spectra of charmonium and bottomonium reinforces our confidence in the power-counting rules and in the utility of a nonrelativistic framework for studying quarkonium.

The total angular momentum J , the parity P , and the charge conjugation C are exactly conserved quantum numbers in NRQCD, as well as in full QCD. Thus, the energy eigenstates $|H\rangle$ of heavy quarkonium can be labelled by the quantum numbers J^{PC} . By the arguments given above, the dominant component in the Fock state expansion of $|H\rangle$ is a pure quark-antiquark state $|Q\bar{Q}\rangle$. The Fock state $|Q\bar{Q}g\rangle$, in which a dynamical gluon is present, has a probability of order v^2 , and higher Fock states have probabilities of order v^4 or higher. Since our primary interest is in processes in which the Q and \bar{Q} in the quarkonium annihilate,

¹In perturbation theory, ladder-like Coulomb-gluon exchanges between the quark and antiquark give a factor of order α_s/v for each ladder rung. The spin-flip contribution is down by v^2 relative to this Coulomb-ladder contribution. For example, in a two-loop calculation, the Coulomb ladder gives a factor of order $(\alpha_s/v)^2$, while the ladder with one Coulomb exchange and one spin-flip exchange gives a factor of order $v^2(\alpha_s/v)^2 = \alpha_s^2$.

we concentrate on the state of the $Q\bar{Q}$ pair in the various Fock-state components. For a general Fock state, the $Q\bar{Q}$ pair can be in either a color-singlet state or a color-octet state. Its angular-momentum state can be denoted by the spectroscopic notation $^{2S+1}L_J$, where $S = 0, 1$ is the total spin of the quark and antiquark, $L = 0, 1, 2, \dots$ (or $L = S, P, D, \dots$) is the orbital angular momentum, and J is the total angular momentum. A $Q\bar{Q}$ pair in a $^{2S+1}L_J$ state has parity $P = (-1)^{L+1}$; if it is in a color-singlet state, it has charge-conjugation number $C = (-1)^{L+S}$.

In the Fock state $|Q\bar{Q}\rangle$, the $Q\bar{Q}$ pair must be in a color-singlet state and in an angular-momentum state $^{2S+1}L_J$ that is consistent with the quantum numbers J^{PC} of the meson. Conservation of J^{PC} implies that mixing is allowed only between the angular-momentum states $^3(J-1)_J$ and $^3(J+1)_J$. For example, a $^3S_1 Q\bar{Q}$ state can mix with a 3D_1 state. However, such mixing is suppressed because operators that change the orbital angular momentum must contain at least one power of ∇ . In general, up to corrections of order v^2 , we can regard the $Q\bar{Q}$ component of the meson as being in a definite angular-momentum state $^{2S+1}L_J$. Of course, if the contribution of the dominant angular-momentum state is suppressed in a given process, then the contribution of the subdominant states takes on increased importance. We will present examples of this phenomenon in the discussions of the decay and production of P-wave states.

We turn next to the Fock state $|Q\bar{Q}g\rangle$ of the meson, which includes a dynamical gluon and has a component whose probability is of order v^2 . In spite of the fact that the dynamics of the soft gluon is nontrivial, NRQCD tells us much about the quantum numbers of the $Q\bar{Q}$ pair in the $Q\bar{Q}g$ component whose probability is of order v^2 . The pair must of course be in a color-octet state. Heavy-quark spin symmetry implies that the total spin quantum number S for the $Q\bar{Q}$ pair is the same as in the dominant Fock state $|Q\bar{Q}\rangle$. But NRQCD also tells us that the orbital state of the $Q\bar{Q}$ pair is closely related to that in the Fock state $|Q\bar{Q}\rangle$. The reason for this is that the coupling of the soft gluon can be analyzed using a multipole expansion, and the usual selection rules for multipole expansions apply.

The leading interaction that couples the dominant Fock state $|Q\bar{Q}\rangle$ to the state $|Q\bar{Q}g\rangle$ is the electric-dipole part of the operator $\psi^\dagger g\mathbf{A} \cdot \nabla\psi$ in $\mathcal{L}_{\text{heavy}}$, and this changes the orbital-angular-momentum quantum number L of the $Q\bar{Q}$ pair by ± 1 . Higher multipoles bring in additional powers of v , as does second-order perturbation theory. Thus, if the $Q\bar{Q}$ pair in the dominant Fock state $|Q\bar{Q}\rangle$ has angular-momentum quantum numbers $^{2S+1}L_J$, then the Fock state $|Q\bar{Q}g\rangle$ has a probability of order v^2 only if the $Q\bar{Q}$ pair has total spin S and orbital angular momentum $L+1$ or $L-1$. For example, if the dominant Fock state consists of a $Q\bar{Q}$ pair in a 3S_1 state, then the Fock state $|Q\bar{Q}g\rangle$ has a probability of order v^2 only if the $Q\bar{Q}$ pair is in a color-octet state with angular-momentum quantum numbers 3P_0 , 3P_1 , or 3P_2 . If the dominant Fock state consists of a $Q\bar{Q}$ pair in a 1P_1 state, then the Fock state $|Q\bar{Q}g\rangle$ has a probability of order v^2 only if the $Q\bar{Q}$ pair is in a color-octet 1S_0 or 1D_2 state.

The above discussion applies to Fock states $|Q\bar{Q}g\rangle$ in which the $Q\bar{Q}$ pair has the same total spin quantum number S as in the dominant $|Q\bar{Q}\rangle$ state. The probabilities for Fock states $|Q\bar{Q}g\rangle$ that can be reached from the dominant Fock state by a spin-flip transition also scale in a definite way with v . The probability for such a Fock state to contain a dynamical gluon with momentum of order Mv is of order v^3 , just as in the case of a non-spin-flip transition. However, in the case of a spin-flip transition, this momentum region dominates because, as we have seen, gluons with softer momenta, on the order of Mv^2 , are suppressed by the multipole expansion. Thus, if the $Q\bar{Q}$ pair in the dominant Fock state has angular-momentum quantum numbers $^{2S+1}L_J$, then the Fock state $|Q\bar{Q}g\rangle$, with the $Q\bar{Q}$ pair in a color-octet state with the same value of L but different total spin quantum number, has a probability of order v^3 . For example, if the dominant Fock state consists of a $Q\bar{Q}$ pair in a 3S_1 state, then the Fock state $|Q\bar{Q}g\rangle$ with the $Q\bar{Q}$ pair in a color-octet 1S_0 state has a probability of order v^3 . If the dominant Fock state consists of a $Q\bar{Q}$ pair in a 1P_1 state, then the Fock state $|Q\bar{Q}g\rangle$ with the $Q\bar{Q}$ pair in a color-octet 3P_J state has probability of order v^3 .

E. Space-Time Structure of Annihilation

As we will explain in this subsection, the annihilation of a heavy $Q\bar{Q}$ pair into gluons (or light quarks) occurs at distances that are typically of order $1/M$, that is, at momentum scales of order M . Because of the large momentum scales involved, the details of the annihilation process cannot be described accurately within a nonrelativistic effective theory such as NRQCD. Nevertheless, as we will argue in the next subsection, the effects of annihilation can be incorporated into NRQCD through 4-fermion operators in the term $\delta\mathcal{L}$ in the NRQCD lagrangian. To show that the required operators are local, it is sufficient to show that the interactions they account for occur over short distances of order $1/M$. Strictly local operators are then obtained by expanding the short-distance interaction in a Taylor series in the 3-momentum \mathbf{p} of the heavy quark multiplied by the characteristic size $1/M$.

Now we wish to argue that the annihilation process is indeed local, *i.e.* that the annihilation does occur within a distance of order $1/M$. We note that any annihilation must result in at least two hard gluons (or light quarks), each with momentum of order M . This has two consequences. First, the heavy quark and antiquark must come within a distance of order $1/M$ in order to annihilate. That is because the emission of a hard gluon from, say, the heavy quark puts it into a highly virtual state, which can propagate only a short distance before the quark must annihilate with the antiquark. Thus, the total annihilation amplitude can be expressed as the sum of point-like annihilation amplitudes, where the sum extends over the possible annihilation points inside the meson. The annihilation rate is the square of the total annihilation amplitude, summed over all possible final states. The second consequence of the hard gluons is that there is no overlap between one annihilation amplitude and the complex conjugate of another if the two annihilation points are separated by a distance greater than about $1/M$. This might seem surprising, since the gluons are, in effect, on their mass shells (that is, they fragment into jets with invariant masses much less than M). There is no highly virtual state to constrain the distance between the annihilation points for two amplitudes that produce the same final-state jets. Nevertheless,

the annihilation points must be in close proximity to each other in order for there to be an overlap between the final states. In order to see why this is so, we note that, in classical mechanics, we could trace the two final-state jets back to the annihilation vertex, and there would be no ambiguity whatsoever as to its space-time position. In quantum mechanics, the uncertainty principle tells us that we can know the position of the annihilation vertex only to a precision of order $1/M$, since the jet momenta are of order M . Hence, in quantum mechanics, $Q\bar{Q}$ annihilation is not a point-like process, but it *is* a localized process, with a size of order $1/M$.

In a field-theoretic calculation of the annihilation rate at leading order in α_s , the localization of the annihilation process would manifest itself as follows. The annihilation rate involves the imaginary part $\Gamma(P, p, p')$ of the scattering amplitude for a $Q\bar{Q}$ pair with total momentum P and initial and final relative momenta p and p' . Consider the Fourier transform of $\Gamma(P, p, p')$ with respect to all three momentum variables:

$$\int d^4P d^4p d^4p' e^{iP \cdot (X-X')} e^{ip \cdot (x_1-x_2)} e^{ip' \cdot (x'_1-x'_2)} \Gamma(P, p, p'). \quad (2.7)$$

Here, x_1 and x_2 correspond to quark and antiquark interaction points in one annihilation amplitude, x'_1 and x'_2 correspond to quark and antiquark interaction points in the complex conjugate of a second annihilation amplitude, and $X = (x_1 + x_2)/2$ and $X' = (x'_1 + x'_2)/2$ are average annihilation points for the first and second amplitudes. The fact that $\Gamma(P, p, p')$ is insensitive to changes in p and p' that are much less than M implies that, in the Fourier transform, x_1 (x'_1) is localized to within a distance of order $1/M$ of x_2 (x'_2). Similarly, the fact that Γ is insensitive to changes in P that are much less than M implies that the first and second amplitudes have significant overlap only if X and X' are separated by a distance of order $1/M$ or less. Note that, if one puts a restriction in the annihilation rate on one of the components of the jet momentum, then Γ becomes sensitive to that component of P , and the annihilation vertices are no longer localized along that direction. This is a consequence of the uncertainty principle, which says that knowledge of a component of the jet momentum along a given direction reduces our potential knowledge of the position of the annihilation

vertex along that direction.

The radiation of soft or collinear gluons might seem to violate this simple localization picture that appears at leading order in the coupling constant. Gluon radiation from the initial $Q\bar{Q}$ pair is not a problem, since infrared divergences can be factored into the long-distance matrix elements of the 4-fermion operators that mediate the annihilation process in NRQCD, and collinear divergences are controlled by the heavy-quark mass. We must, however, worry about infrared or collinear divergences from the radiation of gluons from the final-state hard gluons. In the presence of such soft or collinear radiation, the hard gluon can propagate almost on its mass shell from the annihilation point to the emission vertex. The energetic final-state gluon jet points back to the emission vertex, rather than to the annihilation point, which may be far away. In perturbation theory, infrared and collinear divergences occur in individual Feynman diagrams and produce a sensitivity to the heavy-quark momenta in Γ . However, the Kinoshita-Lee-Nauenberg (KLN) theorem [19] guarantees that, when one sums over the contributions of all nearly degenerate final states, as is done in forming the inclusive annihilation rate, the infrared divergences cancel between diagrams involving real and virtual gluon emission. We can think of this KLN cancellation as a consequence of a generalized form of the uncertainty principle: we can localize the annihilation point, provided that we do not require too much knowledge about the final state—that is, provided that we do not distinguish between the various states that contribute to the inclusive cross section.

The locality of the annihilation process is spoiled if the final-state gluons form a narrow resonance, such as a glueball. This is because the jets produced by the decay of the resonance point back to the place where the resonance decayed. If the resonance is narrow, this may be far from the point where the heavy quark and antiquark annihilated. That is why perturbation theory cannot be applied directly to the cross section for e^+e^- annihilation into hadrons in the region of the charmonium or bottomonium resonances. In a field-theoretic calculation, the resonance partially spoils the KLN cancellation of infrared and collinear divergences. While contributions from gluons that have exactly zero momentum or are

exactly collinear still cancel, the real and virtual contributions no longer cancel for soft gluons whose energy is comparable to the resonance width or collinear gluons whose transverse momentum is comparable to the resonance width. In the case of e^+e^- annihilation, one can deal with this problem by forming a suitable average of the cross section over the resonance region [20]. In perturbation theory, the effect of this smearing is to allow virtual soft or collinear emission at one value of the e^+e^- center-of-mass energy \sqrt{s} to cancel real soft or collinear emission at a slightly higher value of \sqrt{s} , but the same value of the energy of the resonating $Q\bar{Q}$ pair. This solution of smearing in the energy is not available to us in the case of quarkonium annihilation. Fortunately, there are no known narrow glueball resonances in the charmonium or bottomonium region, so we do not expect the resonance issue to be a problem in practice.

F. Annihilation into Light Hadrons

Since the annihilation of a $Q\bar{Q}$ pair necessarily produces gluons or light quarks with energies of order M , the annihilation amplitude cannot be described accurately within NRQCD. Nevertheless, the annihilation rate, which is the square of the amplitude summed over final states, can be accounted for in NRQCD. Since the annihilation rate of the $Q\bar{Q}$ pair is localized within a distance of order $1/M$, the annihilation contribution to a low-energy $Q\bar{Q} \rightarrow Q\bar{Q}$ scattering amplitude can be reproduced in NRQCD by local 4-fermion operators in $\delta\mathcal{L}$ involving ψ , χ^\dagger , χ , and ψ^\dagger . The optical theorem relates $Q\bar{Q}$ annihilation rates to the imaginary parts of $Q\bar{Q} \rightarrow Q\bar{Q}$ scattering amplitudes. This relation implies that the coefficients of the 4-fermion operators in $\delta\mathcal{L}$ must have imaginary parts. These imaginary parts are the manifestation of annihilation in NRQCD.

The 4-fermion interactions that represent the effects of $Q\bar{Q}$ annihilation in NRQCD have the general form

$$\delta\mathcal{L}_{4\text{-fermion}} = \sum_n \frac{f_n(\Lambda)}{M^{d_n-4}} \mathcal{O}_n(\Lambda), \quad (2.8)$$

where the \mathcal{O}_n are local 4-fermion operators, such as $\psi^\dagger\chi\chi^\dagger\psi$. The naive scaling dimensions d_n of the operators can be obtained by counting the powers of M using Table I. The factors of M^{d_n-4} in (2.8) have been introduced so as to make the coefficients f_n dimensionless. The operators \mathcal{O}_n must be regularized, and they therefore depend on the ultraviolet cutoff or renormalization scale Λ of the effective theory. The natural scale for this cutoff is M , since $1/M$ is the distance scale of the annihilation process. However, all results are independent of Λ , since the coefficients $f_n(\Lambda)$ depend on Λ in such a way as to cancel the Λ -dependence of the operators. The coefficients can be computed in full QCD as perturbation series in $\alpha_s(M)$, in which individual terms may depend on $\log(M/\Lambda)$.

If the analysis of annihilation rates were carried out completely within full QCD, then the scale Λ would arise as an arbitrary factorization scale that must be introduced in order to separate the momentum scale M from smaller momentum scales of order Mv or less. The factorization scale Λ should not be confused with the renormalization scale μ of the full theory. The coefficients $f_n(\Lambda)$ are independent of μ if they are computed to all orders in $\alpha_s(\mu)$, although some μ -dependence is introduced as usual by the truncation of the perturbation series. Unless we explicitly specify otherwise, we always make the choice $\mu = M$ in this paper.

The dimension-6 4-fermion terms in $\delta\mathcal{L}$ are

$$\begin{aligned} (\delta\mathcal{L}_{4\text{-fermion}})_{d=6} &= \frac{f_1(^1S_0)}{M^2} \mathcal{O}_1(^1S_0) + \frac{f_1(^3S_1)}{M^2} \mathcal{O}_1(^3S_1) \\ &\quad + \frac{f_8(^1S_0)}{M^2} \mathcal{O}_8(^1S_0) + \frac{f_8(^3S_1)}{M^2} \mathcal{O}_8(^3S_1), \end{aligned} \quad (2.9)$$

where the dimension-6 operators are

$$\mathcal{O}_1(^1S_0) = \psi^\dagger\chi\chi^\dagger\psi, \quad (2.10a)$$

$$\mathcal{O}_1(^3S_1) = \psi^\dagger\boldsymbol{\sigma}\chi\cdot\chi^\dagger\boldsymbol{\sigma}\psi, \quad (2.10b)$$

$$\mathcal{O}_8(^1S_0) = \psi^\dagger T^a\chi\chi^\dagger T^a\psi, \quad (2.10c)$$

$$\mathcal{O}_8(^3S_1) = \psi^\dagger\boldsymbol{\sigma}T^a\chi\cdot\chi^\dagger\boldsymbol{\sigma}T^a\psi. \quad (2.10d)$$

The subscript 1 or 8 on the operators and on their coefficients indicates the color structure of

the operator. The arguments $^{2S+1}L_J$ indicate the angular-momentum state of the $Q\bar{Q}$ pair which is annihilated or created by the operator. Normal-ordering of the 4-fermion operators \mathcal{O}_n will always be understood, so that matrix elements of \mathcal{O}_n receive contributions only from annihilation of the Q and \bar{Q} . The dimension-8 terms in the lagrangian for NRQCD include

$$\begin{aligned}
(\delta\mathcal{L}_{4\text{-fermion}})_{d=8} = & \frac{f_1(^1P_1)}{M^4} \mathcal{O}_1(^1P_1) + \frac{f_1(^3P_0)}{M^4} \mathcal{O}_1(^3P_0) + \frac{f_1(^3P_1)}{M^4} \mathcal{O}_1(^3P_1) \\
& + \frac{f_1(^3P_2)}{M^4} \mathcal{O}_1(^3P_2) + \frac{g_1(^1S_0)}{M^4} \mathcal{P}_1(^1S_0) + \frac{g_1(^3S_1)}{M^4} \mathcal{P}_1(^3S_1) \\
& + \frac{g_1(^3S_1, ^3D_1)}{M^4} \mathcal{P}_1(^3S_1, ^3D_1) + \dots .
\end{aligned} \tag{2.11}$$

The dimension-8 operators included explicitly in (2.11) are

$$\mathcal{O}_1(^1P_1) = \psi^\dagger(-\frac{i}{2}\vec{\mathbf{D}})\chi \cdot \chi^\dagger(-\frac{i}{2}\vec{\mathbf{D}})\psi, \tag{2.12a}$$

$$\mathcal{O}_1(^3P_0) = \frac{1}{3} \psi^\dagger(-\frac{i}{2}\vec{\mathbf{D}} \cdot \boldsymbol{\sigma})\chi \chi^\dagger(-\frac{i}{2}\vec{\mathbf{D}} \cdot \boldsymbol{\sigma})\psi, \tag{2.12b}$$

$$\mathcal{O}_1(^3P_1) = \frac{1}{2} \psi^\dagger(-\frac{i}{2}\vec{\mathbf{D}} \times \boldsymbol{\sigma})\chi \cdot \chi^\dagger(-\frac{i}{2}\vec{\mathbf{D}} \times \boldsymbol{\sigma})\psi, \tag{2.12c}$$

$$\mathcal{O}_1(^3P_2) = \psi^\dagger(-\frac{i}{2}\vec{\mathbf{D}}^{(i}\sigma^{j)})\chi \chi^\dagger(-\frac{i}{2}\vec{\mathbf{D}}^{(i}\sigma^{j)})\psi, \tag{2.12d}$$

$$\mathcal{P}_1(^1S_0) = \frac{1}{2} [\psi^\dagger\chi \chi^\dagger(-\frac{i}{2}\vec{\mathbf{D}})^2\psi + \text{h.c.}], \tag{2.12e}$$

$$\mathcal{P}_1(^3S_1) = \frac{1}{2} [\psi^\dagger\boldsymbol{\sigma}\chi \cdot \chi^\dagger\boldsymbol{\sigma}(-\frac{i}{2}\vec{\mathbf{D}})^2\psi + \text{h.c.}], \tag{2.12f}$$

$$\mathcal{P}_1(^3S_1, ^3D_1) = \frac{1}{2} [\psi^\dagger\sigma^i\chi \chi^\dagger\sigma^j(-\frac{i}{2}\vec{\mathbf{D}})^2\vec{\mathbf{D}}^{(i}\vec{\mathbf{D}}^{j)}\psi + \text{h.c.}], \tag{2.12g}$$

where $\vec{\mathbf{D}}$ is the difference between the covariant derivative acting on the spinor to the right and on the spinor to the left: $\chi^\dagger\vec{\mathbf{D}}\psi \equiv \chi^\dagger(\mathbf{D}\psi) - (\mathbf{D}\chi)^\dagger\psi$. We have used the notation $T^{(ij)}$ for the symmetric traceless component of a tensor: $T^{(ij)} = (T^{ij} + T^{ji})/2 - T^{kk}\delta^{ij}/3$. For each of the operators shown explicitly in (2.11), there is a corresponding color-octet operator \mathcal{O}_8 or \mathcal{P}_8 , which contains color matrices T^a inserted between ψ^\dagger and χ and between χ^\dagger and ψ . This exhausts the list of the dimension-8 operators that contribute at tree level to $Q\bar{Q}$ scattering in the center of momentum frame. There are other dimension-8 operators, such as $\nabla(\psi^\dagger\chi) \cdot (\chi^\dagger\vec{\mathbf{D}}\psi)$ or $\mathbf{D}(\psi^\dagger T^a\chi) \cdot \mathbf{D}(\chi^\dagger T^a\psi)$, in which a derivative acts on the product of ψ^\dagger and χ or on the product of χ^\dagger and ψ . Matrix elements of operators such as these are proportional to the total momentum of the $Q\bar{Q}$ pair, and therefore do not receive any

contributions from the dominant Fock state $|Q\bar{Q}\rangle$ in the meson rest frame. They do, however, receive contributions from higher Fock states, such as $|Q\bar{Q}g\rangle$, in which the total momentum of the $Q\bar{Q}$ pair is nonzero.

According to the velocity-scaling rules in Table I, the dimension-6 terms in (2.9) scale as v relative to the leading term $\mathcal{L}_{\text{heavy}}$ in the NRQCD Lagrangian. Thus, if we consider only the dependence on v , the terms in (2.9) appear to be more important than the terms in $\delta\mathcal{L}_{\text{bilinear}}$, which scale as v^2 relative to the terms in $\mathcal{L}_{\text{heavy}}$. However, the contributions from 4-fermion operators contain extra suppression factors, owing to the operator coefficients, whose imaginary parts are of order $\alpha_s^2(M)$ or smaller. Thus, the contributions to annihilation widths from (2.9) are of order $\alpha_s^2(M)v$ or smaller relative to the scale Mv^2 of the splittings between radial excitations and between orbital-angular-momentum excitations. Similarly, the contributions to annihilation widths from the dimension-8 operators in (2.11) are at most of order $\alpha_s^2(M)v^3$ relative to the scale Mv^2 of splittings between energy levels. Thus, the annihilation decay rates for heavy-quarkonium states are tiny perturbations on the energy levels. This is certainly true empirically. In the charmonium system, the ground state η_c has the largest annihilation width, but it is less than 3% of the splitting between the η_c and the first radial or orbital-angular-momentum excitations. For bottomonium, the annihilation widths are always less than 1% of the corresponding splittings.

In order to obtain an expression for the annihilation rate, we recall that the decay rate is -2 times the imaginary part of the energy of the state. The contribution to the imaginary part of the energy that corresponds to annihilation into light hadrons comes from the expectation value of $-\delta\mathcal{L}_{4\text{-fermion}}$, whose coefficients have imaginary parts. Thus, we see that the annihilation rate of a heavy-quarkonium state H into light hadrons is

$$\Gamma(H \rightarrow \text{LH}) = 2 \text{Im} \langle H | \delta\mathcal{L}_{4\text{-fermion}} | H \rangle, \quad (2.13)$$

where LH represents all possible light-hadronic final states. The expectation value is taken in the rest frame of the quarkonium, where its total momentum \mathbf{P} vanishes. The state $|H\rangle \equiv$

$|H(\mathbf{P} = 0)\rangle$ is an eigenstate of the NRQCD hamiltonian.² It has the standard nonrelativistic normalization: $\langle H(\mathbf{P}')|H(\mathbf{P})\rangle = (2\pi)^3\delta^3(\mathbf{P} - \mathbf{P}')$. Inserting the expansion (2.8) into (2.13), we obtain

$$\Gamma(H \rightarrow \text{LH}) = \sum_n \frac{2 \text{Im} f_n(\Lambda)}{M^{d_n-4}} \langle H|\mathcal{O}_n(\Lambda)|H\rangle. \quad (2.14)$$

The equation (2.14) is our central result for the annihilation decays into light hadrons. It expresses the decay rate as a sum of terms, each of which factors into a short-distance coefficient $\text{Im} f_n$ and a long-distance matrix element $\langle H|\mathcal{O}_n|H\rangle$. The coefficients $\text{Im} f_n$ in (2.14) are proportional to the rates for on-shell heavy quarks and antiquarks to annihilate from appropriate initial configurations into hard gluons and light quarks, and can be computed as perturbation series in $\alpha_s(M)$. The matrix elements $\langle H|\mathcal{O}_n|H\rangle$ give the probability for finding the heavy quark and antiquark in a configuration within the meson that is suitable for annihilation, and can be evaluated nonperturbatively using, for example, lattice simulations. The dependence on the arbitrary factorization scale Λ in (2.14) cancels between the coefficients and the operators.

²Radial and orbital-angular-momentum excitations of a quarkonium may decay through the hermitian part of the NRQCD lagrangian to lower-lying quarkonium states plus light hadrons. An example is the decay of $\psi(2S)$ into $\psi\pi\pi$. In this example, the spectrum of states in NRQCD contains a continuum of $\psi\pi\pi$ scattering states, each of which includes a small admixture of the bare $\psi(2S)$ state, and a discrete state, which is mostly the bare $\psi(2S)$ state, but which also contains a small admixture of bare $\psi\pi\pi$ scattering states. The $\psi(2S)$ Breit-Wigner resonance in, for example, the amplitude for $e^+e^- \rightarrow \mu^+\mu^-$ results from the contributions of the complete spectrum of states. However, the resonance in the amplitude can be reproduced by a single state, with complex energy, that is an eigenstate of the nonlocal effective Hamiltonian that one would obtain by integrating out the light-hadron states in NRQCD. One should identify the state $|H\rangle$ in (2.14) with such an eigenstate in applying (2.14) to an excited quarkonium state that decays through the hermitian part of the NRQCD lagrangian into a lower-lying quarkonium state.

In some calculations of the matrix elements in (2.14), such as lattice simulations, it may be useful to approximate the states $|H\rangle$ by eigenstates of the hermitian part of the NRQCD Hamiltonian. We note that corrections to this approximation first appear at third-order in perturbation theory in $\text{Im } \delta\mathcal{L}_{4\text{-fermion}}$, since second-order perturbation theory does not give an imaginary contribution to the energy. The corrections are therefore of order $(\Gamma/Mv^2)^2\Gamma$. This is of relative order $\alpha_s^4(M)v^2$ or smaller, since the leading terms in Γ scale like Mv^3 and are multiplied by short-distance coefficients of order $\alpha_s^2(M)$ or smaller. This level of accuracy is sufficient for most practical purposes.

Applying the velocity-scaling rules of Table I to the matrix elements $\langle H|\mathcal{O}_n(\Lambda)|H\rangle$, one finds that the expression (2.14) for the annihilation decay rate can be organized into an expansion in powers of v . Only a finite number of operators contribute to any given order in v . The coefficients $f_n(\Lambda)$ can be calculated as perturbation series in $\alpha_s(M)$, so (2.14) is really a double expansion in $\alpha_s(M)$ and v . The simultaneous expansion in $\alpha_s(M)$ and v is useful to the extent that these two parameters are both small. Of course, $\alpha_s(M)$ and v are not independent for heavy quarkonium. According to (2.1), v can be identified with $\alpha_s(Mv)$, which is larger than $\alpha_s(M)$. This implies that it would be futile to consider corrections to the coefficients $\text{Im } f_n$ of relative order $\alpha_s^n(M)$ unless matrix elements $\langle H|\mathcal{O}_n|H\rangle$ of relative order v^n have already been included.

The relation between v and $\alpha_s(M)$ implied by (2.1) follows from the dynamics of heavy quarkonium. The factorization formula (2.14) is actually an operator equation, and it can equally well be applied to other problems in which the relation between v and $\alpha_s(M)$ is different. An example in which v and $\alpha_s(M)$ are independent is the annihilation of a pair of heavy-light mesons, such as D and \bar{D} mesons, at small relative velocity $v \ll 1$. As long as v is much larger than Λ_{QCD}/M , which is the typical relative velocity of a heavy quark in the heavy-light meson, it can be identified with the velocity of the heavy quark and the scaling rules of Table I apply.

G. Electromagnetic Annihilation

In addition to annihilating into light hadrons, heavy-quarkonium states can also annihilate into purely electromagnetic final states containing only photons and lepton pairs. The energies of the final-state photons and leptons are of order M . In NRQCD, the effects of electromagnetic annihilation can be accounted for in the same way as the effects of annihilation into light hadrons: by adding 4-fermion terms $\delta\mathcal{L}_{4\text{-fermion}}^{\text{EM}}$ to the effective lagrangian. The primary difference is that in the case of electromagnetic annihilation, the final state, as far as the strong interactions are concerned, is the QCD vacuum state $|0\rangle$. The 4-fermion operators that reproduce the effects of electromagnetic annihilation therefore differ from those in (2.9) and (2.11) by the insertion of an operator $|0\rangle\langle 0|$ that projects onto the QCD vacuum state. The dimension-6 terms that must be added to the lagrangian are

$$\left(\delta\mathcal{L}_{4\text{-fermion}}^{\text{EM}}\right)_{d=6} = \frac{f_{\text{EM}}(^1S_0)}{M^2} \psi^\dagger\chi|0\rangle\langle 0|\chi^\dagger\psi + \frac{f_{\text{EM}}(^3S_1)}{M^2} \psi^\dagger\boldsymbol{\sigma}\chi|0\rangle \cdot \langle 0|\chi^\dagger\boldsymbol{\sigma}\psi. \quad (2.15)$$

Note that color-octet operators, such as $\psi^\dagger T^a\chi|0\rangle\langle 0|\chi^\dagger T^a\psi$, are omitted because they cannot contribute to matrix elements between color-singlet heavy-quarkonium states. The dimension-8 terms that must be added to the lagrangian include

$$\begin{aligned} \left(\delta\mathcal{L}_{4\text{-fermion}}^{\text{EM}}\right)_{d=8} = & \frac{f_{\text{EM}}(^3P_0)}{M^4} \frac{1}{3} \psi^\dagger\left(-\frac{i}{2}\vec{\mathbf{D}}\right) \cdot \boldsymbol{\sigma}\chi|0\rangle \langle 0|\chi^\dagger\left(-\frac{i}{2}\vec{\mathbf{D}}\right) \cdot \boldsymbol{\sigma}\psi \\ & + \frac{f_{\text{EM}}(^3P_2)}{M^4} \psi^\dagger\left(-\frac{i}{2}\vec{D}^{(i}\sigma^j)\right)\chi|0\rangle \langle 0|\chi^\dagger\left(-\frac{i}{2}\vec{D}^{(i}\sigma^j)\right)\psi \\ & + \frac{g_{\text{EM}}(^1S_0)}{M^4} \frac{1}{2} \left[\psi^\dagger\chi|0\rangle\langle 0|\chi^\dagger\left(-\frac{i}{2}\vec{\mathbf{D}}\right)^2\psi + \text{h.c.}\right] \\ & + \frac{g_{\text{EM}}(^3S_1)}{M^4} \frac{1}{2} \left[\psi^\dagger\boldsymbol{\sigma}\chi|0\rangle \cdot \langle 0|\chi^\dagger\boldsymbol{\sigma}\left(-\frac{i}{2}\vec{\mathbf{D}}\right)^2\psi + \text{h.c.}\right] + \dots \end{aligned} \quad (2.16)$$

We have shown only four of the possible dimension-8 terms. In particular, there are terms corresponding to each of the operators shown explicitly in (2.11). The coefficients of the operators in (2.15) and (2.16) can be computed as perturbation expansions in $\alpha_s(M)$.

The decay rate of a heavy quarkonium state H into electromagnetic final states (EM) can be expressed in a factored form that is analogous to that given in (2.14) for decays into light hadrons:

$$\Gamma(H \rightarrow \text{EM}) = \sum_n \frac{2 \text{Im} f_{\text{EM},n}(\Lambda)}{M^{d_n-4}} \langle H | \psi^\dagger \mathcal{K}'_n \chi(\Lambda) | 0 \rangle \langle 0 | \chi^\dagger \mathcal{K}_n \psi(\Lambda) | H \rangle, \quad (2.17)$$

where \mathcal{K}_n and \mathcal{K}'_n are products of the unit color matrix, a spin matrix (the unit matrix or σ^i), and a polynomial in the covariant derivative \mathbf{D} and other fields, as in (2.15) and (2.16). The possible electromagnetic final states EM include the multiphoton states $\gamma\gamma$ and 3γ and the lepton pairs $\ell^+\ell^-$, where $\ell = e, \mu, \tau$.

H. Computation of the Coefficients of the 4-Fermion Operators

The nonperturbative long-distance dynamics of QCD is described equally well by full QCD and by NRQCD. The perturbation expansions for full QCD and NRQCD also give equivalent descriptions of the long-distance dynamics, although the description is incorrect. For example, perturbation theory allows quarks and antiquarks to appear as asymptotic states. However, because the coefficients of the NRQCD operators are insensitive to the long-distance dynamics, we can exploit the equivalence of perturbative QCD and perturbative NRQCD at long distances as a device to calculate the coefficients of the four-fermion operators. We compute in perturbation theory in full QCD the annihilation part $A(Q\bar{Q} \rightarrow Q\bar{Q})$ of the scattering amplitude for an on-shell quark and antiquark with small relative momenta. Then we use perturbation theory in NRQCD to compute the matrix elements of 4-fermion operators \mathcal{O}_n between on-shell $Q\bar{Q}$ states. The short-distance coefficients are determined by the matching condition

$$A(Q\bar{Q} \rightarrow Q\bar{Q}) \Big|_{\text{pert. QCD}} = \sum_n \frac{f_n(\Lambda)}{M^{d_n-4}} \langle Q\bar{Q} | \mathcal{O}_n(\Lambda) | Q\bar{Q} \rangle \Big|_{\text{pert. NRQCD}}. \quad (2.18)$$

By expanding the left and right sides of (2.18) as Taylor series in the relative momenta \mathbf{p} and \mathbf{p}' of the initial and final $Q\bar{Q}$ pairs, we can identify the coefficients of the individual operators. These correspond to the infrared-finite parts of the parton-level amplitudes for $Q\bar{Q}$ scattering. Because of the equivalence of NRQCD and full QCD at long distances, all of the infrared divergences contained in $A(Q\bar{Q} \rightarrow Q\bar{Q})$ on the left side of (2.18) reside on the right side in the NRQCD matrix elements $\langle Q\bar{Q} | \mathcal{O}_n(\Lambda) | Q\bar{Q} \rangle$.

The application of the matching condition (2.18) is illustrated in Appendix A. The imaginary parts of the coefficients f_n that enter into the annihilation rates of S-wave states through relative order v^2 and the annihilation rates of P-wave states at leading order in v are computed to order α_s^2 . In order to illustrate the use of the matching condition (2.18) beyond leading order in α_s , we also calculate the coefficient $\text{Im } f_1(^1S_0)$ at next-to-leading order in α_s .

III. MATRIX ELEMENTS FOR HEAVY QUARKONIUM

The factorization formula (2.14) expresses the decay rate of an arbitrary heavy quarkonium state H into light hadrons as a sum over all 4-fermion operators \mathcal{O}_n . If we truncate the expansion at a given order in the heavy-quark velocity v , then only finitely many of the operators contribute. In this section, we show how the number of independent matrix elements can be reduced further by exploiting heavy-quark spin symmetry and by using the vacuum-saturation approximation. We identify the matrix elements that contribute to the decays of S-wave states through relative order v^2 and the matrix elements that contribute to the decays of P-wave states at leading order in v . We also discuss the relation between these matrix elements and Coulomb-gauge wavefunctions, as well as the dependence of the matrix elements on the factorization scale. For the sake of clarity, we use the lowest S-wave and P-wave states of charmonium for the purpose of illustration. However, our results apply equally well to other sets of S-wave and P-wave states, and they can be extended readily to higher orbital-angular-momentum states as well. The lowest-lying S-wave states in the charmonium system are the $J^{PC} = 0^{-+}$ state η_c and the 1^{--} state J/ψ (henceforth referred to simply as ψ). The lowest-lying P-wave states are the 1^{+-} state h_c and the J^{++} states χ_{cJ} , $J = 0, 1, 2$.

A. Powers of Velocity

We wish to determine the relative importance of the matrix elements $\langle H|\mathcal{O}_n|H\rangle$ of 4-fermion operators \mathcal{O}_n for a heavy quarkonium state $|H\rangle$. The velocity-scaling rules in Table I suggest that $\langle H|\mathcal{O}_n|H\rangle$ is of the same order in v for all the dimension-6 operators in (2.9), and that all the dimension-8 operators in (2.11) are down by a power of v^2 . There can, however, be additional suppression by powers of v , depending on the quantum numbers of the state H . The velocity-scaling rules in Table I give the correct result only if the operator \mathcal{O}_n annihilates and creates a color-singlet $Q\bar{Q}$ pair with the same angular-momentum $^{2S+1}L_J$ as

the $Q\bar{Q}$ pair in the dominant Fock state $|Q\bar{Q}\rangle$ of the state $|H\rangle$. (In the notation for 4-fermion operators used in (2.9) and (2.11), the subscript 1 or 8 and the argument $^{2S+1}L_J$ indicate the color and angular-momentum state of the $Q\bar{Q}$ pair that is annihilated and created by the operator.) The matrix element $\langle H|\mathcal{O}_n|H\rangle$ is suppressed by only one additional power of v^2 , relative to the velocity-scaling rules in Table 1, if \mathcal{O}_n annihilates and creates $Q\bar{Q}$ pairs in the same color-spin-orbital state as appears in one of the Fock states $|Q\bar{Q}g\rangle$ whose probability is of order v^2 . In particular, if the dominant $Q\bar{Q}$ component is $^{2S+1}L_J$, the $Q\bar{Q}$ pair in the component $|Q\bar{Q}g\rangle$ must be in a color-octet state with spin quantum number S and orbital-angular-momentum quantum number $L \pm 1$. The matrix element is suppressed by v^3 relative to the velocity-scaling rules in Table I if \mathcal{O}_n annihilates and creates $Q\bar{Q}$ pairs in the same color-spin-orbital state as appears in one of the Fock states $|Q\bar{Q}g\rangle$ that can be obtained from the dominant Fock state by a spin-flip transition. In such a Fock state, the $Q\bar{Q}$ pair must be in a color-octet state with the same orbital-angular-momentum quantum number L as in the dominant $|Q\bar{Q}\rangle$ state, but with different total spin quantum number. In all other cases, the matrix element is down by v^4 or more relative to the velocity-scaling result from Table I.

If perturbation theory remained accurate down to the scale Mv , then the spin-flip matrix elements would be suppressed by an additional power of v . The reason for this is that the contribution to a spin-flip matrix element that is suppressed by only v^3 relative to the velocity-scaling rules is power ultraviolet divergent. Therefore, one could carry out a renormalization of the matrix element in which this contribution is subtracted. The corresponding contribution to the decay rate would then reside in the short-distance coefficient of the matrix element that is associated with the dominant Fock state. (Such a subtraction is carried out automatically if dimensional regularization is used to cut off the ultraviolet divergences in the matrix element.) Once the subtraction has been made, the leading contribution to the spin-flip matrix element comes from the scale Mv^2 . It is subject to the usual multipole suppression and scales as v^4 relative to the velocity-scaling rules. In practice, one usually

makes such subtractions perturbatively. It is not clear, in the charmonium and bottomonium systems, that perturbation theory is sufficiently accurate at the scale Mv to remove the v^3 contribution completely. Therefore, we assume in the error estimates below that the spin-flip matrix elements scale as v^3 relative to the velocity-scaling rules.

We can now identify the operators that contribute to the annihilation of the η_c into light hadrons through relative order v^2 . The $J^{PC} = 0^{-+}$ state $|\eta_c\rangle$ consists predominantly of the Fock state $|Q\bar{Q}\rangle$, with the $Q\bar{Q}$ pair in a color-singlet 1S_0 state, but it also contains, with probability of order v^2 , the Fock state $|Q\bar{Q}g\rangle$, with the $Q\bar{Q}$ pair in a color-octet 1P_1 state. The $Q\bar{Q}$ pair in the dominant Fock state $|Q\bar{Q}\rangle$ is annihilated and created by the leading operator $\mathcal{O}_1(^1S_0) = \psi^\dagger\chi\chi^\dagger\psi$, and by the operator $\mathcal{P}_1(^1S_0) = \psi^\dagger\chi\chi^\dagger(-\frac{i}{2}\vec{\mathbf{D}})^2\psi + \text{h.c.}$, which is down by v^2 . All other operators are suppressed by v^3 or more relative to $\mathcal{O}_1(^1S_0)$. For example, the operator $\mathcal{O}_8(^1P_1) = \psi^\dagger(-\frac{i}{2}\vec{\mathbf{D}})T^a\chi\cdot\chi^\dagger(-\frac{i}{2}\vec{\mathbf{D}})T^a\psi$ scales as v^2 relative to $\mathcal{O}_1(^1S_0)$, but it contributes through the Fock state $|Q\bar{Q}g\rangle$, which gives an additional suppression by v^2 . The operator $\mathcal{O}_1(^3S_1) = \psi^\dagger\boldsymbol{\sigma}\chi\cdot\chi^\dagger\boldsymbol{\sigma}\psi$ scales as $\mathcal{O}_1(^1S_0)$, but it contributes through the Fock state $|Q\bar{Q}gg\rangle$, and is therefore suppressed by an additional probability factor of v^4 . As a final example, the operator $\nabla(\psi^\dagger\chi)\cdot\nabla(\chi^\dagger\psi)$ scales as v^2 relative to $\mathcal{O}_1(^1S_0)$, but its matrix element is proportional to the total momentum of the $Q\bar{Q}$ pair, which vanishes for the Fock state $|Q\bar{Q}\rangle$ in the meson rest frame. Thus, there are only two operators that contribute to the decay rate of the η_c into light hadrons through relative order v^2 :

$$\begin{aligned} \Gamma(\eta_c \rightarrow \text{LH}) &= \frac{2 \text{Im } f_1(^1S_0)}{M^2} \langle \eta_c | \mathcal{O}_1(^1S_0) | \eta_c \rangle \\ &\quad + \frac{2 \text{Im } g_1(^1S_0)}{M^4} \langle \eta_c | \mathcal{P}_1(^1S_0) | \eta_c \rangle + O(v^3\Gamma). \end{aligned} \quad (3.1)$$

The analysis of the operators that contribute to the decays of the ψ is similar to that for the η_c . The 1^{--} state $|\psi\rangle$ consists predominantly of the Fock state $|Q\bar{Q}\rangle$, with the $Q\bar{Q}$ pair in a color-singlet 3S_1 state, but it contains, with a probability of order v^2 , the Fock state $|Q\bar{Q}g\rangle$, with the $Q\bar{Q}$ pair in a color-octet 3P_0 , 3P_1 , or 3P_2 state. At leading order in v , only the operator $\mathcal{O}_1(^3S_1)$ contributes to the decay rate of the ψ into light hadrons. At relative order v^2 , the only additional contribution comes from the operator $\mathcal{P}_1(^3S_1)$. As in the case

of the η_c , all contributions from Fock states containing dynamical gluons, such as $|Q\bar{Q}g\rangle$, are of order $v^3\Gamma$ or higher.

We next determine the operators that contribute to the annihilation decays of the P-wave states at leading order in v . In contrast to the S-wave states, we find that Fock states containing dynamical gluons play an important role. The 1^{+-} state $|h_c\rangle$ consists predominantly of the Fock state $|Q\bar{Q}\rangle$, with the $Q\bar{Q}$ pair in a color-singlet 1P_1 state, but it has a probability of order v^2 for the Fock state $|Q\bar{Q}g\rangle$, with the $Q\bar{Q}$ pair in a color-octet 1S_0 or 1D_2 state. The Fock state $|Q\bar{Q}\rangle$ is created and annihilated by the dimension-8 operator $\mathcal{O}_1(^1P_1) = \psi^\dagger(-\frac{i}{2}\vec{\mathbf{D}})\chi \cdot \chi^\dagger(-\frac{i}{2}\vec{\mathbf{D}})\psi$. The Fock state $|Q\bar{Q}g\rangle$, with the $Q\bar{Q}$ pair in a color-octet 1S_0 state, also contributes to the decay at the same order in v through the operator $\mathcal{O}_8(^1S_0) = \psi^\dagger T^a \chi \chi^\dagger T^a \psi$. The operator scales as v^{-2} relative to $\mathcal{O}_1(^1P_1)$, but there is also a suppression factor of v^2 from the probability for the $Q\bar{Q}g$ state. Thus, the Fock state $|Q\bar{Q}g\rangle$, which contains a dynamical gluon, contributes to the decay rate into light hadrons at the same order in v as the dominant Fock state $|Q\bar{Q}\rangle$. The resulting expression for the decay rate is

$$\begin{aligned} \Gamma(h_c \rightarrow \text{LH}) &= \frac{2 \text{Im } f_1(^1P_1)}{M^4} \langle h_c | \mathcal{O}_1(^1P_1) | h_c \rangle \\ &+ \frac{2 \text{Im } f_8(^1S_0)}{M^2} \langle h_c | \mathcal{O}_8(^1S_0) | h_c \rangle + O(v^2\Gamma). \end{aligned} \quad (3.2)$$

The analysis of the operators that contribute to the decays of the χ_{c0} , χ_{c1} , and χ_{c2} is similar to that for h_c . The J^{++} state $|\chi_{cJ}\rangle$ consists predominantly of the Fock state $|Q\bar{Q}\rangle$, with the $Q\bar{Q}$ pair in a color-singlet 3P_J state. It also contains, with a probability of order v^2 , the Fock state $|Q\bar{Q}g\rangle$, with the $Q\bar{Q}$ pair in a color-octet 3S_1 , 3D_1 , 3D_2 , or 3D_3 state. The Fock state $|Q\bar{Q}\rangle$ contributes to the annihilation at leading order in v through the dimension-8 operator $\mathcal{O}_1(^3P_J)$. The Fock state $|Q\bar{Q}g\rangle$, with the $Q\bar{Q}$ pair in a color-octet 3S_1 state, also contributes to the annihilation rate at the same order in v , through the operator $\mathcal{O}_8(^3S_1) = \psi^\dagger \boldsymbol{\sigma} T^a \chi \cdot \chi^\dagger \boldsymbol{\sigma} T^a \psi$.

The analysis of the electromagnetic operators that contribute to the decays of S-wave and P-wave states is identical to that of the operators that contribute to the decays into

light hadrons, except that there are no color-octet operators. We find, therefore, that there are two operators that contribute to the decay of the η_c into two photons through relative order v^2 : $\psi^\dagger\chi|0\rangle\langle 0|\chi^\dagger\psi$ and $\psi^\dagger\chi|0\rangle\langle 0|\chi^\dagger(-\frac{i}{2}\overleftrightarrow{\mathbf{D}})^2\psi + \text{h.c.}$. Thus, the decay rate for $\eta_c \rightarrow \gamma\gamma$ is

$$\Gamma(\eta_c \rightarrow \gamma\gamma) = \frac{2 \operatorname{Im} f_{\gamma\gamma}(^1S_0)}{M^2} \left| \langle 0|\chi^\dagger\psi|\eta_c \rangle \right|^2 + \frac{2 \operatorname{Im} g_{\gamma\gamma}(^1S_0)}{M^4} \operatorname{Re} \left(\langle \eta_c|\psi^\dagger\chi|0 \rangle \langle 0|\chi^\dagger(-\frac{i}{2}\overleftrightarrow{\mathbf{D}})^2\psi|\eta_c \rangle \right) + O(v^4\Gamma). \quad (3.3)$$

Here, it is expressed in terms of the vacuum-to- η_c matrix elements $\langle 0|\chi^\dagger\psi|\eta_c \rangle$ and $\langle 0|\chi^\dagger(-\frac{i}{2}\overleftrightarrow{\mathbf{D}})^2\psi|\eta_c \rangle$. Similarly the decay rate for $\psi \rightarrow e^+e^-$ can be computed at relative order v^2 in terms of $\langle 0|\chi^\dagger\boldsymbol{\sigma}\psi|\psi \rangle$ and $\langle 0|\chi^\dagger\boldsymbol{\sigma}(-\frac{i}{2}\overleftrightarrow{\mathbf{D}})^2\psi|\psi \rangle$. For the decay $\chi_{c0} \rightarrow \gamma\gamma$, the only operator that contributes at leading order in v is $\psi^\dagger(-\frac{i}{2}\overleftrightarrow{\mathbf{D}} \cdot \boldsymbol{\sigma})\chi|0\rangle\langle 0|\chi^\dagger(-\frac{i}{2}\overleftrightarrow{\mathbf{D}} \cdot \boldsymbol{\sigma})\psi$, so the decay rate can be expressed in terms of the single vacuum-to- χ_{c0} matrix element $\langle 0|\chi^\dagger(-\frac{i}{2}\overleftrightarrow{\mathbf{D}} \cdot \boldsymbol{\sigma})\psi|\chi_{c0} \rangle$. Similarly the decay rate for $\chi_{c2} \rightarrow \gamma\gamma$ can be calculated to leading order in v in terms of the matrix element $\langle 0|\chi^\dagger(-\frac{i}{2}\overleftrightarrow{D}^{(i}\sigma^j)})\psi|\chi_{c2} \rangle$ only.

B. Heavy-Quark Spin Symmetry

Heavy-quark spin symmetry provides approximate relations between matrix elements for the various spin states of a given radial and orbital excitation of heavy quarkonium. The leading violations of heavy-quark spin symmetry come from the spin-flip terms in (2.5), whose effects are of relative order v^2 . Consequently, the equalities that follow from heavy-quark spin symmetry hold only through relative order v^2 . Nevertheless, these relations can significantly reduce the number of independent matrix elements that contribute to the decays of the various spin states.

When applied to the S-wave states, heavy-quark spin symmetry relates the η_c and the 3 spin states of the ψ . For the matrix elements that contribute to their decays into light hadrons through relative order v^2 , the spin-symmetry relations are

$$\langle \psi|\mathcal{O}_1(^3S_1)|\psi \rangle = \langle \eta_c|\mathcal{O}_1(^1S_0)|\eta_c \rangle \left(1 + O(v^2) \right), \quad (3.4a)$$

$$\langle \psi | \mathcal{P}_1(^3S_1) | \psi \rangle = \langle \eta_c | \mathcal{P}_1(^1S_0) | \eta_c \rangle \left(1 + O(v^2) \right). \quad (3.4b)$$

The 12 spin states of the P-wave states h_c , χ_{c0} , χ_{c1} , and χ_{c2} form a spin-symmetry multiplet. The spin-symmetry relations between the matrix elements that contribute to the decays of the P-wave states into light hadrons at leading order in v are

$$\langle \chi_{cJ} | \mathcal{O}_1(^3P_J) | \chi_{cJ} \rangle = \langle h_c | \mathcal{O}_1(^1P_1) | h_c \rangle \left(1 + O(v^2) \right), \quad J = 0, 1, 2, \quad (3.5a)$$

$$\langle \chi_{cJ} | \mathcal{O}_8(^3S_1) | \chi_{cJ} \rangle = \langle h_c | \mathcal{O}_8(^1S_0) | h_c \rangle \left(1 + O(v^2) \right), \quad J = 0, 1, 2. \quad (3.5b)$$

Heavy-quark spin symmetry also relates the matrix elements that contribute to the electromagnetic annihilation decay rates. For the matrix elements that contribute to the decays of η_c and ψ , the spin-symmetry relations are

$$\boldsymbol{\epsilon}^* \cdot \langle 0 | \chi^\dagger \boldsymbol{\sigma} \psi | \psi(\boldsymbol{\epsilon}) \rangle = \langle 0 | \chi^\dagger \psi | \eta_c \rangle \left(1 + O(v^2) \right), \quad (3.6a)$$

$$\boldsymbol{\epsilon}^* \cdot \langle 0 | \chi^\dagger \boldsymbol{\sigma} \left(-\frac{i}{2} \vec{\mathbf{D}} \right)^2 \psi | \psi(\boldsymbol{\epsilon}) \rangle = \langle 0 | \chi^\dagger \left(-\frac{i}{2} \vec{\mathbf{D}} \right)^2 \psi | \eta_c \rangle \left(1 + O(v^2) \right), \quad (3.6b)$$

where the polarization vector $\boldsymbol{\epsilon}$ satisfies $\boldsymbol{\epsilon}^* \cdot \boldsymbol{\epsilon} = 1$. For the matrix elements that contribute to the decays of the χ_{c0} and χ_{c2} into two photons, the spin-symmetry relations are

$$\epsilon^{ij*} \langle 0 | \chi^\dagger \left(\frac{1}{2} \vec{\mathbf{D}}^i \sigma^j \right) \psi | \chi_{c2}(\boldsymbol{\epsilon}) \rangle = \frac{1}{\sqrt{3}} \langle 0 | \chi^\dagger \left(\frac{1}{2} \vec{\mathbf{D}} \cdot \boldsymbol{\sigma} \right) \psi | \chi_{c0} \rangle \left(1 + O(v^2) \right), \quad (3.7)$$

where the symmetric polarization tensor ϵ^{ij} satisfies $\text{tr}(\boldsymbol{\epsilon}) = 0$ and $\text{tr}(\boldsymbol{\epsilon}^\dagger \boldsymbol{\epsilon}) = 1$.

C. Vacuum-Saturation Approximation

The 4-fermion operators in (2.9) and (2.11) that contribute to the decays of heavy quarkonium into light hadrons are distinct from those in (2.15) and (2.16) that contribute to electromagnetic annihilation. The electromagnetic matrix elements can be obtained from the corresponding light hadronic matrix elements by making use of the ‘‘vacuum-saturation approximation’’: insert a complete set of light hadronic states $\sum_X |X\rangle \langle X|$ between χ^\dagger and χ and assume that the sum is ‘‘saturated’’ by the lowest-energy state, the QCD vacuum

$|0\rangle$. The vacuum-saturation approximation has been used in many other contexts in particle physics, but it is usually just a simplifying assumption without any rigorous basis. In the case of heavy quarkonium, we can show that the vacuum-saturation approximation is actually a controlled approximation.

Consider the matrix element of a color-singlet operator of the form $\mathcal{O}_n = \psi^\dagger \mathcal{K}'_n \chi \chi^\dagger \mathcal{K}_n \psi$, where \mathcal{K}_n and \mathcal{K}'_n are products of a unit color matrix, a spin matrix (the unit matrix or σ^i), and a polynomial in \mathbf{D} and other fields. The vacuum-saturation approximation to the matrix element $\langle H | \mathcal{O}_n | H \rangle$ is obtained by inserting a complete set of states $|X\rangle$ between χ and χ^\dagger , and assuming that the sum is well approximated by the term involving the vacuum state $|0\rangle$:

$$\begin{aligned} \langle H | \mathcal{O}_n | H \rangle &= \sum_X \langle H | \psi^\dagger \mathcal{K}'_n \chi | X \rangle \langle X | \chi^\dagger \mathcal{K}_n \psi | H \rangle \\ &\approx \langle H | \psi^\dagger \mathcal{K}'_n \chi | 0 \rangle \langle 0 | \chi^\dagger \mathcal{K}_n \psi | H \rangle \end{aligned} \quad (3.8)$$

If the last step in (3.8) is to be a controlled approximation, we must show that the contributions from all other states, such as multigluon states, are suppressed by powers of v . One example for which this can be done is the matrix element $\langle \eta_c | \psi^\dagger \chi \chi^\dagger \psi | \eta_c \rangle$. In the vacuum-saturation approximation, the last line of (3.8) reduces to $|\langle 0 | \chi^\dagger \psi | \eta_c \rangle|^2$. This approximation would be exact if the η_c were a pure 1S_0 $Q\bar{Q}$ state. The point-like operator $\chi^\dagger \psi$ would then annihilate the η_c completely, leaving the vacuum state. However, the η_c also has Fock-state components, such as $|Q\bar{Q}g\rangle$ and $|Q\bar{Q}gg\rangle$, which include dynamical gluons. Corrections to the vacuum-saturation approximation can be attributed to contributions from intermediate states $|X\rangle$ containing such dynamical gluons. For the matrix element $\langle \eta_c | \psi^\dagger \chi \chi^\dagger \psi | \eta_c \rangle$, a single-gluon intermediate state is forbidden by color conservation, so the leading corrections to the vacuum-saturation approximation come from two-gluon intermediate states $|gg\rangle$. The leading contribution to $\langle \eta_c | \psi^\dagger \chi | gg \rangle \langle gg | \chi^\dagger \psi | \eta_c \rangle$ comes from the $|Q\bar{Q}gg\rangle$ component of the η_c , which has a probability of order v^4 . Thus, the vacuum-saturation approximation for $\langle \eta_c | \psi^\dagger \chi \chi^\dagger \psi | \eta_c \rangle$ holds up to corrections of relative order v^4 .

The vacuum-saturation approximation holds up to corrections of relative order v^4 for

any matrix element in which the operator creates and annihilates the dominant $Q\bar{Q}$ component of the quarkonium state. For the matrix elements that contribute to the decay rates of the S-wave states into light hadrons through relative order v^2 , the vacuum-saturation approximation gives

$$\langle \eta_c | \mathcal{O}_1(^1S_0) | \eta_c \rangle = \left| \langle 0 | \chi^\dagger \psi | \eta_c \rangle \right|^2 \left(1 + O(v^4) \right), \quad (3.9a)$$

$$\langle \psi | \mathcal{O}_1(^3S_1) | \psi \rangle = \left| \langle 0 | \chi^\dagger \boldsymbol{\sigma} \psi | \psi \rangle \right|^2 \left(1 + O(v^4) \right), \quad (3.9b)$$

$$\langle \eta_c | \mathcal{P}_1(^1S_0) | \eta_c \rangle = \text{Re} \left(\langle \eta_c | \psi^\dagger \chi | 0 \rangle \langle 0 | \chi^\dagger (-\frac{i}{2} \vec{\mathbf{D}})^2 \psi | \eta_c \rangle \right) \left(1 + O(v^4) \right), \quad (3.9c)$$

$$\langle \psi | \mathcal{P}_1(^3S_1) | \psi \rangle = \text{Re} \left(\langle \psi | \psi^\dagger \boldsymbol{\sigma} \chi | 0 \rangle \cdot \langle 0 | \chi^\dagger \boldsymbol{\sigma} (-\frac{i}{2} \vec{\mathbf{D}})^2 \psi | \psi \rangle \right) \left(1 + O(v^4) \right). \quad (3.9d)$$

In the case of P-wave states, the vacuum-saturation approximation can be applied to the matrix elements of the color-singlet 4-fermion operators of dimension 8:

$$\langle h_c | \mathcal{O}_1(^1P_1) | h_c \rangle = \left| \langle 0 | \chi^\dagger (-\frac{i}{2} \vec{\mathbf{D}}) \psi | h_c \rangle \right|^2 \left(1 + O(v^4) \right), \quad (3.10a)$$

$$\langle \chi_{c0} | \mathcal{O}_1(^3P_0) | \chi_{c0} \rangle = \frac{1}{3} \left| \langle 0 | \chi^\dagger (-\frac{i}{2} \vec{\mathbf{D}} \cdot \boldsymbol{\sigma}) \psi | \chi_{c0} \rangle \right|^2 \left(1 + O(v^4) \right), \quad (3.10b)$$

$$\langle \chi_{c1} | \mathcal{O}_1(^3P_1) | \chi_{c1} \rangle = \frac{1}{2} \left| \langle 0 | \chi^\dagger (-\frac{i}{2} \vec{\mathbf{D}} \times \boldsymbol{\sigma}) \psi | \chi_{c1} \rangle \right|^2 \left(1 + O(v^4) \right), \quad (3.10c)$$

$$\langle \chi_{c2} | \mathcal{O}_1(^3P_2) | \chi_{c2} \rangle = \sum_{ij} \left| \langle 0 | \chi^\dagger (-\frac{i}{2} \vec{D}^{(i} \sigma^{j)}) \psi | \chi_{c2} \rangle \right|^2 \left(1 + O(v^4) \right). \quad (3.10d)$$

The vacuum-saturation approximation cannot be applied to matrix elements of color-octet operators, such as $\langle h_c | \psi^\dagger T^a \chi \chi^\dagger T^a \psi | h_c \rangle$, because the matrix element $\langle X | \chi^\dagger T^a \psi | h_c \rangle$ vanishes if $\langle X |$ is the vacuum or any other color-singlet state.

D. Relation to Wavefunctions

In most previous work on the annihilation decays of heavy quarkonium, the nonperturbative factors in the decay rates were expressed in terms of wavefunctions, or their derivatives, evaluated at the origin. These “wavefunctions” were often identified with the Schrödinger

wavefunctions calculated in potential models for heavy quarkonium. The wavefunction factors were never given rigorous field-theoretic definitions, so the accuracy of the approximations that were involved was always vague. By expressing the decay rates in terms of matrix elements of NRQCD, we have provided a rigorous field-theoretic definition of the nonperturbative factors in the decay rates. Since heavy quarks and antiquarks are described in NRQCD by a Schrödinger field theory, the nonrelativistic wavefunctions can also be given rigorous field-theoretic definitions, and their relations to the nonperturbative factors in the decay rates can be clarified.

Nonrelativistic Coulomb-gauge wavefunctions can be defined naturally as NRQCD Bethe-Salpeter $Q\bar{Q}$ wavefunctions, evaluated at equal time. For example, the radial wavefunction $R_{\eta_c}(r)$ for the η_c can be defined as

$$R_{\eta_c}(r) \frac{1}{\sqrt{4\pi}} \equiv \frac{1}{\sqrt{2N_c}} \langle 0 | \chi^\dagger(-\mathbf{r}/2) \psi(+\mathbf{r}/2) | \eta_c \rangle \Big|_{\text{Coulomb}}. \quad (3.11)$$

The Pauli spinor fields $\psi(\mathbf{r}/2)$ and $\chi^\dagger(-\mathbf{r}/2)$ are understood to be evaluated at the same time $t = 0$. The factor $1/\sqrt{4\pi}$ on the left is the spherical harmonic $Y_{00}(\hat{\mathbf{r}})$, while the factor of $\sqrt{2N_c}$ on the left takes into account the traces of the spin wavefunction $\delta^{m+m',0}/\sqrt{2}$ and the color wavefunction $\delta^{ij}/\sqrt{N_c}$ of the $|Q\bar{Q}\rangle$ component of the η_c . In the absence of a regulator, the wave function or its derivatives may be singular as $\mathbf{r} \rightarrow 0$. We can define regularized “radial wavefunctions at the origin” $\overline{R}_{\eta_c}(\Lambda)$ for η_c and $\overline{R}_\psi(\Lambda)$ for ψ by

$$\overline{R}_{\eta_c}(\Lambda) \equiv \sqrt{\frac{2\pi}{N_c}} \langle 0 | \chi^\dagger \psi(\Lambda) | \eta_c \rangle, \quad (3.12a)$$

$$\overline{R}_\psi(\Lambda) \boldsymbol{\epsilon} \equiv \sqrt{\frac{2\pi}{N_c}} \langle 0 | \chi^\dagger \boldsymbol{\sigma} \psi(\Lambda) | \psi(\boldsymbol{\epsilon}) \rangle, \quad (3.12b)$$

where $\boldsymbol{\epsilon}$ is the polarization vector of the ψ . The local operators $\chi^\dagger \psi(\Lambda)$ and $\chi^\dagger \boldsymbol{\sigma} \psi(\Lambda)$ can be defined by dimensional regularization with scale Λ , together with minimal subtraction. They can also be defined by a lattice regulator, or any other convenient regularization scheme. As is suggested by the overline, the intuitive interpretation of $\overline{R}_{\eta_c}(\Lambda)$ and $\overline{R}_\psi(\Lambda)$ is that they are the radial wavefunctions averaged over a region of size $1/\Lambda$ centered at the origin. Note

that the regularized matrix elements in (3.12) are precisely those that enter into the decay rates for $\eta_c \rightarrow \gamma\gamma$ and $\psi \rightarrow e^+e^-$ at leading order in v .

The matrix element $\langle 0|\chi^\dagger(-\frac{i}{2}\overleftrightarrow{\mathbf{D}})^2\psi|\eta_c\rangle$ that contributes to the decay rate for $\eta_c \rightarrow \gamma\gamma$ at relative order v^2 can also be related to the Coulomb-gauge wavefunction defined in (3.11). By the velocity-scaling rules of Table I, it differs from the matrix element $\langle 0|\chi^\dagger(-\frac{i}{2}\overleftrightarrow{\nabla})^2\psi|\eta_c\rangle$ in Coulomb gauge only at relative order v^2 . With appropriate regularization, the latter matrix element can be identified with the limit as $r \rightarrow 0$ of $-\nabla^2 R(r)$, where $R(r)$ is the radial wavefunction defined in (3.11). The operator $\chi^\dagger(\frac{1}{2}\overleftrightarrow{\nabla})^2\psi$ contains a linear ultraviolet divergence proportional to $\chi^\dagger\psi(\Lambda)$, which we subtract, and a logarithmic divergence that is cut off at the scale Λ . This subtraction and cutoff define a renormalized laplacian of the radial wavefunction at the origin, which we denote by $\overline{\nabla^2 R_{\eta_c}}$:

$$\overline{\nabla^2 R_{\eta_c}}(\Lambda) \equiv \sqrt{\frac{2\pi}{N_c}} \left. \langle 0|\chi^\dagger(\frac{1}{2}\overleftrightarrow{\nabla})^2\psi(\Lambda)|\eta_c\rangle \right|_{\text{Coulomb}}. \quad (3.13)$$

The analogous quantity $\overline{\nabla^2 R_\psi}$ for the ψ can be defined in a similar way. The corresponding gauge-invariant matrix elements differ from $\overline{\nabla^2 R_{\eta_c}}$ and $\overline{\nabla^2 R_\psi}$ only at relative order v^2 :

$$\langle 0|\chi^\dagger(-\frac{i}{2}\overleftrightarrow{\mathbf{D}})^2\psi(\Lambda)|\eta_c\rangle = -\sqrt{\frac{N_c}{2\pi}} \overline{\nabla^2 R_{\eta_c}}(\Lambda) \left(1 + O(v^2) \right). \quad (3.14a)$$

$$\boldsymbol{\epsilon}^* \cdot \langle 0|\chi^\dagger\boldsymbol{\sigma}(-\frac{i}{2}\overleftrightarrow{\mathbf{D}})^2\psi(\Lambda)|\psi(\boldsymbol{\epsilon})\rangle = -\sqrt{\frac{N_c}{2\pi}} \overline{\nabla^2 R_\psi}(\Lambda) \left(1 + O(v^2) \right). \quad (3.14b)$$

The intuitive interpretations of $\overline{\nabla^2 R_{\eta_c}}(\Lambda)$ and $\overline{\nabla^2 R_\psi}(\Lambda)$ are somewhat obscured by the subtractions needed to define the renormalized matrix elements.

Heavy-quark spin symmetry implies that the wavefunctions of the η_c and ψ are identical up to corrections of relative order v^2 :

$$R_\psi(r) = R_{\eta_c}(r) \left(1 + O(v^2) \right). \quad (3.15)$$

It is convenient to introduce an average radial wavefunction $R_S(r)$ for the $1S$ states η_c and ψ , which can be used when the differences of relative order v^2 can be neglected:

$$R_S(r) \equiv \frac{R_{\eta_c}(r) + 3R_\psi(r)}{4}. \quad (3.16)$$

Because of the heavy-quark spin symmetry, the regularized quantities $\overline{R_{\eta_c}}(\Lambda)$ and $\overline{R_\psi}(\Lambda)$ differ only at relative order v^2 , as do the renormalized quantities $\overline{\nabla^2 R_{\eta_c}}(\Lambda)$ and $\overline{\nabla^2 R_\psi}(\Lambda)$. Weighted averages $\overline{R_S}(\Lambda)$ and $\overline{\nabla^2 R_S}(\Lambda)$ for the S-wave states can be defined as in (3.16). The S-wave radial wavefunction that is computed in nonrelativistic potential models can be interpreted as a phenomenological estimate of the wavefunction (3.16). Thus, the value $R_S(r=0)$ that is obtained from potential models can be used as an estimate of the regularized quantity $\overline{R_S}(\Lambda)$ at a scale Λ of order Mv . The relation between $\overline{\nabla^2 R_S}(\Lambda)$ and $\nabla^2 R_S(r=0)$ in potential models is more obscure, because of the subtraction that is required to define the renormalized matrix element in (3.13), and because $\nabla^2 R_S(r)$ diverges linearly as $r \rightarrow 0$ if the potential is Coulombic at short distances.

Nonrelativistic wavefunctions for the P-wave states can be defined through matrix elements in Coulomb gauge that are analogous to (3.11). For example, the radial wavefunction $R_{h_c}(r)$ for the h_c can be defined as

$$R_{h_c}(r) \left(\sqrt{\frac{3}{4\pi}} \hat{\mathbf{r}} \cdot \boldsymbol{\epsilon} \right) \equiv \frac{1}{\sqrt{2N_c}} \langle 0 | \chi^\dagger(-\mathbf{r}/2) \psi(+\mathbf{r}/2) | h_c(\boldsymbol{\epsilon}) \rangle \Big|_{\text{Coulomb}}, \quad (3.17)$$

where the polarization vector satisfies $\boldsymbol{\epsilon} \cdot \boldsymbol{\epsilon}^* = 1$. A regularized derivative of the radial wavefunction at the origin $\overline{R'_{h_c}}(\Lambda)$ can be defined by

$$\overline{R'_{h_c}}(\Lambda) \boldsymbol{\epsilon} \equiv \sqrt{\frac{2\pi}{3N_c}} \langle 0 | \chi^\dagger(\frac{1}{2} \overleftrightarrow{\nabla}) \psi(\Lambda) | h_c(\boldsymbol{\epsilon}) \rangle \Big|_{\text{Coulomb}}. \quad (3.18)$$

Analogous quantities $\overline{R'_{\chi_{cJ}}}(\Lambda)$ can be defined for the χ_{cJ} states. Since no subtractions are required in order to define the operator on the right side of (3.18), the quantity $\overline{R'_{h_c}}(\Lambda)$ has a straightforward intuitive interpretation as the derivative of the radial wavefunction averaged over a region of size $1/\Lambda$ centered at the origin. In the gauge-invariant analog of the matrix element (3.18), the derivative $\overleftrightarrow{\nabla}$ is replaced by the covariant derivative $\overleftrightarrow{\mathbf{D}}$. From the velocity-scaling rules of Table I, we see that these matrix elements differ only at relative order v^2 :

$$\langle 0 | \chi^\dagger(\frac{1}{2} \overleftrightarrow{\mathbf{D}}) \psi(\Lambda) | h_c(\boldsymbol{\epsilon}) \rangle = \sqrt{\frac{3N_c}{2\pi}} \overline{R'_{h_c}}(\Lambda) \boldsymbol{\epsilon} \left(1 + O(v^2) \right), \quad (3.19a)$$

$$\frac{1}{\sqrt{3}} \langle 0 | \chi^\dagger (\frac{1}{2} \vec{D} \cdot \boldsymbol{\sigma}) \psi(\Lambda) | \chi_{c0} \rangle = \sqrt{\frac{3N_c}{2\pi}} \overline{R'_{\chi_{c0}}}(\Lambda) \left(1 + O(v^2) \right), \quad (3.19b)$$

$$\frac{1}{\sqrt{2}} \langle 0 | \chi^\dagger (-\frac{i}{2} \vec{D} \times \boldsymbol{\sigma}) \psi(\Lambda) | \chi_{c1}(\epsilon) \rangle = \sqrt{\frac{3N_c}{2\pi}} \overline{R'_{\chi_{c1}}}(\Lambda) \epsilon \left(1 + O(v^2) \right), \quad (3.19c)$$

$$\langle 0 | \chi^\dagger (\frac{1}{2} \vec{D}^{(i} \sigma^{j)}) \psi(\Lambda) | \chi_{c2}(\epsilon) \rangle = \sqrt{\frac{3N_c}{2\pi}} \overline{R'_{\chi_{c2}}}(\Lambda) \epsilon^{ij} \left(1 + O(v^2) \right). \quad (3.19d)$$

By heavy-quark spin symmetry, $\overline{R'_{h_c}}(\Lambda)$ differs from $\overline{R'_{\chi_{cJ}}}(\Lambda)$, $J = 0, 1, 2$, only at relative order v^2 . For applications in which v^2 corrections can be neglected, these wavefunctions can all be replaced by the average over the 16 P-wave spin states, which we denote by $\overline{R'_P}(\Lambda)$. The value $R'_P(0)$ for the derivative of the radial wavefunction at the origin that is obtained from nonrelativistic potential models can be interpreted as a phenomenological estimate of the regularized quantity $\overline{R'_P}(\Lambda)$ at a scale Λ of order Mv .

The vacuum-saturation approximation discussed in Section III C allows the matrix elements of some 4-fermion operators to be expressed in terms of the regularized and renormalized wavefunction parameters defined above. Combining (3.9) with (3.12) and (3.14), we obtain the following expressions for the matrix elements that contribute to the decays of the η_c and the ψ into light hadrons:

$$\langle \eta_c | \mathcal{O}_1(^1S_0) | \eta_c \rangle = \frac{N_c}{2\pi} |\overline{R_{\eta_c}}|^2 \left(1 + O(v^4) \right). \quad (3.20a)$$

$$\langle \psi | \mathcal{O}_1(^3S_1) | \psi \rangle = \frac{N_c}{2\pi} |\overline{R_\psi}|^2 \left(1 + O(v^4) \right) \quad (3.20b)$$

$$\langle \eta_c | \mathcal{P}_1(^1S_0) | \eta_c \rangle = -\frac{N_c}{2\pi} \text{Re}(\overline{R_S}^* \overline{\nabla^2 R_S}) \left(1 + O(v^2) \right), \quad (3.20c)$$

$$\langle \psi | \mathcal{P}_1(^3S_1) | \psi \rangle = -\frac{N_c}{2\pi} \text{Re}(\overline{R_S}^* \overline{\nabla^2 R_S}) \left(1 + O(v^2) \right). \quad (3.20d)$$

In (3.20c) and (3.20d), we have used heavy-quark spin symmetry to replace $\overline{R_{\eta_c}}$ and $\overline{R_\psi}$ by their weighted average $\overline{R_S}$ and to replace $\overline{\nabla^2 R_{\eta_c}}$ and $\overline{\nabla^2 R_\psi}$ by $\overline{\nabla^2 R_S}$ without any loss of accuracy. If we were to make the same replacement in (3.20a) and (3.20b), the relative accuracy would be decreased to v^2 . For the decays of the P-wave states into light hadrons at leading order in v , the vacuum-saturation approximation together with heavy-quark spin symmetry can be used to express all the color-singlet matrix elements in terms of the average

regularized quantity $\overline{R'_P}$. Combining (3.10) with (3.19), we obtain the approximations

$$\langle h_c | \mathcal{O}_1(^1P_1) | h_c \rangle = \frac{3N_c}{2\pi} |\overline{R'_P}|^2 \left(1 + O(v^2) \right), \quad (3.21a)$$

$$\langle \chi_{cJ} | \mathcal{O}_1(^3P_J) | \chi_{cJ} \rangle = \frac{3N_c}{2\pi} |\overline{R'_P}|^2 \left(1 + O(v^2) \right), \quad J = 0, 1, 2. \quad (3.21b)$$

E. Factorization-Scale Dependence

The matrix elements $\langle H | \mathcal{O}_n | H \rangle$ that appear in the factorization formula (2.14) are ultraviolet finite only if the 4-fermion operators \mathcal{O}_n are properly regularized. The regularization introduces dependence on the ultraviolet cutoff Λ of NRQCD, and this cutoff-dependence must be understood in order to make quantitative predictions. We assume that the operator \mathcal{O}_n is normal-ordered: $\langle 0 | \mathcal{O}_n | 0 \rangle = 0$. This guarantees that in the matrix element $\langle H | \mathcal{O}_n | H \rangle$, the operator \mathcal{O}_n annihilates the heavy quark and antiquark in the initial quarkonium state $|H\rangle$. In addition to normal-ordering, regularization is needed to control power and logarithmic divergences. If a cutoff Λ is imposed on loop momenta, there are power divergences in $\langle H | \mathcal{O}_n | H \rangle$ that are proportional to Λ^p , where $p = 1, 2, \dots$. If the operator \mathcal{O}_n has dimension d_n , then the coefficient of Λ^p is, by dimensional analysis, the sum of matrix elements of 4-fermion operators of dimension $d_n - p$ or larger. If the dimension is larger than $d_n - p$, the extra dimensions are balanced by powers of $1/M$. Similarly the coefficients of logarithmic divergences are proportional to matrix elements of 4-fermion operators of dimension d_n or larger.

The power and logarithmic divergences associated with loop corrections to NRQCD operators can be regularized by a variety of means. A convenient regularization scheme for analytic calculations is dimensional regularization with minimal subtraction. The scale associated with the dimensional regularization then plays the role of the NRQCD cutoff Λ . An advantage in using a mass-independent regulator, such as dimensional regularization, is that power divergences are automatically discarded. In other approaches, such as lattice regularization, the regularized operator may contain divergences that are proportional to

powers of Λ . These power divergences are simply artifacts of the regularization scheme and have no physical content. Since physical quantities are renormalization-group invariants, they have no dependence on Λ . Hence, any power divergences in NRQCD operator matrix elements must ultimately be cancelled by power divergences in operator coefficients.

Once one has removed the power divergences, either by employing a mass-independent regularization scheme or by making explicit subtractions, the 4-fermion operators satisfy simple evolution equations of the form

$$\Lambda \frac{d}{d\Lambda} \mathcal{O}_n(\Lambda) = \sum_k \frac{\gamma_{nk}(\Lambda)}{M^{d_k-d_n}} \mathcal{O}_k(\Lambda), \quad (3.22)$$

where the sum ranges over all 4-fermion operators $\mathcal{O}_k(\Lambda)$ with dimensions $d_k \geq d_n$. The anomalous-dimension coefficients $\gamma_{nk}(\Lambda)$ are computable as power series in the running coupling constant $\alpha_s(\Lambda)$. For $d_n = d_k$, the coefficients γ_{nk} are of order α_s^2 , because logarithmic ultraviolet divergences in one-loop diagrams in NRQCD arise only from transverse gluons, whose coupling to the heavy quark lines brings in a factor of v . The coefficients γ_{nk} for $d_n = 6$ and $d_k = 8$ are computed to order α_s in Appendix B.

By taking the matrix elements of (3.22) between heavy quarkonium states $|H\rangle$, we obtain the evolution equations for the matrix elements $\langle H | \mathcal{O}_n(\Lambda) | H \rangle$ that appear in the general factorization formula (2.14):

$$\Lambda \frac{d}{d\Lambda} \langle H | \mathcal{O}_n(\Lambda) | H \rangle = \sum_k \frac{\gamma_{nk}(\Lambda)}{M^{d_k-d_n}} \langle H | \mathcal{O}_k(\Lambda) | H \rangle. \quad (3.23)$$

The leading v behavior of the matrix elements can be determined by using the velocity-scaling rules developed in the previous sections. At any given order in v , there is only a finite number of terms that contribute to the evolution equation (3.23). The evolution equations for the dimension-6 4-fermion operators are calculated to order α_s in Appendix B. The operator evolution equations for $\mathcal{O}_1(^1S_0)$ and $\mathcal{O}_1(^3S_1)$ are given in (B16) and (B19a). Taking the matrix elements of these equations and keeping only those terms on the right sides that are of relative order v^2 , we find that only the operators \mathcal{P}_1 survive, and we obtain

$$\Lambda \frac{d}{d\Lambda} \langle \eta_c | \mathcal{O}_1(^1S_0) | \eta_c \rangle = -\frac{8C_F\alpha_s(\Lambda)}{3\pi M^2} \langle \eta_c | \mathcal{P}_1(^1S_0) | \eta_c \rangle, \quad (3.24a)$$

$$\Lambda \frac{d}{d\Lambda} \langle \psi | \mathcal{O}_1(^3S_1) | \psi \rangle = -\frac{8C_F\alpha_s(\Lambda)}{3\pi M^2} \langle \psi | \mathcal{P}_1(^3S_1) | \psi \rangle, \quad (3.24b)$$

where $C_F = (N_c^2 - 1)/(2N_c)$. If the evolution equations are truncated at leading order in v , the right sides of (3.24a) and (3.24b) vanish and we find that the matrix elements $\langle \eta_c | \mathcal{O}_1(^1S_0) | \eta_c \rangle$ and $\langle \psi | \mathcal{O}_1(^3S_1) | \psi \rangle$ are renormalization-scale invariant through order α_s . The dimension-8 matrix elements $\langle \eta_c | \mathcal{P}_1(^1S_0) | \eta_c \rangle$ and $\langle \psi | \mathcal{P}_1(^3S_1) | \psi \rangle$ are also renormalization-scale invariant through order α_s and at leading order in v :

$$\Lambda \frac{d}{d\Lambda} \langle \eta_c | \mathcal{P}_1(^1S_0) | \eta_c \rangle = 0, \quad (3.25a)$$

$$\Lambda \frac{d}{d\Lambda} \langle \psi | \mathcal{P}_1(^3S_1) | \psi \rangle = 0. \quad (3.25b)$$

Truncated at order α_s , the evolution equations can be solved analytically for the Λ -dependence of the matrix elements. For example, the solution to (3.24a) is

$$\langle \eta_c | \mathcal{O}_1(^1S_0; \Lambda) | \eta_c \rangle = \langle \eta_c | \mathcal{O}_1(^1S_0; \Lambda_0) | \eta_c \rangle - \frac{8C_F}{3\beta_0 M^2} \log \left(\frac{\alpha_s(\Lambda_0)}{\alpha_s(\Lambda)} \right) \langle \eta_c | \mathcal{P}_1(^1S_0) | \eta_c \rangle, \quad (3.26)$$

where $\beta_0 = (11N_c - 2n_f)/6$ is the first coefficient in the beta function for QCD with n_f flavors of light quarks: $\mu(d/d\mu)\alpha_s = -\beta_0\alpha_s^2/\pi + \dots$

We next consider the evolution of the matrix elements that contribute to P-wave annihilation at leading order in v . The color-singlet dimension-8 matrix elements are renormalization-scale-invariant to this order in α_s :

$$\Lambda \frac{d}{d\Lambda} \langle h_c | \mathcal{O}_1(^1P_1) | h_c \rangle = 0, \quad (3.27a)$$

$$\Lambda \frac{d}{d\Lambda} \langle \chi_{cJ} | \mathcal{O}_1(^3P_J) | \chi_{cJ} \rangle = 0, \quad J = 0, 1, 2. \quad (3.27b)$$

Taking the matrix elements of (B17) and (B19b) in Appendix B, we find that the color-octet dimension-6 matrix elements have nontrivial scaling behavior at order α_s :

$$\Lambda \frac{d}{d\Lambda} \langle h_c | \mathcal{O}_8(^1S_0) | h_c \rangle = \frac{4C_F\alpha_s(\Lambda)}{3N_c\pi M^2} \langle h_c | \mathcal{O}_1(^1P_1) | h_c \rangle, \quad (3.28a)$$

$$\Lambda \frac{d}{d\Lambda} \langle \chi_{cJ} | \mathcal{O}_8(^3S_1) | \chi_{cJ} \rangle = \frac{4C_F\alpha_s(\Lambda)}{3N_c\pi M^2} \langle \chi_{cJ} | \mathcal{O}_1(^3P_J) | \chi_{cJ} \rangle. \quad (3.28b)$$

To this order in α_s , we find that the evolution equations can be solved analytically. For example, the solution to (3.28a) is

$$\langle h_c | \mathcal{O}_8(^1S_0; \Lambda) | h_c \rangle = \langle h_c | \mathcal{O}_8(^1S_0; \Lambda_0) | h_c \rangle + \frac{4C_F}{3N_c\beta_0 M^2} \log\left(\frac{\alpha_s(\Lambda_0)}{\alpha_s(\Lambda)}\right) \langle h_c | \mathcal{O}_1(^1P_1) | h_c \rangle. \quad (3.29)$$

The solution (3.29) to the evolution equation can be used to provide a crude estimate of the color-octet matrix element $\langle h_c | \mathcal{O}_8(^1S_0; \Lambda) | h_c \rangle$ in terms of the color-singlet matrix element $\langle h_c | \mathcal{O}_1(^1P_1) | h_c \rangle$. Suppose that we approximate (3.29) by the evolution term on the right side. The evolution term is largest, relative to the matrix element $\langle h_c | \mathcal{O}_8(^1S_0; \Lambda_0) | h_c \rangle$, when the scales Λ_0 and Λ are as widely separated as possible. However, the logarithmic evolution holds only down to scales of order Mv . Thus, we choose $\Lambda_0 = Mv$. Then, setting $\Lambda = M$, neglecting the initial matrix element in (3.29), and assuming that $\alpha_s(\Lambda_0) = \alpha_s(Mv) \sim v$, we find that (3.29) reduces to

$$\langle h_c | \mathcal{O}_8(^1S_0; M) | h_c \rangle \approx \frac{4C_F}{3N_c\beta_0 M^2} \log\left(\frac{v}{\alpha_s(M)}\right) \langle h_c | \mathcal{O}_1(^1P_1) | h_c \rangle. \quad (3.30)$$

The same method can be used to obtain crude estimates for the corresponding matrix elements for the χ_{cJ} states:

$$\langle \chi_{cJ} | \mathcal{O}_8(^3S_1; M) | \chi_{cJ} \rangle \approx \frac{4C_F}{3N_c\beta_0 M^2} \log\left(\frac{v}{\alpha_s(M)}\right) \langle \chi_{cJ} | \mathcal{O}_1(^3P_J) | \chi_{cJ} \rangle. \quad (3.31)$$

The terms that we have retained in obtaining these estimates are enhanced by one power of $\log[v/\alpha_s(M)]$ relative to the terms that we have neglected. Since this is not a large enhancement factor, particularly in the case of charmonium, these estimates should be regarded as giving only the orders of magnitude of the matrix elements.

IV. ANNIHILATION DECAYS OF HEAVY QUARKONIUM

In Section III, we derived a factorization formula (2.14) for the decay rates of heavy quarkonium states into light hadrons. In this section, we apply this formula to the decays of S-wave states, up to corrections of relative order v^3 , and to the decays of P-wave states, up to corrections of relative order v^2 . We also treat the decays into the electromagnetic final states by using the analogous formula (2.17). As in Section III, we use the lowest-lying S-wave and P-wave states of charmonium for the purpose of illustration.

A. S-wave Annihilation

Most previous treatments of the annihilation rates of the S-wave states of heavy quarkonium have been restricted to leading order in v . In these analyses, long-distance effects were absorbed into a nonperturbative factor $|R_S(0)|^2$, where $R_S(0)$ is the radial wavefunction at the origin. We improve on these previous treatments by providing a rigorous definition of the nonperturbative factor in terms of matrix elements of NRQCD. We also extend the analysis of the decay rates to relative order v^2 , and show that 3 independent nonperturbative factors are sufficient to calculate all the S-wave annihilation rates through this order.

We first consider the decays of the $J^{PC} = 0^{-+}$ state η_c and the 1^{--} state ψ into light hadrons. As was shown in Section III A, there are only two operators that contribute to each of these decay rates through relative order v^2 . According to (2.14), the decay rates into light hadrons are therefore

$$\begin{aligned} \Gamma(\eta_c \rightarrow \text{LH}) = & \frac{2 \operatorname{Im} f_1(^1S_0)}{M^2} \langle \eta_c | \mathcal{O}_1(^1S_0) | \eta_c \rangle + \frac{2 \operatorname{Im} g_1(^1S_0)}{M^4} \langle \eta_c | \mathcal{P}_1(^1S_0) | \eta_c \rangle \\ & + O(v^3\Gamma), \end{aligned} \quad (4.1a)$$

$$\begin{aligned} \Gamma(\psi \rightarrow \text{LH}) = & \frac{2 \operatorname{Im} f_1(^3S_1)}{M^2} \langle \psi | \mathcal{O}_1(^3S_1) | \psi \rangle + \frac{2 \operatorname{Im} g_1(^3S_1)}{M^4} \langle \psi | \mathcal{P}_1(^3S_1) | \psi \rangle \\ & + O(v^3\Gamma). \end{aligned} \quad (4.1b)$$

The imaginary parts of the coefficients in (4.1) are calculated at order α_s^2 in Appendix A 2, and $\operatorname{Im} f_1(^1S_0)$ and $\operatorname{Im} f_1(^3S_1)$ are given through next-to-leading order in α_s in Appendix A 3.

According to the factorization formula (2.17) for electromagnetic annihilation, the decay rates for $\eta_c \rightarrow \gamma\gamma$ and $\psi \rightarrow e^+e^-$ are

$$\begin{aligned} \Gamma(\eta_c \rightarrow \gamma\gamma) &= \frac{2 \operatorname{Im} f_{\gamma\gamma}(^1S_0)}{M^2} \left| \langle 0 | \chi^\dagger \psi | \eta_c \rangle \right|^2 \\ &+ \frac{2 \operatorname{Im} g_{\gamma\gamma}(^1S_0)}{M^4} \operatorname{Re} \left(\langle \eta_c | \psi^\dagger \chi | 0 \rangle \langle 0 | \chi^\dagger (-\frac{i}{2} \vec{\mathbf{D}})^2 \psi | \eta_c \rangle \right) + O(v^4\Gamma), \end{aligned} \quad (4.2a)$$

$$\begin{aligned} \Gamma(\psi \rightarrow e^+e^-) &= \frac{2 \operatorname{Im} f_{ee}(^3S_1)}{M^2} \left| \langle 0 | \chi^\dagger \boldsymbol{\sigma} \psi | \psi \rangle \right|^2 \\ &+ \frac{2 \operatorname{Im} g_{ee}(^3S_1)}{M^4} \operatorname{Re} \left(\langle \psi | \psi^\dagger \boldsymbol{\sigma} \chi | 0 \rangle \cdot \langle 0 | \chi^\dagger \boldsymbol{\sigma} (-\frac{i}{2} \vec{\mathbf{D}})^2 \psi | \psi \rangle \right) + O(v^4\Gamma). \end{aligned} \quad (4.2b)$$

The decay rate for $\psi \rightarrow \gamma\gamma\gamma$ is given by an expression that is identical to (4.2b), but with coefficients $f_{3\gamma}(^3S_1)$ and $g_{3\gamma}(^3S_1)$. The imaginary parts of the coefficients in (4.2) are calculated at order α^2 in Appendix A 4, and order- α_s corrections are given for $\operatorname{Im} f_{\gamma\gamma}(^1S_0)$, $\operatorname{Im} f_{ee}(^3S_1)$, and $\operatorname{Im} f_{3\gamma}(^3S_1)$. The matrix elements in (4.1) and (4.2) can be computed using lattice simulations of NRQCD. Since matrix elements of relative order v^3 have been omitted, there is nothing to be gained by computing the dimension-6 matrix elements to an accuracy of better than v^2 . Similarly, the dimension-8 matrix elements need be computed only at leading order in v .

At the level of accuracy in (4.1) and (4.2), the matrix elements are not all independent. The vacuum-saturation approximation (3.9) can be used to express the 4-fermion matrix elements in (4.1) in terms of the vacuum-to-quarkonium matrix elements in (4.2). Furthermore, the heavy-quark spin-symmetry relation (3.6) can be used to equate the matrix elements in the second terms on the right sides of (4.2a) and (4.2b). The net result is that the 8 matrix elements in (4.1) and (4.2) can be reduced to 3 independent nonperturbative quantities, which we can take to be $|\overline{R_{\eta_c}}|^2$, $|\overline{R_\psi}|^2$, and $\operatorname{Re}(\overline{R_S^*} \overline{\nabla^2 R_S})$. The resulting expressions for the decay rates are

$$\Gamma(\eta_c \rightarrow \text{LH}) = \frac{N_c \operatorname{Im} f_1(^1S_0)}{\pi M^2} |\overline{R_{\eta_c}}|^2 - \frac{N_c \operatorname{Im} g_1(^1S_0)}{\pi M^4} \operatorname{Re}(\overline{R_S^*} \overline{\nabla^2 R_S}) + O(v^3\Gamma), \quad (4.3a)$$

$$\Gamma(\psi \rightarrow \text{LH}) = \frac{N_c \operatorname{Im} f_1(^3S_1)}{\pi M^2} |\overline{R_\psi}|^2 - \frac{N_c \operatorname{Im} g_1(^3S_1)}{\pi M^4} \operatorname{Re}(\overline{R_S^*} \overline{\nabla^2 R_S}) + O(v^3\Gamma), \quad (4.3b)$$

$$\Gamma(\eta_c \rightarrow \gamma\gamma) = \frac{N_c \operatorname{Im} f_{\gamma\gamma}(^1S_0)}{\pi M^2} |\overline{R_{\eta_c}}|^2 - \frac{N_c \operatorname{Im} g_{\gamma\gamma}(^1S_0)}{\pi M^4} \operatorname{Re}(\overline{R_S^*} \overline{\nabla^2 R_S}) + O(v^4\Gamma), \quad (4.3c)$$

$$\Gamma(\psi \rightarrow e^+e^-) = \frac{N_c \text{Im} f_{ee}(^3S_1)}{\pi M^2} |\overline{R_\psi}|^2 - \frac{N_c \text{Im} g_{ee}(^3S_1)}{\pi M^4} \text{Re}(\overline{R_S^*} \overline{\nabla^2 R_S}) + O(v^4\Gamma). \quad (4.3d)$$

The quantities $\overline{R_{\eta_c}}$, $\overline{R_\psi}$, and $\overline{\nabla^2 R_S}$ are defined in Section IIID in terms of vacuum-to-quarkonium matrix elements in NRQCD, and can, therefore, be calculated using nonperturbative methods, such as lattice simulations. They can also be estimated using the wavefunctions that are obtained from nonrelativistic potential models of quarkonium. Alternatively, since there are more decay rates than there are parameters, they can be treated as purely phenomenological parameters, to be determined by experiment.

The approximations to the matrix elements that have been made in (4.3) imply restrictions on the order in $\alpha_s(M)$ to which the coefficients can be included meaningfully. Because of the identification of v with $\alpha_s(Mv)$ in (2.1), we should consider v to be less than or of order $\alpha_s(M)$. There is no point in calculating the coefficients to relative order α_s^n unless we have included all operators whose matrix elements are of relative order v^n or less. Hence, there is no gain in accuracy if the coefficients of $|\overline{R_{\eta_c}}|^2$ and $|\overline{R_\psi}|^2$ are calculated beyond relative order α_s^3 , or if the coefficients of $\text{Re}(\overline{R_S^*} \overline{\nabla^2 R_S})$ are calculated beyond relative order α_s .

If we require accuracy only to leading order in v , then the decay rates in (4.3) can be simplified further. The difference between $\overline{R_{\eta_c}}$ and $\overline{R_\psi}$ is of relative order v^2 , so both can be replaced by their weighted average $\overline{R_S}$. The factor $\text{Re}(\overline{R_S^*} \overline{\nabla^2 R_S})$ is of order v^2 relative to $|\overline{R_S}|^2$ and can therefore be set to 0. We thereby recover the familiar factorization formulas assumed in previous work:

$$\Gamma(\eta_c \rightarrow \text{LH}) = \frac{N_c \text{Im} f_1(^1S_0)}{\pi M^2} |\overline{R_S}|^2 + O(v^2\Gamma), \quad (4.4a)$$

$$\Gamma(\psi \rightarrow \text{LH}) = \frac{N_c \text{Im} f_1(^3S_1)}{\pi M^2} |\overline{R_S}|^2 + O(v^2\Gamma), \quad (4.4b)$$

$$\Gamma(\eta_c \rightarrow \gamma\gamma) = \frac{N_c \text{Im} f_{\gamma\gamma}(^1S_0)}{\pi M^2} |\overline{R_S}|^2 + O(v^2\Gamma), \quad (4.4c)$$

$$\Gamma(\psi \rightarrow e^+e^-) = \frac{N_c \text{Im} f_{ee}(^3S_1)}{\pi M^2} |\overline{R_S}|^2 + O(v^2\Gamma). \quad (4.4d)$$

Because corrections of relative order v^2 have been neglected in (4.4), there is no point in calculating the regularized wavefunction at the origin $\overline{R_S}$ to an accuracy of relative order v^2 .

Similarly, because of the identification of v with $\alpha_s(Mv)$, there is no increase in accuracy if the coefficients of $|\overline{R_S}|^2$ in (4.4) are calculated beyond next-to-leading order in α_s . The effects of matrix elements of relative order v^2 are probably more important than perturbative corrections to the coefficients that are of relative order α_s^2 .

B. P-wave Annihilation

In most previous work on the annihilation decays of P-wave states, it was assumed that long-distance effects could be factored into a single nonperturbative quantity $|R'_P(0)|^2$, where $R'_P(0)$ is the derivative of the radial wavefunction at the origin. By explicit calculation, Barbieri *et al.* [7,8] found that the coefficients of $|R'_P(0)|^2$ depend logarithmically on an infrared cutoff on the energies of the final-state gluons. In subsequent phenomenological applications of these calculations, the infrared cutoff has been identified with the binding energy of the quarkonium state, which is of order Mv^2 , the inverse of the radius of the bound state, which is of order Mv , or the inverse of the confinement radius, which is of order Λ_{QCD} . It should be clear, however, that the infrared divergence is a signal of the breakdown of the factorization assumption upon which the calculation is based. The solution to the problem of infrared divergences in the calculation of the P-wave decay rates into light hadrons was first presented in Ref. [10]. We will review the resolution of this problem later in this subsection.

As was shown in Section III A, there are two 4-fermion operators that contribute to the decay rates of any of the P-wave states into light hadrons at leading order in v . According to our factorization formula (2.14), the decay rates of the four P-wave states into light hadrons are

$$\begin{aligned} \Gamma(h_c \rightarrow \text{LH}) &= \frac{2 \operatorname{Im} f_1(^1P_1)}{M^4} \langle h_c | \mathcal{O}_1(^1P_1) | h_c \rangle \\ &\quad + \frac{2 \operatorname{Im} f_8(^1S_0)}{M^2} \langle h_c | \mathcal{O}_8(^1S_0) | h_c \rangle + O(v^2\Gamma), \end{aligned} \quad (4.5a)$$

$$\begin{aligned} \Gamma(\chi_{cJ} \rightarrow \text{LH}) &= \frac{2 \operatorname{Im} f_1(^3P_J)}{M^4} \langle \chi_{cJ} | \mathcal{O}_1(^3P_J) | \chi_{cJ} \rangle \\ &\quad + \frac{2 \operatorname{Im} f_8(^3S_1)}{M^2} \langle \chi_{cJ} | \mathcal{O}_8(^3S_1) | \chi_{cJ} \rangle + O(v^2\Gamma), \quad J = 0, 1, 2. \end{aligned} \quad (4.5b)$$

The imaginary parts of the coefficients $f_1(^3P_0)$, $f_1(^3P_2)$, $f_8(^1S_0)$, and $f_8(^3S_1)$ are calculated in order α_s^2 in Appendix A 2. The color-octet matrix elements in the factorization formulas (4.5) represent contributions to the annihilation rates from the Fock states $|Q\bar{Q}g\rangle$. Thus, we see that the decays of P-wave (and higher orbital-angular-momentum states) can probe components of the meson wavefunction that involve dynamical gluons. For the decays of the χ_{c0} and χ_{c2} into two photons, there is only one operator that contributes at leading order in v :

$$\Gamma(\chi_{c0} \rightarrow \gamma\gamma) = \frac{2 \operatorname{Im} f_{\gamma\gamma}(^3P_0)}{M^4} \frac{1}{3} \left| \langle 0 | \chi^\dagger (-\frac{i}{2} \vec{D} \cdot \boldsymbol{\sigma}) \psi | \chi_{c0} \rangle \right|^2 + O(v^2\Gamma), \quad (4.6a)$$

$$\Gamma(\chi_{c2} \rightarrow \gamma\gamma) = \frac{2 \operatorname{Im} f_{\gamma\gamma}(^3P_2)}{M^4} \sum_{ij} \left| \langle 0 | \chi^\dagger (-\frac{i}{2} \vec{D}^{(i} \sigma^{j)}) \psi | \chi_{c2} \rangle \right|^2 + O(v^2\Gamma). \quad (4.6b)$$

The coefficients $\operatorname{Im} f_{\gamma\gamma}(^3P_0)$ and $\operatorname{Im} f_{\gamma\gamma}(^3P_2)$ are calculated at order α^2 in Appendix A 4, and the order- α_s corrections are given as well. There is no increase in accuracy if the matrix elements in (4.5) and (4.6) are calculated to an accuracy of relative order v^2 , since matrix elements of relative order v^2 have been omitted. Because of the identification (2.1) of v with $\alpha_s(Mv)$, there is no increase in accuracy if the coefficients in (4.5) and (4.6) are calculated beyond next-to-leading order in $\alpha_s(M)$. Perturbative corrections of relative order $\alpha_s^2(M)$ are probably less important than contributions of other matrix elements of relative order v^2 .

To the order in v that is being considered in (4.5) and (4.6), the matrix elements are not all independent. The vacuum-saturation approximation (3.10) can be used to express the matrix elements of $\mathcal{O}_1(^1P_1)$ and $\mathcal{O}_1(^3P_J)$ in (4.5) in terms of vacuum-to-quarkonium matrix elements. These matrix elements can be related to regularized derivatives of radial wavefunctions at the origin by using (3.19). Because of the heavy-quark spin symmetry, the derivatives of the radial wavefunctions at the origin can all be replaced by the average value $\overline{R'_P}$ for the 12 spin states of the P-wave system, without any loss of accuracy. The heavy-quark spin-symmetry relation (3.5b) also implies that the matrix elements of $\mathcal{O}_8(^1S_0)$ and $\mathcal{O}_8(^3S_1)$ in (4.5) are the same, up to corrections of relative order v^2 . Thus, the decay rates (4.5) and (4.6) can all be expressed in terms of two nonperturbative quantities $|\overline{R'_P}|^2$ and $\langle h_c | \mathcal{O}_8(^1S_0) | h_c \rangle$ (or, alternatively, the average of the color-octet matrix elements for the

12 P-wave spin states):

$$\Gamma(h_c \rightarrow \text{LH}) = \frac{3N_c \text{Im} f_1(^1P_1)}{\pi M^4} |\overline{R'_P}|^2 + \frac{2 \text{Im} f_8(^1S_0)}{M^2} \langle h_c | \mathcal{O}_8(^1S_0) | h_c \rangle + O(v^2\Gamma), \quad (4.7a)$$

$$\begin{aligned} \Gamma(\chi_{cJ} \rightarrow \text{LH}) &= \frac{3N_c \text{Im} f_1(^3P_J)}{\pi M^4} |\overline{R'_P}|^2 + \frac{2 \text{Im} f_8(^3S_1)}{M^2} \langle h_c | \mathcal{O}_8(^1S_0) | h_c \rangle \\ &\quad + O(v^2\Gamma), \quad J = 0, 1, 2, \end{aligned} \quad (4.7b)$$

$$\Gamma(\chi_{cJ} \rightarrow \gamma\gamma) = \frac{3N_c \text{Im} f_{\gamma\gamma}(^3P_J)}{\pi M^4} |\overline{R'_P}|^2 + O(v^2\Gamma), \quad J = 0, 2. \quad (4.7c)$$

Since $\overline{R'_P}$ is proportional to a vacuum-to-quarkonium matrix element, it can be calculated more easily in lattice NRQCD simulations than can $\langle h_c | \mathcal{O}_8(^1S_0) | h_c \rangle$, which is a matrix element between quarkonium states.

As we have already mentioned, in the calculations of Barbieri *et al.* of the P-wave decay rates into light hadrons [7,8,21], a logarithmic dependence on an infrared cutoff appeared in the coefficients of $|R'_P(0)|^2$. We now explain why this infrared-cutoff dependence is absent in the factorization formulas (4.7). The coefficients of $|\overline{R'_P}|^2$ in (4.7) depend logarithmically on the NRQCD cutoff Λ . In these coefficients, Λ plays the same role as did the infrared cutoff in the Barbieri *et al.* calculations. According to the evolution equation (3.28a), the matrix element $\langle h_c | \mathcal{O}_8(^1S_0) | h_c \rangle$, also depends logarithmically on Λ . In this case, Λ plays the role of an ultraviolet cutoff. Because physical quantities, such as decay rates, are renormalization-group invariants, the Λ -dependence in $\langle h_c | \mathcal{O}_8(^1S_0) | h_c \rangle$ cancels the Λ -dependence in the coefficients of $|\overline{R'_P}|^2$ in (4.7). Thus, we see that the inclusion of the color-octet term proportional to $\langle h_c | \mathcal{O}_8(^1S_0) | h_c \rangle$ in the factorization formulas removes the dependence of the decay rate on an arbitrary infrared cutoff.

The factorization formulas (4.7) for the annihilation decays of P-waves at leading order in v were first given in Ref. [10] in the form

$$\Gamma(h_c \rightarrow \text{LH}) = H_1 \widehat{\Gamma}_1(Q\overline{Q}(^1P_1) \rightarrow \text{partons}) + H_8 \widehat{\Gamma}_8(Q\overline{Q}(^1S_0) \rightarrow \text{partons}), \quad (4.8a)$$

$$\begin{aligned} \Gamma(\chi_{cJ} \rightarrow \text{LH}) &= H_1 \widehat{\Gamma}_1(Q\overline{Q}(^3P_J) \rightarrow \text{partons}) + H_8 \widehat{\Gamma}_8(Q\overline{Q}(^3S_1) \rightarrow \text{partons}), \\ &\quad J = 0, 1, 2, \end{aligned} \quad (4.8b)$$

$$\Gamma(\chi_{cJ} \rightarrow \gamma\gamma) = H_1 \widehat{\Gamma}_1(Q\overline{Q}(^3P_J) \rightarrow \gamma\gamma), \quad J = 0, 2. \quad (4.8c)$$

The coefficients $\widehat{\Gamma}_1$ and $\widehat{\Gamma}_8$ in (4.8) are proportional to the annihilation rates of on-shell $Q\bar{Q}$ pairs in color-singlet P-wave and color-octet S-wave states, respectively. The nonperturbative parameters H_1 and H_8 that were introduced in Ref. [10] can be defined rigorously in terms of matrix elements in NRQCD:

$$H_1 = \frac{1}{M^4} \langle h_c | \mathcal{O}_1(^1P_1) | h_c \rangle , \quad (4.9a)$$

$$H_8(\Lambda) = \frac{1}{M^2} \langle h_c | \mathcal{O}_8(^1S_0) | h_c \rangle . \quad (4.9b)$$

The factors of $1/M^4$ and $1/M^2$ in (4.9a) and (4.9b) were chosen in Ref. [10] so that H_1 and H_8 would be the combinations of NRQCD matrix elements and quark masses that are determined in experimental measurements of the P-wave decay rates.

In retrospect, the choice made in Ref. [10] to include factors of $1/M$ in the definitions of H_1 and H_8 in (4.9) was unfortunate. The factors of $1/M$ are more properly associated with the coefficients $\widehat{\Gamma}_1$ and $\widehat{\Gamma}_8$, since they involve short-distance physics at scales of order $1/\Lambda$ or less. The factorization formulas (4.7) are, therefore, to be preferred over the forms (4.8), because they incorporate all effects of the short distance scale $1/M$ into the coefficients, leaving matrix elements that depend only on physics at length scales $1/(Mv)$ and longer.

V. PERTURBATIVE FACTORIZATION

In this section, we sketch the connection between the NRQCD approach and conventional perturbative methods for demonstrating the factorization of cross sections involving large momentum transfer in QCD. In perturbative proofs of factorization, the aim is to demonstrate that, to all orders in perturbation theory, infrared and collinear divergences either cancel or can be absorbed into well-defined nonperturbative long-distance quantities. Some familiar examples of such nonperturbative quantities are parton distributions in the case of deep-inelastic lepton-hadron scattering and fragmentation functions in the case of inclusive hadron production at large transverse momentum in e^+e^- annihilation. The cross sections can be written as sums of products of long-distance quantities with infrared-safe (*i.e.*, short-distance) parton-level cross sections. Our factorization formula for heavy quarkonium annihilation rates is also of this form, and it is illuminating to see how it could be derived from a more conventional perturbative analysis.

A. Topological Factorization

We remind the reader that, in QCD, infrared (or soft) divergences are logarithmic and arise only from the emission of a gluon for which all components of the 4-momentum are small. Collinear divergences (or mass singularities) are also logarithmic, and arise when one parton (gluon or light quark) splits into two or more partons and all of their 4-momenta are parallel. Collinear divergences are cut off by quark masses, which necessarily introduce a non-parallel component into the 4-momenta of the splitting partons.

Let us focus first on the infrared divergences that arise in the radiation of gluons from final-state partons and on the collinear divergences that arise in the splitting of a final-state parton into collinear partons. The Kinoshita-Lee-Nauenberg theorem [19] guarantees that all such divergences cancel when one sums over those final-state cuts of a given diagram that contribute to an inclusive cross section. For example, the diagram shown in Fig. 1

has three cuts that correspond to gluonic final states, and each cut contains infrared and collinear divergences. However, these divergences cancel when one adds the real-emission cut of Fig. 1(b) to the virtual-emission cuts of Figs. 1(a) and 1(c). This step in the proof of perturbative factorization is related to the localization of the annihilation vertex, which was discussed in Section II E.

Next, let us consider the radiation of gluons from the heavy-quark lines. Such contributions are protected from collinear divergences by the heavy-quark mass, so we need consider only the possibility of infrared divergences. One key to analyzing the infrared divergences is the concept of a “controlling momentum”. The essential idea is that the infrared divergence associated with an integration over propagators and vertices in some portion of a Feynman diagram is cut off by the largest external momentum that enters the propagators. For example, an infrared divergence could potentially arise from the square of the diagram in Fig. 4(c) when all components of the 4-momentum of the middle gluon become small. However, because of simple kinematics, the other two final-state gluons must both carry large momenta, some of whose components are of order M . That large momentum must flow through the heavy-quark propagator to which the soft gluon attaches, and, consequently, it cuts off the potential infrared divergence.

In this example, and in general, the concept of a controlling momentum tells us that an infrared divergence can never arise from a soft gluon that attaches to a propagator that is off-shell by order M . That means that the infrared-divergent part of a Feynman diagram can always be separated from the “short-distance part” by cutting through heavy-quark propagators that are off the mass shell by amounts that are much less than M . (By the short-distance part, we mean that part of the diagram that includes the hard final-state partons and all propagators that are off-shell by order M .) This “topological factorization” is the crucial step in a perturbative demonstration of factorization. It implies that the infrared divergences can be disentangled from the short-distance part of the diagram and absorbed into the long-distance part of the diagram, which also includes the quarkonium wavefunctions.

The topological factorization of the annihilation rate of heavy quarkonium is represented schematically in Fig. 2. The shaded ovals represent the wavefunction for a quarkonium state. A typical Fock state contains a $Q\bar{Q}$ pair and zero or more gluons or light quark pairs. The short-distance part of the annihilation rate is represented by the circle labelled **H** (for *hard*). At leading order in v , the only lines that attach to the short-distance part are the incoming Q and \bar{Q} and the outgoing Q and \bar{Q} . The long-distance part includes the wavefunction of the initial meson and its complex conjugate. These wavefunctions are connected by any extra partons that may be present in the Fock state, which are represented in Fig. 2 by gluon lines. The long-distance part also includes soft-gluon interactions between the extra partons, which are represented by the circle labelled **S** (for *soft*).

Once topological factorization has been demonstrated, two additional steps are required in order to complete the proof of perturbative factorization. First, one must decouple the relative 4-momentum p of the heavy quark and antiquark from the short-distance part of the amplitude by expanding the short-distance part as a Taylor series in p . Second, one must decouple the Dirac indices and color indices that connect the short-distance part to the long-distance part. This can be accomplished by making use of Fierz rearrangements. In the factored decay rate, the long-distance parts correspond to the matrix elements of the NRQCD 4-fermion operators in the quarkonium state; the short-distance parts correspond to the imaginary parts of the coefficients of those operators in the NRQCD lagrangian.

In order to see in more detail how the perturbative analysis leads to the results that we have obtained from NRQCD, let us consider two examples: annihilation of S-wave and P-wave quarkonium at leading nontrivial order in v and through order α_s^3 in QCD perturbation theory. We use the specific example of decays into 2 and 3 gluons in the discussions below. However, the essential ingredients of the discussion apply also to decays into a light quark-antiquark pair and decays into a $q\bar{q}$ pair and a gluon.

B. Annihilation of S-wave Quarkonium

The first step in the analysis of annihilation of S-wave quarkonium is to identify the short-distance part in the topological factorization of the amplitude. The dominant component of the bound-state wavefunction consists of a heavy quark and antiquark in a color-singlet state. We take the $Q\bar{Q}$ pair to have total 4-momentum P and relative 4-momentum $2p$. We assume that, owing to the bound-state dynamics, the Q and \bar{Q} have inverse propagators $(\frac{1}{2}P \pm p)^2 - M^2$ of order M^2v^2 , with $v^2 \ll 1$. In the meson rest frame, the energies $\frac{1}{2}P_0 \pm p_0$ of the Q and \bar{Q} then differ from the mass M by order Mv^2 and their momenta $\frac{1}{2}\mathbf{P} \pm \mathbf{p}$ are of order Mv . At order α_s^2 , the $Q\bar{Q}$ pair can annihilate into two gluons through the diagrams in Fig. 3. By energy conservation, the two gluons must both have momenta of order M . At this order, the topological factorization of the annihilation rate is trivial. The $Q\bar{Q}$ annihilation amplitude belongs entirely to the short-distance part of the annihilation rate in Fig. 2, while the quarkonium wavefunction belongs to the long-distance part.

We next consider the annihilation rate of the $Q\bar{Q}$ pair at order α_s^3 . This rate has contributions from the annihilation into three gluons through the diagrams in Fig. 4, and also from the annihilation into two gluons, due to the interference between next-to-leading order diagrams such as those in Fig. 5 and the leading-order diagrams in Fig. 3. We begin by examining the infrared divergences in the diagrams for the emission of a real gluon of 4-momentum l shown in Fig. 4. As we have already explained, the diagram in Fig. 4(c) contains no infrared divergence. For the diagrams in Figs. 4(a) and (b), we identify the infrared contribution that is leading in v by assuming that $P_0 \approx 2M$, that $l_0 = |\mathbf{l}|$, \mathbf{P} , and \mathbf{p} are of order Mv , and that p_0 is of order Mv^2 . The emission vertex for the gluon with momentum l and the two adjacent heavy-quark propagators can then be approximated as follows:

$$\begin{aligned} & \frac{(\pm\frac{1}{2}P + p) \cdot \gamma + M}{(\pm\frac{1}{2}P + p)^2 - M^2 + i\epsilon} \gamma^\mu \frac{(\pm\frac{1}{2}P + p \mp l) \cdot \gamma + M}{(\pm\frac{1}{2}P + p \mp l)^2 - M^2 + i\epsilon} \\ & \approx \frac{M(1 \pm \gamma_0)}{(\pm\frac{1}{2}P + p)^2 - M^2 + i\epsilon} \gamma^\mu \frac{M(1 \pm \gamma_0)}{-2Ml_0 + i\epsilon} \end{aligned}$$

$$= \frac{M(1 \pm \gamma_0)}{(\pm \frac{1}{2}P + p)^2 - M^2 + i\epsilon} \begin{pmatrix} \pm g^{\mu 0} \\ -|\mathbf{l}| \end{pmatrix}, \quad (5.1)$$

where the upper and lower signs correspond to Fig. 4(a) and Fig. 4(b), respectively. (In the case of the lower sign, the order of the gamma matrices should actually be reversed, but the last line is unaffected.) The factor $\pm g^{\mu 0}$ is called the “eikonal vertex”, and the factor $1/(-l_0 + i\epsilon) = 1/(-|\mathbf{l}|)$ is called the “eikonal propagator”. Their product is called the “eikonal factor”. We see that the eikonal factor for the contribution of Fig. 4(a) is equal and opposite in sign to the eikonal factor for the contribution of Fig. 4(b). All other propagator and vertex factors in the two diagrams are the same. If the $Q\bar{Q}$ pair is in a color-singlet state, then the color factors in the two diagrams are also the same, and the infrared contributions from the region $|\mathbf{l}| \rightarrow 0$ cancel. This cancellation is a consequence of the fact that, in the infrared limit, the soft gluon couples to the color charges of the quark and antiquark. Since the quarkonium is a color singlet, the quark and antiquark have opposite color charges.

Because of the infrared cancellation, the topological factorization of the real-emission diagrams in Fig. 4 is trivial. The amplitudes for $Q\bar{Q} \rightarrow ggg$ all belong to the short distance part of the annihilation rate in Fig. 2, while the quarkonium wavefunction belongs to the long-distance part.

Now let us turn to the virtual-gluon-emission diagrams shown in Fig. 5. Once again, we can identify the infrared part by neglecting l and p compared to M . As in the preceding example, the eikonal vertices are proportional to $g^{\mu 0}$ times the quark (or antiquark) charge. For Fig. 5(a), the eikonal propagator factors associated with the exchange of the gluon with momentum l are $[1/(-l_0 + i\epsilon)][-1/(l_0 + i\epsilon)]$. Each of the diagrams of Figs. 5(b) and (c) contains a mass renormalization, which we subtract. The remaining contribution is a wavefunction renormalization, half of which we absorb into the quarkonium wavefunction. The other half yields the eikonal propagator factor $(-1/2)[1/(-l_0 + i\epsilon)]^2$. (The squared propagator appears after subtraction of the mass-renormalization contribution.) The eikonal factors from the three diagrams would cancel, were it not for the $i\epsilon$'s in the propagator denominators. Instead, the eikonal factors yield

$$\frac{1}{-l_0 + i\epsilon} \frac{-1}{l_0 + i\epsilon} - \frac{1}{-l_0 + i\epsilon} \frac{1}{-l_0 + i\epsilon} = 2\pi i \delta(l_0) \frac{1}{-l_0 + i\epsilon}. \quad (5.2)$$

The $\delta(l_0)$ contribution arises because of the pinch in the l_0 integration contour in the contribution of the diagram of Fig. 5(a). This $\delta(l_0)$ contribution corresponds to the exchange of a space-like gluon with temporal polarization between the quark and antiquark. That is, it corresponds to the Coulomb scattering of the quark and antiquark. Note that the factor multiplying $\delta(l_0)$ is divergent at $l_0 = 0$. This somewhat unexpected divergence has arisen because we have neglected the relative momentum \mathbf{p} of the heavy quark and antiquark. Had we retained that momentum in the propagator denominators, we would have obtained a $1/v$ singularity, where v is the relative velocity of the quark and antiquark. [This $1/v$ contribution is calculated in detail in (A20)–(A22).] Ordinarily, in the absence of a collinear singularity, the phase space for two partons to be moving with small relative velocity would be unimportant. Here, that region of phase space is important by virtue of the quarkonium bound state. (In fact, it is the $1/v$ singularity that builds up the bound-state wave function in a perturbative analysis of the Bethe-Salpeter equation for positronium.)

At this point, the topological factorization of the virtual-emission diagrams can be carried out. For the diagrams in Fig. 5, one factors the following contributions into the long-distance part: the wavefunctions, with which we associate the square root of each quark or antiquark wavefunction renormalization, and the $1/v$ singularity that arises from the diagram of Fig. 5(a). The remaining contributions from these diagrams are factored into the short-distance part.

Many discussions of perturbative factorization make use of the Grammer-Yennie technique [22] for analyzing infrared divergences. As an aside, let us indicate briefly how that technique would apply to the example at hand. From our previous discussion, we see that, in the infrared limit, the infrared-gluon vertex V^μ is well approximated by $g^{\mu 0} V_0$. Then we can write

$$V^\mu \approx g^{\mu 0} \frac{V \cdot l}{l_0 - i\epsilon}, \quad (5.3)$$

provided that l_0 is not small compared with the other components of l . This is always

the case for real emission. For virtual emission, we can eliminate the region of small l_0 by deforming the l_0 contour of integration into the lower half of the complex plane. As can be seen from an examination of the propagator denominators, all of the singularities in the lower half of the complex plane are order M^0 away from the origin, except in the diagram of Fig. 5(a). This is the momentum-space manifestation of the fact that a space-like gluon (with small l_0) can be exchanged causally only between co-moving particles. In carrying out the contour deformation for the diagram of Fig. 5(a), and only in this case, we unavoidably pick up the residue of a pole at $l_0 \approx 0$. This residue yields the $1/v$ singularity in (5.2) that was noted earlier. Along the deformed contours, the Grammer-Yennie approximation (5.3) is valid. Substituting (5.3) for the infrared vertices, we can make use of Ward identities (current conservation) to show that the contributions of the deformed contours cancel. In order to obtain this Ward-identity cancellation, one needs, in addition to the Grammer-Yennie contributions of Figs. 4 and 5, Grammer-Yennie contributions in which the infrared gluon attaches to the short-distance part of the process. But, as we have already argued, these diagrams give contributions that vanish in the infrared region, so there is no harm in applying the Grammer-Yennie approximation to them.

After topological factorization, the short-distance and long-distance parts of the annihilation rate are still tied together by integrations over the relative 4-momenta p and p' of the $Q\bar{Q}$ pairs entering and leaving the short distance part and by sums over the color and Dirac indices associated with the heavy-quark propagators. To complete the factorization, we must decouple these integrals and sums.

The decoupling of the integration over p and p' is accomplished simply by expanding the short-distance contribution in a Taylor series in p and p' . Taking \mathbf{p} and \mathbf{p}' to be of order Mv and p_0 and p'_0 to be of order Mv^2 , we see that the Taylor expansion of the short-distance part corresponds to an expansion in powers of v . All of the dependence on p and p' is now in the long-distance part and in the explicit powers of p and p' from the Taylor expansion. To analyze S-wave decays at leading order in v , we need keep only the zeroth order terms in the Taylor expansion, which amounts to setting $p = p' = 0$. In the meson rest frame, the

$Q\bar{Q}$ pair has total energy P_0 which differs from $2M$ by an amount of order Mv^2 , and total momentum \mathbf{P} of order Mv . At leading order in v , we can set $P_0 = 2M$ and $\mathbf{P} = 0$ in the short-distance part of the annihilation rate. Thus the incoming quark and antiquark can be taken to be on their mass shells and at threshold.

The decoupling of the color indices connecting the short-distance and long-distance parts of the annihilation rate is straightforward. The short-distance part is a color tensor $C_{ij,kl}$, with color indices i and j for the incoming Q and \bar{Q} and j and k for the outgoing Q and \bar{Q} . The indices i and j can be decoupled from the tensor by using the Fierz rearrangement

$$\delta_{i'i} \delta_{jj'} = \frac{1}{N_c} \delta_{ji} \delta_{i'j'} + 2 T_{ji}^a T_{i'j'}^a. \quad (5.4)$$

A similar rearrangement can be used for the indices k and l . By color symmetry, $T_{ij}^a C_{ij,kl}$ must vanish and $T_{ij}^a C_{ij,kl} T_{lk}^b$ must be proportional to the unit tensor δ^{ab} . The resulting rearrangement formula is

$$C_{ij,kl} = \frac{1}{N_c^2} \delta_{ji} (C_{i'i',j'j'}) \delta_{kl} + \frac{4}{N_c^2 - 1} T_{ji}^a \left(T_{i'j'}^b C_{i'j',k'l'} T_{l'k'}^b \right) T_{kl}^a. \quad (5.5)$$

The indices have been decoupled from the tensor by decomposing it into a term in which both pairs of indices are projected onto a color-singlet state and a term in which both pairs of indices are projected onto a color-octet state. For S-wave quarkonium, the dominant Fock state contains a color-singlet $Q\bar{Q}$ pair, so only the first term on the right side of (5.5) contributes at leading order in v .

The Dirac indices connecting the short-distance and long-distance parts of the amplitude can be decoupled in a similar way, although the algebra is a little more cumbersome than it is for the color indices. Having set $p = p' = 0$ and $P = (2M, \mathbf{0})$ in the short-distance part of the amplitude, we find that the numerators of the four propagators connecting it to the long-distance part reduce to $M(\gamma_0 + 1)$ for the quarks and $M(-\gamma_0 + 1)$ for the antiquarks. The Dirac structure of the short-distance part of the amplitude is therefore a tensor $\Gamma_{ij,kl}$, in which the Dirac indices i and k of the quarks are contracted with projectors $P_+ = (1 + \gamma_0)/2$, and the Dirac indices j and l of the antiquarks are contracted with projectors $P_- = (1 - \gamma_0)/2$. The indices i and j can be decoupled from the Dirac tensor by using the Fierz rearrangement

$$(P_+)_{i'i} (P_-)_{jj'} = \frac{1}{2} (\gamma_5 P_+)_{ji} (\gamma_5 P_-)_{i'j'} + \frac{1}{2} (\sigma^a \gamma_5 P_+)_{ji} (\sigma^a \gamma_5 P_-)_{i'j'}, \quad (5.6)$$

where $\sigma^i = (i/2)\epsilon^{0ijk}[\gamma^j, \gamma^k]$. A similar Fierz rearrangement can be used to decouple the indices k and l from the Dirac tensor. Since all 3-momenta have been set to 0 in the Dirac tensor $\Gamma^{ij,kl}$, there is no 3-vector on which $\Gamma^{ij,kl}$ can depend. Its transformation properties under rotations then imply that the vector $(\sigma^a \gamma_5 P_-)_{ij} \Gamma_{ij,kl} (\gamma_5 P_+)_{lk}$ must vanish, while the tensor $(\sigma^a \gamma_5 P_-)_{ij} \Gamma_{ij,kl} (\sigma^b \gamma_5 P_+)_{lk}$ must be proportional to the Cartesian unit tensor δ^{ab} . Consequently, one obtains the rearrangement formula

$$\begin{aligned} & (P_+)_{i'i} (P_-)_{jj'} \Gamma_{i'j',k'l'} (P_+)_{kk'} (P_-)_{l'l} \\ &= \frac{1}{4} (\gamma_5 P_+)_{ji} \left[(\gamma_5 P_-)_{i'j'} \Gamma_{i'j',k'l'} (\gamma_5 P_+)_{l'k'} \right] (\gamma_5 P_-)_{kl} \\ &+ \frac{1}{12} (\sigma^m \gamma_5 P_+)_{ji} \left[(\sigma^a \gamma_5 P_-)_{i'j'} \Gamma_{i'j',k'l'} (\sigma^a \gamma_5 P_+)_{l'k'} \right] (\sigma^m \gamma_5 P_-)_{kl}. \end{aligned} \quad (5.7)$$

This rearrangement of the Dirac indices corresponds to the decomposition of the Dirac tensor into spin-singlet and spin-triplet pieces. The Dirac matrix $\gamma_5 P_- = P_+ \gamma_5$ projects a $Q\bar{Q}$ pair at rest onto a state with total spin 0, as can be seen from the identity

$$\sum_{mm'} \langle 0, 0 | \frac{1}{2}, m; \frac{1}{2}, m' \rangle u_m \bar{v}_{m'} = \frac{1}{\sqrt{2}} (\gamma_5 P_-), \quad (5.8)$$

where u_m and $\bar{v}_{m'}$ are Dirac spinors evaluated at zero 3-momentum. Similarly, the Dirac matrix $\sigma^i \gamma_5 P_- = P_+ \sigma^i \gamma_5$ projects a $Q\bar{Q}$ pair at rest onto a state of total spin 1:

$$\sum_{mm'} \langle 1, M | \frac{1}{2}, m; \frac{1}{2}, m' \rangle u_m \bar{v}_{m'} = \frac{1}{\sqrt{2}} U^{Mi} (\sigma^i \gamma_5 P_-), \quad (5.9)$$

where U^{Mi} is the unitary matrix that transforms from the Cartesian basis to the basis of angular-momentum eigenstates.

Now that we have decoupled the integrations over p and p' and the sums over color and Dirac indices, the factorization of the annihilation rate is complete. In the rearrangement identity (5.7), the factors on the right side that are enclosed in square brackets belong to the short-distance part of the annihilation rate. They correspond to the operator coefficients in the NRQCD approach. The remaining factors to the right and to the left of the square

brackets belong to the long-distance part. It is evident that the long-distance parts of the annihilation rate can be reproduced by matrix elements of local operators in the quarkonium state. The two operators that contribute to the annihilation of S-wave states at leading order in v may be identified as

$$-\bar{\Psi}\gamma_5 P_+ \Psi \bar{\Psi}\gamma_5 P_- \Psi \quad \approx \mathcal{O}_1(^1S_0), \quad (5.10a)$$

$$-\bar{\Psi}\boldsymbol{\sigma}\gamma_5 P_+ \Psi \cdot \bar{\Psi}\boldsymbol{\sigma}\gamma_5 P_- \Psi \approx \mathcal{O}_1(^3S_1), \quad (5.10b)$$

where Ψ is the Dirac field for the heavy quark. For matrix elements between quarkonium states, these operators reduce at leading order in v to the NRQCD operators $\mathcal{O}_1(^1S_0) = \psi^\dagger \chi \chi^\dagger \psi$ and $\mathcal{O}_1(^3S_1) = \psi^\dagger \boldsymbol{\sigma} \chi \cdot \chi^\dagger \boldsymbol{\sigma} \psi$, respectively. Thus, perturbative factorization yields the same operator matrix elements as appear in the NRQCD analysis. It should be noted, however, that the identifications (5.10) are not unique. For example, the operator $-\bar{\Psi}\gamma_5 \Psi \bar{\Psi}\gamma_5 \Psi$, when sandwiched between quarkonium states, also reduces at leading order in v to $\mathcal{O}_1(^1S_0)$ and both $-\bar{\Psi}\boldsymbol{\sigma}\gamma_5 \Psi \cdot \bar{\Psi}\boldsymbol{\sigma}\gamma_5 \Psi$ and $-\bar{\Psi}\boldsymbol{\gamma}\Psi \cdot \bar{\Psi}\boldsymbol{\gamma}\Psi$ reduce to $\mathcal{O}_1(^3S_1)$.

C. Annihilation of P-wave Quarkonium

Now let us analyze the annihilation of P-wave quarkonium at leading nontrivial order in v . First we note that, because the spatial part of the P-wave quarkonium wavefunction transforms under rotations like a vector, the \mathbf{p} -independent part of the $Q\bar{Q}$ annihilation amplitude vanishes on carrying out the angular part of the integration over \mathbf{p} . Thus, we must retain terms with one factor of \mathbf{p} in the annihilation amplitude, which means that the leading amplitude is down by one power of v relative to the S-wave case.

At order α_s^2 , the annihilation proceeds through the diagrams in Fig. 3. In this case, the factor of \mathbf{p} in the $Q\bar{Q}$ annihilation amplitude can come only from expanding the propagator of the virtual heavy quark, which is off its mass-shell by an amount of order M . The topological factorization is therefore trivial. The amplitude for $Q\bar{Q} \rightarrow gg$ belongs to the short-distance part of Fig. 2, and the quarkonium wavefunction belongs to the long-distance part.

We next consider the annihilation at order α_s^3 , which receives contributions from the real-emission diagrams in Fig. 4 and from the virtual-emission diagrams in Fig. 5. The factor of \mathbf{p} can come from one of two sources: the purely short-distance (infrared-safe) part of the diagram, or the potentially infrared-divergent part, which consists of the soft gluon and the heavy-quark propagators to which it attaches.

If the factor of \mathbf{p} comes from the short-distance part of the diagram, then the analysis of the infrared divergences goes through exactly as in the S-wave case. Infrared divergences cancel between the real-emission diagrams, but the exchange of a virtual gluon between the Q and \bar{Q} [Fig. 5(c)] results in a $1/v$ singularity. Topological factorization is trivial, except for this $1/v$ singularity. It must be factored into the long-distance part of the annihilation rate.

We proceed to consider the case in which the factor of \mathbf{p} comes from the potentially infrared-divergent part of the diagram. We consider separately the cases of virtual-gluon emission and real-gluon emission.

The diagrams for virtual-gluon emission are shown in Fig. 5. The potentially infrared-divergent part of the amplitude includes the factors in the first line of (5.1). The required factor of \mathbf{p} can come either from a $\mathbf{p} \cdot \boldsymbol{\gamma}$ in the numerator of a propagator or from expanding out the denominator. The terms with a factor of \mathbf{p} that comes from a propagator denominator are easily seen to be suppressed by a power of v . The terms that contain a $\mathbf{p} \cdot \boldsymbol{\gamma}$ in the numerator are also suppressed by a factor of v because of the Dirac structure. To see this, first consider the case of a soft gluon with temporal polarization. From the identity $P_+ \mathbf{p} \cdot \boldsymbol{\gamma} = \mathbf{p} \cdot \boldsymbol{\gamma} P_-$, one can see that the factor $\mathbf{p} \cdot \boldsymbol{\gamma}$ connects “large” components of Dirac matrices to “small” components. This gives rise to the suppression by a factor of v . Now consider the case of a virtual gluon with spatial polarization vector $\boldsymbol{\epsilon}$. Both of the spatial-gluon vertices bring in factors of $\boldsymbol{\epsilon} \cdot \boldsymbol{\gamma}$. The combined effect of these two factors and the factor of $\mathbf{p} \cdot \boldsymbol{\gamma}$ is again to connect large and small components, which costs a factor of v . Thus for virtual-gluon emission, there are no infrared divergences at leading order in v . The topological factorization is therefore trivial. The amplitude for $Q\bar{Q} \rightarrow gg$ belongs

entirely to the short-distance factor in the annihilation rate, aside from the square root of each heavy-quark or heavy-antiquark wavefunction renormalization, which we associate with the quarkonium wavefunction.

Finally, we consider the case of real-gluon emission through the diagrams in Fig. 4. Let us examine the infrared limit of the diagrams in Fig. 4(a) and 4(b) for the case in which the soft gluon with momentum l has spatial polarization vector $\boldsymbol{\epsilon}$. The emission vertex and the adjacent heavy-quark propagators can be approximated as follows:

$$\begin{aligned}
& \frac{(\pm\frac{1}{2}P + p) \cdot \gamma + M}{(\pm\frac{1}{2}P + p)^2 - M^2 + i\epsilon} \boldsymbol{\epsilon} \cdot \boldsymbol{\gamma} \frac{(\pm\frac{1}{2}P + p \mp l) \cdot \gamma + M}{(\pm\frac{1}{2}P + p \mp l)^2 - M^2 + i\epsilon} \\
& \approx \frac{M(1 \pm \gamma_0) - \mathbf{p} \cdot \boldsymbol{\gamma}}{(\pm\frac{1}{2}P + p)^2 - M^2 + i\epsilon} \boldsymbol{\epsilon} \cdot \boldsymbol{\gamma} \frac{M(1 \pm \gamma_0) - \mathbf{p} \cdot \boldsymbol{\gamma}}{-2Ml_0 + i\epsilon} \\
& \approx \frac{M(1 \pm \gamma_0)}{(\pm\frac{1}{2}P + p)^2 - M^2 + i\epsilon} \left(\frac{2\mathbf{p} \cdot \boldsymbol{\epsilon}}{-|\mathbf{l}|} \right). \tag{5.11}
\end{aligned}$$

The upper and lower signs apply to Figs. 4(a) and 4(b), respectively. (For the lower sign, the order of the Dirac matrices should actually be reversed.) In the last line of (5.11), we have retained only those numerator terms that contain one power of \mathbf{p} . The factor $2\mathbf{p} \cdot \boldsymbol{\epsilon}/(-|\mathbf{l}|)$ is the infrared-emission factor. In contrast with the S-wave case, the infrared contributions from the two real-emission diagrams add, rather than cancelling. Because we have retained one power of \mathbf{p} , the soft gluon couples to the color current of the heavy quark, rather than to the color charge. Since the heavy quark and antiquark have opposite color charges and, in the CM frame, opposite momenta, their color currents are equal. Note that, because of the vector \mathbf{p} in the infrared-emission factor, the emission of the soft gluon changes the orbital-angular-momentum quantum number of the $Q\bar{Q}$ pair by one unit, but it does not flip the spin of the quark or antiquark. Thus, it converts the heavy quark and antiquark from a color-singlet P-wave state to a color-octet S-wave state.

In the decay rate, we must integrate the infrared emission factors from the square of the sum of the amplitudes over the phase space of the gluon. Keeping only the logarithmically divergent part of the integral, we find the result

$$4 \int_{\lambda}^M \frac{d^3l}{(2\pi)^3} \frac{1}{2|\mathbf{l}|} \left(\frac{2\mathbf{p} \cdot \boldsymbol{\epsilon}}{-|\mathbf{l}|} \right) \left(\frac{2\mathbf{p}' \cdot \boldsymbol{\epsilon}^*}{-|\mathbf{l}|} \right) = \frac{4\mathbf{p} \cdot \boldsymbol{\epsilon} \mathbf{p}' \cdot \boldsymbol{\epsilon}^*}{\pi^2} \left(\log \frac{M}{\Lambda} + \log \frac{\Lambda}{\lambda} \right), \tag{5.12}$$

where λ is an infrared cutoff of order Mv , and we have arbitrarily set the upper limit on $|\mathbf{l}|$ to M . We have introduced a factorization scale Λ to separate the infrared divergence from the short-distance part of the integral. The long-distance contribution that is proportional to $\log(\Lambda/\lambda)$ in (5.12) can be interpreted as the probability for a heavy quark and antiquark in a color-singlet P-wave state to make a transition to a color-octet S-wave state by radiating a soft gluon.

We can now carry out the topological factorization of the diagrams in Fig. 4 for real gluon emission. The square of the amplitude for $Q\bar{Q} \rightarrow ggg$, integrated over phase space, belongs to the short-distance part of the annihilation rate in Fig. 2, except for the second term on the right side of (5.12). This term, which contains the infrared divergent contribution that arises from the emission of the soft gluon in Figs. 4(a) and 4(b), is included in the long-distance part, along with the quarkonium wavefunction. The soft gluon is an example of a light parton that connects the initial and final wavefunctions in Fig. 2. Note that, in this contribution to the annihilation rate, the heavy quark and antiquark enter the short-distance part in a color-octet S-wave state. We call this contribution to the annihilation rate the “color-octet contribution”. In all the other contributions to the P-wave annihilation rate at this order, the heavy quark and antiquark enter the short-distance part in a color-singlet P-wave state. We refer to those contributions as the “color-singlet contribution”.

At this point, we have identified the long- and short-distance parts in the topological factorization of the annihilation rate. It remains only to decouple the integrations over the relative momenta p and p' of the $Q\bar{Q}$ pairs and the sums over color and Dirac indices.

We first discuss the color-singlet contribution. The color indices of the short-distance and long-distance parts are easily decoupled by using the rearrangement identity (5.5). Only the first term on the right side of (5.5) contributes, since the $Q\bar{Q}$ pair is in a color-singlet state. In order to decouple the integrals over the relative momenta p and p' of the initial and final $Q\bar{Q}$ pairs, we expand the short distance part as a Taylor series in p and p' . At leading order in v , we set $p_0 = p'_0 = 0$ and keep only those terms linear in both \mathbf{p} and \mathbf{p}' .

The resulting amplitude has the structure $p^m \Gamma_{ij,kl}^{mn} p'^m$, in which the Dirac indices i and k of the quark are contracted with projectors P_+ and the Dirac indices j and l of the antiquarks are contracted with projectors P_- . The Dirac indices of the initial and final $Q\bar{Q}$ pair are decoupled from the short distance factor $\Gamma_{ij,kl}^{mn}$ by applying the Fierz identity (5.6) to both the initial and final indices. The resulting rearrangement identity can be greatly simplified by making use of the fact that the Fierz-decoupled short-distance parts transform like tensors under rotations and the fact that there are no three-vectors on which $\Gamma_{ij,kl}^{mn}$ can depend. For example, the tensor $(\gamma_5 P_+)_{ij} \Gamma_{ij,kl}^{mn} (\gamma_5 P_+)_{lk}$ must be proportional to the unit tensor δ^{mn} , and the tensor $(\sigma^a \gamma_5 P_+)_{ij} \Gamma_{ij,kl}^{mn} (\gamma_5 P_+)_{lk}$ must be proportional to the totally antisymmetric tensor ϵ^{amn} . Since $(\sigma^a \gamma_5 P_+)_{ij} \Gamma_{ij,kl}^{mn} (\sigma^b \gamma_5 P_+)_{lk}$ is a Cartesian tensor in 3 dimensions with 4 indices, it can be decomposed into a linear combination of the three tensors $\delta^{am} \delta^{bn}$, $\epsilon^{amx} \epsilon^{bnx}$, and $\frac{1}{2}(\delta^{ab} \delta^{mn} + \delta^{an} \delta^{mb}) - \frac{1}{3} \delta^{am} \delta^{bn}$, which correspond to total angular momentum 0, 1, and 2, respectively. Consequently, one obtains the rearrangement formula

$$\begin{aligned}
& (P_+)_{i'i} (P_-)_{jj'} \left(p^m \Gamma_{i'j',k'l'}^{mn} p'^m \right) (P_+)_{kk'} (P_-)_{l'l} \\
&= \frac{1}{12} (p^m \gamma_5 P_+)_{ji} \left[(\gamma_5 P_-)_{i'j'} \Gamma_{i'j',k'l'}^{aa} (\gamma_5 P_+)_{l'k'} \right] (p'^m \gamma_5 P_-)_{kl} \\
&\quad + \frac{1}{36} (\mathbf{p} \cdot \boldsymbol{\sigma} \gamma_5 P_+)_{ji} \left[(\sigma^a \gamma_5 P_-)_{i'j'} \Gamma_{i'j',k'l'}^{ab} (\sigma^b \gamma_5 P_+)_{l'k'} \right] (\mathbf{p}' \cdot \boldsymbol{\sigma} \gamma_5 P_-)_{kl} \\
&\quad + \frac{1}{24} ((\mathbf{p} \times \boldsymbol{\sigma})^m \gamma_5 P_+)_{ji} \left[(\sigma^{[a} \gamma_5 P_-)_{i'j'} \Gamma_{i'j',k'l'}^{b] [b} (\sigma^a] \gamma_5 P_+)_{l'k'} \right] ((\mathbf{p}' \times \boldsymbol{\sigma})^m \gamma_5 P_-)_{kl} \\
&\quad + \frac{1}{20} (p^{(m} \sigma^n) \gamma_5 P_+)_{ji} \left[(\sigma^{(a} \gamma_5 P_-)_{i'j'} \Gamma_{i'j',k'l'}^{b)(a} (\sigma^b) \gamma_5 P_+)_{l'k'} \right] (p'^{(m} \sigma^n) \gamma_5 P_-)_{kl} \\
&\quad - \frac{1}{24} ((\mathbf{p} \times \boldsymbol{\sigma})^m \gamma_5 P_+)_{ji} \left[\epsilon^{abc} (\sigma^a \gamma_5 P_-)_{i'j'} \Gamma_{i'j',k'l'}^{bc} (\gamma_5 P_+)_{l'k'} \right] (p'^m \gamma_5 P_-)_{kl} \\
&\quad + \frac{1}{24} (p^m \gamma_5 P_+)_{ji} \left[\epsilon^{abc} (\gamma_5 P_-)_{i'j'} \Gamma_{i'j',k'l'}^{ab} (\sigma^c \gamma_5 P_+)_{l'k'} \right] ((\mathbf{p}' \times \boldsymbol{\sigma})^m \gamma_5 P_-)_{kl}. \tag{5.13}
\end{aligned}$$

We use the notation $T^{(ab)}$ for the symmetric traceless part of a tensor T^{ab} and $T^{[ab]} = \frac{1}{2}(T^{ab} - T^{ba})$ for the antisymmetric part.

At this point, the factorization of the color-singlet contribution to the annihilation rate is complete. The factors in square brackets on the right side of (5.13) belong to the short-distance part, while the factors to the right and to the left of the square brackets belong to the long-distance part. It is apparent from the rearrangement identity (5.13) that the

long-distance parts can be reproduced by matrix elements of the following local operators:

$$-\bar{\Psi}(-\frac{i}{2}\vec{\mathbf{D}})\gamma_5 P_+ \Psi \cdot \bar{\Psi}(-\frac{i}{2}\vec{\mathbf{D}})\gamma_5 P_- \Psi \quad \approx \mathcal{O}_1(^1P_1), \quad (5.14a)$$

$$-\frac{1}{3}\bar{\Psi}(-\frac{i}{2}\vec{\mathbf{D}} \cdot \boldsymbol{\sigma})\gamma_5 P_+ \Psi \bar{\Psi}(-\frac{i}{2}\vec{\mathbf{D}} \cdot \boldsymbol{\sigma})\gamma_5 P_- \Psi \quad \approx \mathcal{O}_1(^3P_0), \quad (5.14b)$$

$$-\frac{1}{2}\bar{\Psi}(-\frac{i}{2}\vec{\mathbf{D}} \times \boldsymbol{\sigma})\gamma_5 P_+ \Psi \cdot \bar{\Psi}(-\frac{i}{2}\vec{\mathbf{D}} \times \boldsymbol{\sigma})\gamma_5 P_- \Psi \approx \mathcal{O}_1(^3P_1), \quad (5.14c)$$

$$-\bar{\Psi}(-\frac{i}{2}\vec{\mathbf{D}}^{(i\sigma^j)})\gamma_5 P_+ \Psi \bar{\Psi}(-\frac{i}{2}\vec{\mathbf{D}}^{(i\sigma^j)})\gamma_5 P_- \Psi \quad \approx \mathcal{O}_1(^3P_2), \quad (5.14d)$$

$$-\bar{\Psi}(-\frac{i}{2}\vec{\mathbf{D}})\gamma_5 P_+ \Psi \cdot \bar{\Psi}(-\frac{i}{2}\vec{\mathbf{D}} \times \boldsymbol{\sigma})\gamma_5 P_- \Psi, \quad (5.14e)$$

$$-\bar{\Psi}(-\frac{i}{2}\vec{\mathbf{D}} \times \boldsymbol{\sigma})\gamma_5 P_- \Psi \cdot \bar{\Psi}(-\frac{i}{2}\vec{\mathbf{D}})\gamma_5 P_+ \Psi. \quad (5.14f)$$

The matrix elements of the last two operators vanish for a quarkonium state that is a charge-conjugation eigenstate. The other four operators reduce at leading order in v to the NRQCD operators $\mathcal{O}(^1P_1)$ and $\mathcal{O}(^3P_J)$, $J = 0, 1, 2$, respectively.

Finally, we consider the factorization of the color-octet contribution to the annihilation rate, for which the short-distance part involves the annihilation of a $Q\bar{Q}$ pair in a color-octet S-wave state. The color indices of the short-distance and long-distance parts are easily decoupled by using the rearrangement identity (5.5). Only the second term on the right side of (5.5) is non-vanishing for the color-octet contribution. The decoupling of the momentum integrations and the Dirac indices proceeds along the same lines as for S-wave quarkonium, which was discussed in subsection VB. The momentum integrations are decoupled by Taylor-expanding the short-distance part in p and p' , and setting $p = p' = 0$. The decoupling of the Dirac indices is accomplished by using the rearrangement formula (5.7). The factors in square brackets in (5.7) belong to the short-distance part of the annihilation rate, while the factors to the right and to the left belong to the long-distance part. From the rearrangement identities (5.5) and (5.7), it is evident that the long-distance parts are reproduced by matrix elements of the operators

$$-\bar{\Psi}\gamma_5 T^a P_+ \Psi \bar{\Psi}\gamma_5 T^a P_- \Psi \quad \approx \mathcal{O}_8(^1S_0), \quad (5.15a)$$

$$-\bar{\Psi}\boldsymbol{\sigma}\gamma_5 T^a P_+ \Psi \cdot \bar{\Psi}\boldsymbol{\sigma}\gamma_5 T^a P_- \Psi \approx \mathcal{O}_8(^3S_1). \quad (5.15b)$$

These operators reduce, at leading order in v , to the operators $\mathcal{O}_8(^1S_0) = \psi^\dagger T^a \chi \chi^\dagger T^a \psi$ and

$\mathcal{O}_8(^3S_1) = \psi^\dagger \boldsymbol{\sigma} T^a \chi \cdot \chi^\dagger \boldsymbol{\sigma} T^a \psi$ in the NRQCD analysis. The matrix elements of $\mathcal{O}_8(^1S_0)$ and $\mathcal{O}_8(^3S_1)$ include the probability factor proportional to $\log(\Lambda/\lambda)$ in (5.12). The logarithmic dependence on Λ is reflected in the evolution of these operators, which is given in (3.28a) and (3.28b). Thus, the factorization scale Λ in the perturbative approach can be identified with the ultraviolet cutoff of NRQCD.

VI. PRODUCTION OF HEAVY QUARKONIUM

In this section, we present a general factorization formula for computing inclusive heavy-quarkonium production rates in high-energy processes that involve a momentum transfer Q^2 that is of order M^2 or larger. In the case of S-wave quarkonium, our factorization formalism coincides with the “color-singlet model” for quarkonium production [23] in the nonrelativistic limit, but it also allows the systematic calculation of relativistic corrections that are suppressed by powers of v . In the case of P-wave quarkonium, our formalism reveals that the color-singlet model is incomplete, even at leading order in v , and must be supplemented by including the “color-octet mechanism” for P-wave quarkonium production [24].

A. Factorization of the Production Rate

Our goal, as in the discussion of heavy-quarkonium annihilation, is to express the inclusive production rate for a quarkonium state in a factored form. That is, we wish to write the production rate as a sum of terms, each of which consists of a short-distance part, which can be calculated in QCD perturbation theory, multiplied by a long-distance part that can be expressed as a matrix element in NRQCD. Our arguments for the factorization of the production rate are based on the all-orders properties of QCD perturbation theory. In this sense, the level of rigor of these arguments is comparable to that in the proofs of factorization for the Drell-Yan process for lepton pair-production in hadron-hadron collisions [25]. These arguments are less rigorous than those that we have given for the factorization of the quarkonium annihilation rate. The latter arguments rely only on the general space-time structure of the annihilation process and on the validity of the effective-field-theory approach. Their level of rigor is comparable to that in the proofs of factorization in deep-inelastic lepton-hadron scattering, which can be formulated in terms of the operator-product expansion.

When a quarkonium state is produced in a process that involves momentum transfer Q^2 of order M^2 or larger, the production of the $Q\bar{Q}$ pair that forms the bound state takes place at short distances of order $1/M$ or smaller. A simple example of such a process, which the reader can keep in mind throughout the following discussion, is the production in e^+e^- annihilation at a center-of-mass energy $\sqrt{s} \gg M$ of a heavy quarkonium H , with 4-momentum P , recoiling against two light hadron jets. At leading order in QCD perturbation theory, the relevant parton process is $e^+e^- \rightarrow Q\bar{Q}gg$. We take the Q and \bar{Q} to have momenta $P/2 + p$ and $P/2 - p$. The relative 3-momentum \mathbf{p} must be of order Mv in the $\mathbf{P} = 0$ frame in order for the $Q\bar{Q}$ pair to have a significant probability for forming the bound state H . The amplitude for the production of the $Q\bar{Q}$ pair is insensitive to changes in the relative 4-momentum p that are much less than M , and therefore the quark and antiquark are produced with a separation of order $1/M$ or less. Similarly, the square of the amplitude is insensitive to changes in the the total 4-momentum P of the heavy pair that are much less than M . Thus, the product of one amplitude and the complex conjugate of a second will contribute significantly to the $Q\bar{Q}$ -production cross section only if the corresponding production points are separated by a distance of order $1/M$ or less. We therefore conclude that the production of the $Q\bar{Q}$ pair is indeed a short-distance process that takes place within a distance of order $1/M$.

In the framework of NRQCD, the effect of the short-distance part of a production amplitude is simply to create a $Q\bar{Q}$ pair at a spacetime point. The formation of the quarkonium state H from the $Q\bar{Q}$ pair takes place over distances that are of order $1/(Mv)$ or larger in the quarkonium rest frame, so it is described accurately by NRQCD. Therefore, in NRQCD, the production rate (the square of the amplitude summed over final states) involves the creation of a $Q\bar{Q}$ pair at a spacetime point, its propagation into the asymptotic future, where the out state includes the quarkonium H , and, finally, the propagation of the $Q\bar{Q}$ pair back in time to the creation point. That is, the long-distance part of the production rate is given in NRQCD by vacuum matrix elements of local 4-fermion operators. The effects of the short-distance parts of the production rate are taken into account through the coefficients

of the 4-fermion operators. Since the final state must include a quarkonium, the 4-fermion operators that appear in production cross sections involve projections onto the space of states that contain, in the asymptotic future, the quarkonium state H plus anything else. The generic form of a production operator is

$$\begin{aligned}\mathcal{O}_n^H &= \chi^\dagger \mathcal{K}_n \psi \left(\sum_X \sum_{m_J} |H + X\rangle \langle H + X| \right) \psi^\dagger \mathcal{K}'_n \chi \\ &= \chi^\dagger \mathcal{K}_n \psi \left(a_H^\dagger a_H \right) \psi^\dagger \mathcal{K}'_n \chi,\end{aligned}\tag{6.1}$$

where the sums are over the $2J + 1$ spin states of the quarkonium H and over all other final-state particles X . In the second line of (6.1), the projection has been expressed compactly in terms of the operator a_H^\dagger that creates the quarkonium H in the out state. A sum over the angular-momentum quantum numbers m_J is implicit in $a_H^\dagger a_H$. The factors \mathcal{K}_n and \mathcal{K}'_n in the operator are products of a color matrix (either the unit matrix or T^a), a spin matrix (either the unit matrix or σ^i), and a polynomial in the covariant derivative \mathbf{D} and other fields. The overall operator \mathcal{O}_n^H is invariant under color and spatial rotations.³ We assume that any matrix elements of \mathcal{O}_n^H will be evaluated in the quarkonium rest frame; otherwise the factors \mathcal{K}_n and \mathcal{K}'_n may depend on the 4-momentum of the quarkonium.

It is convenient to introduce notation for the production operators that is analogous to that for the decay operators defined in (2.10) and (2.12). The production operators of dimension 6 are

$$\mathcal{O}_1^H(^1S_0) = \chi^\dagger \psi \left(a_H^\dagger a_H \right) \psi^\dagger \chi,\tag{6.2a}$$

$$\mathcal{O}_1^H(^3S_1) = \chi^\dagger \sigma^i \psi \left(a_H^\dagger a_H \right) \psi^\dagger \sigma^i \chi,\tag{6.2b}$$

$$\mathcal{O}_8^H(^1S_0) = \chi^\dagger T^a \psi \left(a_H^\dagger a_H \right) \psi^\dagger T^a \chi,\tag{6.2c}$$

³Here we consider explicitly only unpolarized production of heavy quarkonium. In the case of polarized production, a_H^\dagger would create a state of definite polarization, and \mathcal{K}_n and \mathcal{K}'_n would, in general, depend on one or more vectors associated with the incoming particles, such as the directions of their spins and momenta.

$$\mathcal{O}_8^H(^3S_1) = \chi^\dagger \sigma^i T^a \psi \left(a_H^\dagger a_H \right) \psi^\dagger \sigma^i T^a \chi. \quad (6.2d)$$

Some of the color-singlet production operators of dimension 8 are

$$\mathcal{O}_1^H(^1P_1) = \chi^\dagger \left(-\frac{i}{2} \vec{D}^i \right) \psi \left(a_H^\dagger a_H \right) \psi^\dagger \left(-\frac{i}{2} \vec{D}^i \right) \chi, \quad (6.3a)$$

$$\mathcal{O}_1^H(^3P_0) = \frac{1}{3} \chi^\dagger \left(-\frac{i}{2} \vec{\mathbf{D}} \cdot \boldsymbol{\sigma} \right) \psi \left(a_H^\dagger a_H \right) \psi^\dagger \left(-\frac{i}{2} \vec{\mathbf{D}} \cdot \boldsymbol{\sigma} \right) \chi, \quad (6.3b)$$

$$\mathcal{O}_1^H(^3P_1) = \frac{1}{2} \chi^\dagger \left(-\frac{i}{2} \vec{\mathbf{D}} \times \boldsymbol{\sigma} \right)^i \psi \left(a_H^\dagger a_H \right) \psi^\dagger \left(-\frac{i}{2} \vec{\mathbf{D}} \times \boldsymbol{\sigma} \right)^i \chi, \quad (6.3c)$$

$$\mathcal{O}_1^H(^3P_2) = \chi^\dagger \left(-\frac{i}{2} \vec{D}^{(i} \sigma^{j)} \right) \psi \left(a_H^\dagger a_H \right) \psi^\dagger \left(-\frac{i}{2} \vec{D}^{(i} \sigma^{j)} \right) \chi, \quad (6.3d)$$

$$\mathcal{P}_1^H(^1S_0) = \frac{1}{2} \left[\chi^\dagger \psi \left(a_H^\dagger a_H \right) \psi^\dagger \left(-\frac{i}{2} \vec{\mathbf{D}} \right)^2 \chi + \text{h.c.} \right], \quad (6.3e)$$

$$\mathcal{P}_1^H(^3S_1) = \frac{1}{2} \left[\chi^\dagger \sigma^i \psi \left(a_H^\dagger a_H \right) \psi^\dagger \sigma^i \left(-\frac{i}{2} \vec{\mathbf{D}} \right)^2 \chi + \text{h.c.} \right]. \quad (6.3f)$$

Given that the long-distance part of the production rate can be expressed in terms of vacuum matrix elements of operators of the form given in (6.1), the inclusive production cross section must have the form

$$\sigma(H) = \sum_n \frac{F_n(\Lambda)}{M^{d_n-4}} \langle 0 | \mathcal{O}_n^H(\Lambda) | 0 \rangle, \quad (6.4)$$

where it is understood that the matrix element is to be evaluated in the quarkonium rest frame. The short-distance coefficients F_n depend on all the kinematic variables of the production process, but they are independent of the quarkonium state H . Equation (6.4) is the equivalent for production of our factorization formula (2.14) for quarkonium decay.

Beyond leading order in perturbation theory, interactions involving soft (infrared) gluons and gluons collinear to the final-state jets potentially spoil this factorization picture, both by making the $Q\bar{Q}$ -production process long-ranged and by making connections between the outgoing quarkonium and the final-state jets that destroy the topological factorization. In the case of quarkonium decay, we were able to use the KLN theorem to argue that such final-state soft and collinear interactions cancel in the inclusive decay rate. In the case of quarkonium production, the KLN theorem does not apply directly because we have specified that the final state contain the quarkonium: some of the cuts in the KLN sum are missing. Cuts are missing only for diagrams in which a soft or collinear gluon attaches to one of the

heavy Q or \bar{Q} lines. If only one end of a gluon attaches to a Q or \bar{Q} line and the other end attaches to a final-state jet, then the sum over cuts along the jet line is sufficient by itself to effect the KLN cancellation. If both ends of a soft gluon attach to a heavy Q or \bar{Q} line, then there is no KLN cancellation. However, this contribution is part of the matrix element of the NRQCD 4-fermion operator.

In the case that \mathcal{O}_n^H is a color-octet operator, one might worry that, because the intermediate states in the first line of (6.1) carry net color charge, the factorization of the cross section in (6.4) is not valid. Owing to the property of confinement, such colored states have infinite energy. (Their energies would be finite in a finite volume, however.) Of course, the complete final state is color neutral and contains only color-singlet hadrons. One can picture the color neutralization of the partons in perturbation theory as a process involving soft-gluon exchanges between the partons. In particular, there can be color-neutralizing soft-gluon exchanges between partons that are comoving with the quarkonium and partons in other hadron jets produced by the short distance process. However, the KLN argument tells us that, at least in perturbation theory, the infrared and collinear divergences from such soft interactions cancel in the inclusive quarkonium production rate. That is, for purposes of computing the inclusive quarkonium production rate, the colored partons can be treated as if they were unconfined. Of course, the complete operator \mathcal{O}_n^H is invariant under color rotations, and one can deal with it without referring to the troublesome colored intermediate states by making use of the form given in the second line of (6.1). This approach might be useful in lattice measurements of the production matrix elements.

If we consider production of quarkonium in hadron-induced processes, then a host of new difficulties arise in proving that the production rate factors. These include exchanges of soft, collinear, and Glauber (quasi-elastic) gluons involving spectator partons in the initial state and exchanges of soft and collinear gluons involving active partons in the initial state. Rather than discuss the resolution of these difficulties here, we will merely assume that the Glauber divergences cancel, that the only noncancelling infrared divergences are those

associated with the matrix elements of the 4-fermion operators, and that the noncancelling collinear divergences can be absorbed into initial parton distributions. We refer the reader to the proofs of factorization of the Drell-Yan cross section [25,26] for detailed discussions of these points. Given these assumptions, the factored form (6.4) holds to all orders in perturbation theory. It should be noted that, in the case of hadron-hadron collisions, there is a limit to the precision of the factored form of the cross section. Generally, because of soft exchanges between spectators, one can prove only that a factored form holds through next-to-leading order in an expansion in inverse powers of the large momentum transfer Q^2 [26]. Beyond that order, factorization is known to fail [27].

B. Relation of Production Matrix Elements to Decay Matrix Elements

The NRQCD matrix elements that appear in the production rate (6.4) are related to the NRQCD matrix elements that appear in decay rates through a crossing of the quarkonium from the final state to the initial state. This relation is analogous to the one between parton distribution functions and parton fragmentation functions [28]. In general, the crossing relation is very complicated. There are, however, two instances in which one can obtain simple results.

Through order α_s in QCD perturbation theory, the crossing relation between $\langle H|\mathcal{O}_n|H\rangle$ and the corresponding production operator $\langle 0|\mathcal{O}_n^H|0\rangle$ is a simple equality, up to a factor of $2J+1$ for the number of spin states. Finite-order perturbation theory is usually of little help in dealing with long-distance matrix elements. It does tell us, though, that, to leading order in α_s , the evolution equations for the production operators are the same as the evolution equations for the corresponding decay operators. For example, the evolution equation for the production matrix element $\langle 0|\mathcal{O}_8^{h_c}(^1S_0)|0\rangle$ in terms of $\langle 0|\mathcal{O}_1^{h_c}(^1P_1)|0\rangle$ is identical at leading order in α_s and in v to the evolution equation (3.28a) for the corresponding decay matrix elements:

$$\Lambda \frac{d}{d\Lambda} \langle 0|\mathcal{O}_8^{h_c}(^1S_0)|0\rangle = \frac{4C_F\alpha_s(\Lambda)}{3N_c\pi M^2} \langle 0|\mathcal{O}_1^{h_c}(^1P_1)|0\rangle. \quad (6.5)$$

When \mathcal{O}_n^H is a color-singlet operator, the vacuum-saturation approximation can sometimes be used to simplify the matrix element. Assuming that the sum over states in the first line of (6.1) is dominated by the quarkonium state H plus the vacuum, we obtain

$$\begin{aligned}
\langle 0|\mathcal{O}_n^H|0\rangle &\approx \langle 0|\chi^\dagger\mathcal{K}_n\psi\left(\sum_{m_J}|H\rangle\langle H|\right)\psi^\dagger\mathcal{K}'_n\chi|0\rangle \\
&= (2J+1)\langle H|\psi^\dagger\mathcal{K}'_n\chi|0\rangle\langle 0|\chi^\dagger\mathcal{K}_n\psi|H\rangle \\
&\approx (2J+1)\langle H|\mathcal{O}_n|H\rangle,
\end{aligned} \tag{6.6}$$

where $\mathcal{O}_n = \psi^\dagger\mathcal{K}'_n\chi\chi^\dagger\mathcal{K}_n\psi$. In the second line, we have used the rotational invariance of the operator $\psi^\dagger\mathcal{K}'_n\chi|0\rangle\langle 0|\chi^\dagger\mathcal{K}_n\psi$, which implies that the matrix element is identical for each of the $2J+1$ angular-momentum states H that differ only in the quantum number m_J . In the last line, we have used the vacuum-saturation approximation (3.8) for the decay matrix element $\langle H|\mathcal{O}_n|H\rangle$.

For the vacuum-saturation approximation to be a controlled approximation, we must be able to show that the contributions of all the other states in the sum in (6.1) are suppressed by powers of v . This is in fact the case if the operator \mathcal{O}_n^H creates and annihilates the $Q\bar{Q}$ pair in the angular-momentum state that corresponds to the dominant Fock state of the meson H . In this case, the vacuum-saturation approximation result (6.6) is correct up to an error of relative order v^4 .

In the case of a color-octet operator, the states $|H+X\rangle$ in the first line of (6.1) have nonzero color, and the vacuum-saturation approximation is not applicable. In perturbation theory, we can approximate the sum by retaining only the terms involving intermediate states $|H+g\rangle$ that contain a single gluon. Similarly, we can approximate the sum for the corresponding decay matrix element by retaining the terms that involve single-gluon intermediate states $|g\rangle$. The resulting matrix elements $\langle 0|\chi^\dagger\mathcal{K}_n\psi|H+g\rangle$ and $\langle g|\chi^\dagger\mathcal{K}'_n\psi|H\rangle$ are related by crossing. Unfortunately the crossing relation is a simple equality only at leading order in perturbation theory. In the absence of any rigorous relation between them, we treat the matrix elements of the color-octet production operators and the color-octet decay operators as independent nonperturbative quantities.

C. Computation of the Operator Coefficients

The short-distance part of the quarkonium production rate is insensitive to the long-distance $Q\bar{Q}$ dynamics. Therefore, following the same reasoning as in Section II H, we can exploit the equivalence of perturbative QCD and perturbative NRQCD at long distances as a device to calculate the coefficients of the matrix elements in (6.4). We compute the production rate for an on-shell $Q\bar{Q}$ pair with small relative momentum using perturbation theory in full QCD. Then we use perturbation theory in NRQCD to compute the matrix elements of 4-fermion operators $\mathcal{O}_n^{Q\bar{Q}}$, which are analogous to those in (6.1) except that the projection is onto on-shell $Q\bar{Q}$ states. The short-distance coefficients are then determined by the matching condition

$$\sigma(Q\bar{Q}) \Big|_{\text{pert. QCD}} = \sum_n \frac{F_n(\Lambda)}{M^{d_n-4}} \langle 0 | \mathcal{O}_n^{Q\bar{Q}}(\Lambda) | 0 \rangle \Big|_{\text{pert. NRQCD}}. \quad (6.7)$$

By expanding the left and right sides of (6.7) as Taylor series in the relative momentum \mathbf{p} between the Q and \bar{Q} , we can identify the coefficients of the individual operators. They correspond to the infrared- and collinear-finite parts of cross sections for $Q\bar{Q}$ production. One useful way to evaluate the left side of (6.7) is to express the projection of the product $u(P/2 + p)\bar{v}(P/2 - p)$ of the Q and \bar{Q} spinors onto a particular angular momentum state in Lorentz-invariant form. We refer the reader to Ref. [29] for examples. Then the left side of (6.7) can be evaluated in any convenient frame, such as the CM frame of the overall production process. It is understood, of course, that the matrix elements on the right side of (6.7) are to be evaluated in the rest frame of the quarkonium.

D. S-wave Production

We now apply the factorization formalism to the production of S-wave quarkonium through relative order v^2 . For definiteness, we use the lowest-lying S-wave levels of charmonium for the purpose of illustration. Of course, the results that we give generalize immediately to other S-wave quarkonium systems. According to (6.4), the cross section for the

inclusive production of S-wave charmonium is

$$\sigma(\eta_c) = \frac{F_1(^1S_0)}{M^2} \langle 0 | \mathcal{O}_1^{\eta_c}(^1S_0) | 0 \rangle + \frac{G_1(^1S_0)}{M^4} \langle 0 | \mathcal{P}_1^{\eta_c}(^1S_0) | 0 \rangle + O(v^3\sigma), \quad (6.8a)$$

$$\sigma(\psi) = \frac{F_1(^3S_1)}{M^2} \langle 0 | \mathcal{O}_1^\psi(^3S_1) | 0 \rangle + \frac{G_1(^3S_1)}{M^4} \langle 0 | \mathcal{P}_1^\psi(^3S_1) | 0 \rangle + O(v^3\sigma). \quad (6.8b)$$

The vacuum-saturation approximation (6.6) can be used to reduce the 4-fermion matrix elements to products of matrix elements between the vacuum and the quarkonium state. These can, in turn, be related to the quarkonium wavefunctions given in Section III D. Finally, heavy-quark spin symmetry can be used to reduce the matrix elements to the same three nonperturbative parameters that appear in charmonium decay: $|\overline{R_{\eta_c}}|^2$, $|\overline{R_\psi}|^2$, and $\text{Re}(\overline{R_S^* \nabla^2 R_S})$. Taking into account factors of $2J + 1$ for the number of spin states, we find that the cross sections are

$$\sigma(\eta_c) = \frac{N_c F_1(^1S_0)}{2\pi M^2} |\overline{R_{\eta_c}}|^2 - \frac{N_c G_1(^1S_0)}{2\pi M^4} \text{Re}(\overline{R_S^* \nabla^2 R_S}) + O(v^3\sigma), \quad (6.9a)$$

$$\sigma(\psi) = \frac{3N_c F_1(^3S_1)}{2\pi M^2} |\overline{R_\psi}|^2 - \frac{3N_c G_1(^3S_1)}{2\pi M^4} \text{Re}(\overline{R_S^* \nabla^2 R_S}) + O(v^3\sigma). \quad (6.9b)$$

If we require only accuracy to leading order in v , then we can simplify the production rates in (6.9) further by dropping the terms proportional to $\text{Re}(\overline{R_S^* \nabla^2 R_S})$ and replacing $\overline{R_{\eta_c}}$ and $\overline{R_\psi}$ by their weighted average $\overline{R_S}$. We then recover the familiar factorization formulas used in most previous work:

$$\sigma(\eta_c) = \frac{N_c F_1(^1S_0)}{2\pi M^2} |\overline{R_S}|^2 + O(v^2\sigma), \quad (6.10a)$$

$$\sigma(\psi) = \frac{3N_c F_1(^3S_1)}{2\pi M^2} |\overline{R_S}|^2 + O(v^2\sigma). \quad (6.10b)$$

In applying the factorization formula (6.4), one should keep in mind that the short-distance coefficients $F_n(\Lambda)$ depend not only on $\alpha_s(M)$ but also on dimensionless ratios of kinematic variables. For example, in the case of production of heavy quarkonium at large transverse momentum p_T , the coefficients $F_n(\Lambda)$ depend strongly on p_T^2/M^2 . In determining the relative importance of the various terms in (6.4), one must take into account not only the size of the matrix element and the leading power of $\alpha_s(M)$ in the short-distance coefficient,

but also the dependence of $F_n(\Lambda)$ on dimensionless ratios of kinematic variables. The terms given explicitly in (6.8) may not be the dominant contributions to the cross sections if the coefficients of the matrix elements are sufficiently suppressed relative to the coefficients of other matrix elements that are of higher order in v .

E. P-wave Production

We next apply the factorization formalism to the production of P-wave quarkonium to leading order in v , using the lowest-lying P-wave levels of charmonium for the purpose of illustration. According to our factorization formula (6.4), the inclusive production rates for P-wave charmonium are

$$\sigma(h_c) = \frac{F_1(^1P_1)}{M^4} \langle 0 | \mathcal{O}_1^{h_c} (^1P_1) | 0 \rangle + \frac{F_8(^1S_0)}{M^2} \langle 0 | \mathcal{O}_8^{h_c} (^1S_0) | 0 \rangle + O(v^2\sigma), \quad (6.11a)$$

$$\begin{aligned} \sigma(\chi_{cJ}) &= \frac{F_1(^3P_J)}{M^4} \langle 0 | \mathcal{O}_1^{\chi_{cJ}} (^3P_J) | 0 \rangle + \frac{F_8(^3S_1)}{M^2} \langle 0 | \mathcal{O}_8^{\chi_{cJ}} (^3S_1) | 0 \rangle \\ &+ O(v^2\sigma), \quad J = 0, 1, 2. \end{aligned} \quad (6.11b)$$

The vacuum-saturation approximation (6.6) can be applied to the color-singlet matrix elements to express them in terms of vacuum-to-quarkonium matrix elements. These matrix elements can be expressed in terms of regularized derivatives of radial wavefunctions at the origin by using (3.19). Because of heavy-quark spin symmetry, they can all be replaced, without loss of accuracy, by their weighted average $\overline{R'_P}$. Heavy-quark spin symmetry also implies that the color-octet matrix elements in (6.11) are proportional to $2J + 1$, up to corrections of relative order v^2 . Thus, the P-wave charmonium production rates can all be expressed in terms of the two nonperturbative parameters $|\overline{R'_P}|^2$ and $\langle 0 | \mathcal{O}_8^{h_c} (^1S_0) | 0 \rangle$ (or, alternatively, the average over the P-wave states of $3/(2J + 1)$ times the color-octet matrix elements):

$$\sigma(h_c) = \frac{9N_c F_1(^1P_1)}{2\pi M^4} |\overline{R'_P}|^2 + \frac{F_8(^1S_0)}{M^2} \langle 0 | \mathcal{O}_8^{h_c} (^1S_0) | 0 \rangle + O(v^2\sigma), \quad (6.12a)$$

$$\begin{aligned} \sigma(\chi_{cJ}) &= \frac{(2J + 1)3N_c F_1(^3P_J)}{2\pi M^4} |\overline{R'_P}|^2 + \frac{(2J + 1)F_8(^3S_1)}{3M^2} \langle 0 | \mathcal{O}_8^{h_c} (^1S_0) | 0 \rangle \\ &+ O(v^2\sigma), \quad J = 0, 1, 2. \end{aligned} \quad (6.12b)$$

Note that the color-octet matrix element $\langle 0 | \mathcal{O}_8^{h_c}({}^1S_0) | 0 \rangle$ in (6.12) cannot be identified with the decay matrix element $\langle h_c | \mathcal{O}_8({}^1S_0) | h_c \rangle$ in (4.7).

The first application of the factorization formulas (6.12) was to the inclusive production of P-wave charmonium states in B -meson decay [24]. The factorization formulas were given in the form

$$\begin{aligned} \Gamma(b \rightarrow h_c + X) &= H_1 \hat{\Gamma}_1 (b \rightarrow c\bar{c}({}^1P_1) + X, \mu) \\ &\quad + 3 H'_8(\mu) \hat{\Gamma}_8 (b \rightarrow c\bar{c}({}^1S_0) + X) , \end{aligned} \quad (6.13a)$$

$$\begin{aligned} \Gamma(b \rightarrow \chi_{cJ} + X) &= H_1 \hat{\Gamma}_1 (b \rightarrow c\bar{c}({}^3P_J) + X, \mu) \\ &\quad + (2J + 1) H'_8(\mu) \hat{\Gamma}_8 (b \rightarrow c\bar{c}({}^3S_1) + X) . \end{aligned} \quad (6.13b)$$

The coefficients $\hat{\Gamma}_1$ and $\hat{\Gamma}_8$ are proportional to the production rates for on-shell $Q\bar{Q}$ pairs in color-singlet P-wave and color-octet S-wave states, respectively. The factors H_1 and H'_8 can be expressed in terms of NRQCD matrix elements divided by appropriate factors of the heavy-quark mass:

$$H_1 = \frac{1}{3M^4} \langle 0 | \mathcal{O}_1^{h_c}({}^1P_1) | 0 \rangle, \quad (6.14a)$$

$$H'_8(\Lambda) = \frac{1}{3M^2} \langle 0 | \mathcal{O}_8^{h_c}({}^1S_0) | 0 \rangle. \quad (6.14b)$$

The definitions (6.14a) and (6.14b) were chosen in Ref. [24] so that H_1 and H'_8 would coincide as closely as possible with the decay matrix elements H_1 and H_8 . Using the vacuum-saturation approximation (6.6), we see that the definition of H_1 given in (6.14a) is equal to that given in (4.9a), up to corrections of relative order v^4 . A crude estimate for $H_8(M)$ in terms of H_1 is given in (3.30). A similar estimate of $H'_8(M)$ in terms of H_1 can be obtained by solving the evolution equation (6.5) and assuming that $\langle 0 | \mathcal{O}_8^{h_c}({}^1S_0; \Lambda) | 0 \rangle$ can be neglected at some initial scale $\Lambda = \Lambda_0$. With the normalizations in (4.9b) and (6.14b), the resulting estimates for $H_8(M)$ and $H'_8(M)$ are equal. However, there is no apparent rigorous relation between these two matrix elements.

As we have already remarked in connection with the decay matrix elements, the factors of $1/M$ in (6.14a) and (6.14b) are more properly associated with the operator coefficients,

since they involve short-distance physics at distance scales of order $1/\Lambda$ or less. Therefore, the factorization formulas (6.12) are preferable to the forms given in (6.13).

In Ref. [24], which discusses the decay of a B meson into a charmonium state, the NRQCD cutoff Λ was set equal to the scale of the large momentum transfer in the process, which is the bottom-quark mass m_b . This choice of cutoff is inappropriate because the NRQCD evolution equation (6.5) accurately reflects the behavior of full QCD only for cutoffs Λ that are less than M . That is, the NRQCD evolution equation cannot be used to sum logarithms of Q^2/M^2 , where Q^2 is the large momentum transfer in a production process. Therefore, a more appropriate choice of NRQCD cutoff for the process analyzed in [24] is $\Lambda = m_c$, where $m_c = M$ is the charmed-quark mass. Note, however, that a change of NRQCD cutoff from m_b to m_c does not affect the short-distance coefficients in the leading-order calculation presented in [24], and is, in general, insignificant numerically.

VII. DISCUSSION AND OUTLOOK

The factorization approach that we have developed in this paper provides a systematic theoretical framework for understanding the annihilation and production of heavy quarkonium. In this section, we discuss the relation between our approach and previous models for quarkonium production and annihilation. We also summarize the current status of theoretical calculations of annihilation rates and production cross sections.

A. Comparison with Previous Approaches

We have presented a rigorous formalism for calculating the inclusive annihilation rates of heavy quarkonia. It is based on the use of NRQCD to separate the annihilation rate into short-distance parts, involving distance scales on the order of $1/M$, and long-distance parts. The short-distance parts are identified with the imaginary parts of coefficients in the NRQCD lagrangian, and can be computed as perturbation expansions in $\alpha_s(M)$. The long-distance parts are expressed as matrix elements of 4-fermion operators in NRQCD and can be computed nonperturbatively by using lattice simulations. We have also developed an analogous formalism for computing inclusive production rates of heavy quarkonia in processes involving large momentum transfers. The cross sections are factored into short-distance parts, which can be computed perturbatively, and long-distance parts, which are expressed as NRQCD matrix elements.

The factorization approach provides a firm theoretical foundation for calculations of the annihilation and production rates for heavy quarkonium. It can be used to assess the degree of validity and the limitations of models used in previous work on heavy quarkonium production and annihilation. The most thoroughly developed model for the calculation of production rates is the “color-singlet model” [30,31,32,33]. Most calculations of annihilation rates have also been carried out within this model. In the color-singlet model, the quarkonium state is modeled by a color-singlet $Q\bar{Q}$ pair that is in the appropriate angular-momentum

state and has vanishing relative momentum. Nonperturbative effects are assumed to factor into a single nonperturbative quantity that is proportional to the square of the radial wavefunction, or one of its derivatives, evaluated at the origin.

The factorization formalism represents a significant advance over the color-singlet model in several respects. First, it provides a systematic framework for calculating perturbative corrections to the short-distance factors to arbitrarily high orders in α_s . The infrared divergences that are encountered at any order of the perturbation expansion can be factored into specific nonperturbative matrix elements. Perturbative calculations in the color-singlet model are based on the assumption that all infrared divergences can be factored into a single nonperturbative quantity. In the case of S-waves, calculations at next-to-leading order in α_s (NLO) provide empirical support for the assumption that long-distance effects can be factored into the quantity $|R_S(0)|^2$. Our formalism reveals that this assumption is, in fact, correct for any specific S-wave process in the nonrelativistic limit to all orders in α_s . It has often been assumed, in addition, that the same quantity $|R_S(0)|^2$ describes processes involving both the 0^{-+} and 1^{--} S-wave states. Our formalism shows that this additional assumption is correct only up to corrections of relative order v^2 . The assumption that the same quantity $|R_S(0)|^2$ describes annihilation into light hadrons and electromagnetic annihilation also fails at relative order v^2 , as does the assumption that the same quantity $|R_S(0)|^2$ describes both annihilation and production processes. In the case of P-waves, explicit calculations of the decay rates into light hadrons reveal that the assumption of a single long-distance factor $|R'_P(0)|^2$ fails at leading order in α_s (LO) for h_c and χ_{c1} [8] and at NLO for χ_{c0} and χ_{c2} [7]. In the context of our formalism, these results follow simply from the existence of a second independent matrix element that contributes to the annihilation rates of P-wave quarkonia in the nonrelativistic limit.

The factorization formalism also improves upon the color-singlet model by allowing the systematic calculation of relativistic corrections to annihilation and production rates. Relativistic corrections are incorporated by including nonperturbative matrix elements that scale as higher powers of v . In the case of S-waves, our formalism for computing the v^2 corrections

is similar at leading order in α_s to a model for relativistic corrections developed by Keung and Muzinich [34]. The major differences are that the factorization formalism provides non-perturbative definitions for the long-distance factors, it allows the short-distance coefficients to be calculated beyond leading order in α_s , and it can be used to treat corrections of order v^3 and higher.

Another advantage of the factorization formalism is that it provides unambiguous field-theoretic definitions of the long-distance factors in annihilation and production rates. This allows one to compute them nonperturbatively using, for example, lattice simulations of NRQCD. Previous approaches have relied either on determining the long-distance factors phenomenologically or on relating them to potential-model wavefunctions. Both of these approaches are of limited utility. The purely phenomenological approach can be applied only in situations in which the number of accurately-measured experimental observables is greater than the number of nonperturbative matrix elements. Potential-model estimates can be used for color-singlet matrix elements that have simple potential-model analogs, but they cannot be used for other matrix elements, such as the color-octet matrix elements that contribute to the annihilation of P-wave states into light hadrons at leading order in v . It is also difficult to gauge the accuracy of potential-model estimates in the absence of a rigorous connection to QCD. Since our formalism provides unambiguous definitions of the long-distance factors in annihilation and production processes, it allows us to quantify relations between these matrix elements and Coulomb-gauge wavefunctions in NRQCD. It also allows us to quantify the differences between matrix elements for decays into light hadrons and matrix elements for decays into electromagnetic final states, as well as the differences between annihilation matrix elements and production matrix elements.

A final advantage of the factorization formalism is that it takes into account the complete Fock-space structure of the quarkonium. In the color-singlet model, the quarkonium is assumed to be simply a $Q\bar{Q}$ pair in a color-singlet state with definite angular-momentum quantum numbers $^{2S+1}L_J$. However, a quarkonium also has a probability of order v^2 to be in a $Q\bar{Q}g$ Fock state, and it has probabilities of order v^4 or smaller for the higher Fock states.

In the case of P-waves, the factorization formalism reveals that the $Q\bar{Q}g$ component can play just as important a role in annihilation and in production as the dominant $Q\bar{Q}$ component. In the case of S-waves, the higher Fock states can be ignored in the nonrelativistic limit, and even at relative order v^2 , but the factorization formalism indicates that they do contribute at relative order v^3 .

The factorization formalism for describing the annihilation of heavy quarkonia is in many ways similar to the operator-product-expansion formalism for calculating the inclusive decay rates of heavy-light mesons [35]. These decay rates can be factored into short distance parts, which involve the weak decay of a heavy quark or its weak annihilation with an antiquark in the meson, and long-distance parts, which can be expressed as NRQCD matrix elements. The main difference between heavy-quarkonium annihilation and heavy-light meson decay is in the relative importance of the various matrix elements. Since the typical momentum of a heavy quark in a heavy-light meson is of order Λ_{QCD} and is independent of M , the relative importance of matrix elements is determined strictly by the dimension of the operator.

Operator-product-expansion methods have also been used to treat exclusive decays of heavy quarkonium into light hadrons at leading order in v [36]. The NRQCD formalism might prove to be useful in extending such analyses to include relativistic corrections. In exclusive processes, a factorization theorem holds, not only for the decay rate, but also for the decay amplitude. Thus, just as in the case of electromagnetic annihilation, the relevant NRQCD matrix elements for exclusive decays are vacuum-to-quarkonium matrix elements of color-singlet operators of the form $\chi^\dagger \mathcal{K}_n \psi$.

Operator-product-expansion methods have also been used in a completely different context in heavy quarkonium physics [3,37]. These methods have been used to treat the interactions of heavy quarkonium with light hadrons whose momenta are small compared to the scale Mv of quarkonium structure. Voloshin [38] has used this approach to calculate nonperturbative corrections to quarkonium annihilation rates that are proportional to the gluon condensate. In our factorization formula, the gluon-condensate contribution would

appear in the long-distance matrix element. In some of the cases considered by Voloshin, the corresponding short-distance part involves the annihilation of the $Q\bar{Q}$ pair in a color-octet state. His approach can therefore be used as a framework for estimating the matrix elements of color-octet operators.

The general factorization formula (6.4) for the production cross section of any specific quarkonium state H takes into account the short-distance production of color-singlet $Q\bar{Q}$ pairs and color-octet $Q\bar{Q}$ pairs in all angular-momentum states. In this respect, our approach has some elements in common with the “color-evaporation model” for quarkonium production [39]. In this model, the total inclusive cross section, summed over all quarkonium states H , is obtained by integrating the perturbative cross section for inclusive $Q\bar{Q}$ production from the quark threshold $2M$ up to the physical threshold for the production of a pair of heavy-light mesons. No constraints are imposed on the color and angular momentum states of the $Q\bar{Q}$ pair. Under the hypothesis of “semilocal duality”, the nonperturbative QCD effects that are responsible for the formation of a color-singlet bound state containing the $Q\bar{Q}$ pair are assumed to be negligible after one sums over all quarkonium states H . In the factorization approach, the nonperturbative effects are not neglected, but are factored into long-distance matrix elements $\langle 0|\mathcal{O}_n^H|0\rangle$. In the color-evaporation model, the production cross section for a specific quarkonium state H is obtained by multiplying the total quarkonium cross section by a purely phenomenological fraction f_H . The relative production rates of different quarkonium states are, therefore, not predicted. In the factorization approach, the relative production rates can be calculated by using perturbative QCD, once the values of the dominant matrix elements $\langle 0|\mathcal{O}_n^H|0\rangle$ have been determined.

B. Present Status of Calculations

The possible applications of the factorization formalism for heavy-quarkonium annihilation and production are almost limitless, since heavy quarkonia play a role in so many high energy processes. In order to highlight some of these applications, we discuss below

the present status of calculations of annihilation and production rates.

In the case of S-wave decays, NLO perturbative corrections have been calculated for all the annihilation rates. In many cases, the NLO corrections are uncomfortably large. In order to develop a better understanding of the origin of these large corrections, it would be desirable to have calculations at NNLO, at least for the simplest processes $\psi \rightarrow e^+e^-$ and $\eta_c \rightarrow \gamma\gamma$. Relativistic corrections to the S-wave annihilation rates have been studied by Keung and Muzinich [34]. From their results, one can extract the coefficients of all the matrix elements of relative order v^2 at leading order in α_s . A phenomenological analysis of the decay rates of the lowest-lying S-wave states of charmonium, including the next-to-leading order corrections in $\alpha_s(M)$ and the corrections of relative order v^2 , is in progress [40].

In the case of P-wave decays, complete NLO perturbative corrections are available only for the electromagnetic decays $\chi_{c0} \rightarrow \gamma\gamma$ and $\chi_{c2} \rightarrow \gamma\gamma$. For the decays of P-wave states into light hadrons, complete results are known only to order α_s^2 [10]. The coefficients of $|\overline{R}'_P|^2$ have been calculated to order α_s^3 [7], but they contain logarithmic infrared divergences that should be factored into matrix elements of the operators $\mathcal{O}_8(^1S_0)$ and $\mathcal{O}_8(^3S_1)$. There are constants under the logarithms that should also be factored into the matrix elements. Unfortunately, these constants cannot be determined readily from the existing calculations. The relativistic corrections to P-wave annihilation rates have not yet been analyzed.

In the case of D-wave decays, the only complete LO calculations are those for the electromagnetic decays of the 3D_1 state into e^+e^- and the 1D_2 state into $\gamma\gamma$ [3]. For the decay of the 1D_2 state into light hadrons, the coefficient of the matrix element corresponding to $|R''_D(0)|^2$ has been calculated at LO [3]. For the decays of the 3D_J states into light hadrons, only the logarithmic infrared divergence in the coefficient of $|R''_D(0)|^2$ has been extracted [41]. This divergence should be factored into other matrix elements that contribute to the annihilation rate in the nonrelativistic limit. These matrix elements can be identified by using the methods of Section III A, and their coefficients can be calculated by using the methods illustrated in Appendix A.

The status of calculations of the production of heavy quarkonium has been reviewed recently in Ref. [23], although many aspects of that review are superseded by the developments described in the present paper. In the case of S-waves, most production processes have been computed only to LO. The only processes for which complete NLO calculations are available are ψ and η_c production in B -meson decay [42] and inclusive η_c production in hadron collisions [43,23]. It would be desirable to have calculations of complete NLO corrections for more production processes, in order to develop a better understanding of the size and behavior of the perturbative corrections. It is also important to calculate the relativistic corrections, which are expected to be typically on the order of 30% for charmonium. Relativistic corrections have been calculated for the photoproduction of the ψ [44] within the model of Keung and Muzinich [34]. The factorization formalism can be used to express those results in terms of well-defined NRQCD matrix elements.

For the production of quarkonia at large transverse momentum p_T , the contributions that are leading in $1/p_T$ sometimes come from beyond leading order in the perturbation expansion, and they can be computed without complete calculations of the NLO or NNLO corrections. These contributions come from fragmentation and can be expressed in terms of process-independent fragmentation functions $D_{i \rightarrow H}(z, \mu)$ for a parton i with invariant mass μ to produce a jet containing the quarkonium H with light-cone momentum fraction z . The fragmentation contribution to a production cross section sometimes appears in a LO calculation, but it often appears first at NLO and sometimes even at NNLO. The fragmentation functions for producing S-wave quarkonia from the fragmentation of gluons [45] and heavy quarks [46] have been calculated at LO in α_s .

For P-wave quarkonia, there are many production processes for which complete calculations are not even available at LO. For most processes, the coefficient of $|\overline{R}_P|^2$ has been calculated [23]. Complete LO calculations, including the coefficient of $\langle 0 | \mathcal{O}_8^H | 0 \rangle$, are available only for the production of P-wave charmonium in B -meson decays [24], Υ decays [47], gluon fragmentation [48], and charm fragmentation [49]. Relativistic corrections to P-wave production processes have not been studied.

In the case of production of D -wave quarkonia, the only perturbative calculations that are available are those for the coefficients of $|R_D''(0)|^2$ in the decay rates for $Z^0 \rightarrow H\gamma$, where H represents any of the 1D_2 or 3D_J states [50].

In the factorization approach, nonperturbative long-distance effects are organized systematically into well-defined NRQCD matrix elements. This allows one to go beyond potential model estimates or phenomenological determinations of the long-distance factors. Instead, they can be calculated from first principles using lattice simulations of NRQCD. Such calculations are still in their infancy. At present, the only vacuum-to-quarkonium matrix elements that have been calculated are $\langle 0|\chi^\dagger\psi|\eta_c\rangle$, $\langle 0|\chi^\dagger\boldsymbol{\sigma}\psi|\psi\rangle$, and $\langle 0|\chi^\dagger\overleftrightarrow{\mathbf{D}}\chi|h_c\rangle$, and their analogs for the bottomonium system [51,52]. The only 4-fermion matrix elements that have been calculated thus far are $\langle \eta_c|\mathcal{O}_1(^1S_0)|\eta_c\rangle$, $\langle h_c|\mathcal{O}_1(^1P_1)|h_c\rangle$, and $\langle h_c|\mathcal{O}_8(^1S_0)|h_c\rangle$ and their analogs for the bottomonium system [52]. Thus far, all matrix elements have been calculated only up to corrections of relative order v^2 and in the absence of dynamical light quarks. Production matrix elements are much more difficult to calculate through lattice simulations, unless they can be related to annihilation matrix elements through the vacuum-saturation approximation.

C. Concluding Remarks

Heavy-quark mesons have long been the best understood of hadrons. Until recently, our understanding has been based almost exclusively on phenomenological quark potential models that are motivated by QCD. Now, lattice QCD simulations are providing systematic analyses that are based directly upon the QCD lagrangian [53]. Heavy-quark systems are particularly well-suited to lattice simulations, and, consequently, they are now of central importance to our exploration of nonperturbative QCD. This new role for quarkonium studies, as a rigorous testing ground for nonperturbative QCD, demands a much higher degree of rigor than was necessary in older phenomenological analyses. Approximations are necessary in tackling most hard problems, but it is essential in a fundamental analysis that there be

systematic procedures for improving the approximations. In this paper, we have developed a formalism for studying annihilation decays of heavy-quark mesons that meets this standard. With our formalism, we can improve upon the nonrelativistic quark potential model by including relativistic corrections in a systematic way. We can also go beyond the quark model to include the dynamical effects of gluons. Thus, we can, for the first time, begin to confront the full richness of nonperturbative QCD in analyses that are systematic and rigorous.

ACKNOWLEDGMENTS

One of us (G.T.B.) would like to thank D. Sinclair for numerous useful discussions. Another one of us (E.B.) would like to express his appreciation to the Fermilab Theory Group for its hospitality while this paper was being written. This work was supported in part by the U.S. Department of Energy, Division of High Energy Physics, under Contract W-31-109-ENG-38 and under Grant DE-FG02-91-ER40684, and by the National Science Foundation.

APPENDIX A: COEFFICIENTS OF 4-FERMION OPERATORS

The coefficients in the lagrangian for nonrelativistic QCD can be determined by matching scattering amplitudes in NRQCD with those in full QCD [14]. In this Appendix, we use these techniques to determine the coefficients for some of the 4-fermion operators that contribute to quarkonium annihilation rates. In Section A 1, we illustrate the method by calculating the coefficients of dimension-6 operators to order α_s . In Section A 2, we apply the method to calculate the imaginary parts of the coefficients of dimension-6 and dimension-8 operators to order α_s^2 . In Section A 3, we demonstrate how the imaginary parts of some of the coefficients can be extracted at next-to-leading order from existing calculations of the decay rates of bound states. We also record coefficients that can be extracted from existing calculations in the literature. Finally, in Section A 4, we give the corresponding coefficients for electromagnetic annihilation rates.

1. Coefficients at Order α_s

We wish to determine the coefficients of the dimension-6 and dimension-8 4-fermion operators at order α_s by using the matching condition (2.18). We consider $Q\bar{Q}$ scattering amplitudes, with the momenta of the heavy quarks and antiquarks small compared to the heavy quark mass M . In full QCD, there are two Feynman diagrams for $Q\bar{Q}$ scattering at tree level. The gluon exchange diagram in Fig. 6(a) is also present in NRQCD. The annihilation diagram in Fig. 6(b) is not present in NRQCD, so its effects must be reproduced by adding 4-fermion terms to the effective lagrangian. We calculate the annihilation contribution to the amplitude for $Q\bar{Q}$ scattering in the center of momentum frame. We take the incoming Q and \bar{Q} to have momenta \mathbf{p} and $-\mathbf{p}$, while the outgoing Q and \bar{Q} have momenta \mathbf{p}' and $-\mathbf{p}'$. By conservation of energy, we have $|\mathbf{p}'| = |\mathbf{p}| \equiv p$.

The scattering amplitude (T-matrix element) in full QCD corresponding to the diagram in Fig. 6(b) is

$$\mathcal{M}_{6(b)} = \frac{\pi\alpha_s}{E^2} \bar{u}(\mathbf{p}')\gamma^\mu T^a v(-\mathbf{p}') \bar{v}(-\mathbf{p})\gamma_\mu T^a u(\mathbf{p}), \quad (\text{A1})$$

where $E = \sqrt{M^2 + p^2}$. We have suppressed the color indices on the 4-component Dirac spinors. Following Ref. [14], we express the 4-component Dirac spinors in the Dirac representation in terms of 2-component Pauli spinors via the substitutions

$$u(\mathbf{p}) = \sqrt{\frac{E+M}{2E}} \begin{pmatrix} \xi \\ \frac{\mathbf{p}\cdot\boldsymbol{\sigma}}{E+M}\xi \end{pmatrix}, \quad (\text{A2a})$$

$$v(-\mathbf{p}) = \sqrt{\frac{E+M}{2E}} \begin{pmatrix} \frac{(-\mathbf{p})\cdot\boldsymbol{\sigma}}{E+M}\eta \\ \eta \end{pmatrix}, \quad (\text{A2b})$$

where ξ and η are 2-component spinors with suppressed color indices. The Dirac spinors $u(\mathbf{p}')$ and $v(-\mathbf{p}')$ have similar expressions in terms of Pauli spinors ξ' and η' . The spinors (A2a) and (A2b) represent fermion states with the standard nonrelativistic normalization. Expanding to second order in the velocity $v = p/E$, we find that the annihilation contribution to the scattering amplitude (A1) from full QCD reduces to

$$\mathcal{M}_{6(b)} = -\frac{\pi\alpha_s}{M^2} \left((1-v^2)\xi'^\dagger \boldsymbol{\sigma} T^a \eta' \cdot \eta^\dagger \boldsymbol{\sigma} T^a \xi - \frac{1}{2}(v^i v^j + v'^i v'^j)\xi'^\dagger \sigma^i T^a \eta' \eta^\dagger \sigma^j T^a \xi \right), \quad (\text{A3})$$

where $\mathbf{v} = \mathbf{p}/E$ and $\mathbf{v}' = \mathbf{p}'/E$. It is convenient to suppress the spinors and write the above matrix element as a direct product of color matrices multiplied by a direct product of spin matrices:

$$\mathcal{M}_{6(b)} = -\frac{\pi\alpha_s}{M^2} (T^a \otimes T^a) \left[(1-v^2)\sigma^i \otimes \sigma^i - \frac{1}{2}(v^i v^j + v'^i v'^j)\sigma^i \otimes \sigma^j \right]. \quad (\text{A4})$$

One can read off the dimension-6 term in the scattering amplitude in terms of the parameters of NRQCD by substituting ξ , ξ'^\dagger , η' , and η^\dagger for ψ , ψ^\dagger , χ , and χ^\dagger in the effective lagrangian (2.9):

$$\begin{aligned} \mathcal{M}_{d=6} &= \frac{1}{M^2} (1 \otimes 1) \left[f_1(^1S_0) 1 \otimes 1 + f_1(^3S_1) \sigma^i \otimes \sigma^i \right] \\ &+ \frac{1}{M^2} (T^a \otimes T^a) \left[f_8(^1S_0) 1 \otimes 1 + f_8(^3S_1) \sigma^i \otimes \sigma^i \right]. \end{aligned} \quad (\text{A5})$$

Comparing (A4) and (A5), we find that only one of the four terms in (2.9) has a nonvanishing coefficient at order α_s :

$$f_8(^3S_1) = -\pi\alpha_s(M). \quad (\text{A6})$$

The coefficients of the remaining three terms in (2.9) are of order α_s^2 .

To determine the dimension-8 coefficients, we need the scattering amplitudes from the term (2.11) in the effective lagrangian:

$$\begin{aligned} \mathcal{M}_{d=8} = \frac{1}{M^2} (1 \otimes 1) & \left[f_1(^1P_1) \mathbf{v}' \cdot \mathbf{v} 1 \otimes 1 + \frac{f_1(^3P_1) + f_1(^3P_2)}{2} \mathbf{v}' \cdot \mathbf{v} \sigma^i \otimes \sigma^i \right. \\ & + \frac{f_1(^3P_0) - f_1(^3P_2)}{3} \mathbf{v}' \cdot \boldsymbol{\sigma} \otimes \mathbf{v} \cdot \boldsymbol{\sigma} + \frac{f_1(^3P_2) - f_1(^3P_1)}{2} \mathbf{v} \cdot \boldsymbol{\sigma} \otimes \mathbf{v}' \cdot \boldsymbol{\sigma} \\ & + g_1(^1S_0) v^2 1 \otimes 1 + \frac{3g_1(^3S_1) - g_1(^3S_1, ^3D_1)}{3} v^2 \sigma^i \otimes \sigma^i \\ & \left. + \frac{g_1(^3S_1, ^3D_1)}{2} (v^i v^j + v'^i v'^j) \sigma^i \otimes \sigma^j \right] + \dots \end{aligned} \quad (\text{A7})$$

There are similar terms with color structure $T^a \otimes T^a$ and coefficients f_8 and g_8 . Comparing with (A4), we find that

$$g_8(^3S_1) = \frac{4\pi}{3}\alpha_s(M), \quad (\text{A8a})$$

$$g_8(^3S_1, ^3D_1) = \pi\alpha_s(M). \quad (\text{A8b})$$

The color-singlet coefficients g_1 and the remaining color-octet coefficients vanish at this order in $\alpha_s(M)$.

2. Imaginary Parts at Order α_s^2

We now turn to the calculation of the imaginary parts of the coefficients at order α_s^2 . They can be determined by matching the imaginary parts of $Q\bar{Q}$ scattering amplitudes in full QCD and NRQCD in accordance with (2.18). In full QCD, the annihilation contributions to the imaginary parts at order α_s^2 come from the one-loop diagrams in Fig. 7. We will determine the imaginary parts of the coefficients of the dimension-6 operators in (2.9). We will also determine the imaginary parts of the coefficients of the dimension-8 operators that contribute to the annihilation of P-wave states at leading order in v and S-wave states through relative order v^2 . The dimension-8 terms in the lagrangian are given in (2.11). To

determine the coefficients, we consider $Q\bar{Q}$ scattering in the center of momentum frame, with the Q and \bar{Q} momenta small compared to the heavy-quark mass M . We calculate the imaginary parts of the diagrams in Fig. 7 in Feynman gauge. After making the substitutions (A2) for the Dirac spinors, we expand in powers of the velocity v .

Below, we list the results for the imaginary parts of each of the diagrams, suppressing the spinors as in (A4). The diagrams in Fig. 7(a) and 7(b) yield, on expansion through second order in the velocity v ,

$$\begin{aligned} \text{Im } \mathcal{M}_{7(a)} = & \frac{\pi\alpha_s^2}{2M^2} (T^a T^b \otimes T^b T^a) \left[\left(1 - \frac{4}{3}v^2 + \frac{1}{3}\mathbf{v} \cdot \mathbf{v}'\right) 1 \otimes 1 \right. \\ & + \left(\frac{1}{3} - \frac{1}{5}v^2 + \frac{2}{5}\mathbf{v} \cdot \mathbf{v}'\right) \sigma^i \otimes \sigma^i \\ & \left. + \left(\frac{2}{5}v^i v'^j + \frac{11}{15}v^i v^j - \frac{11}{30}(v^i v^j + v'^i v'^j)\right) \sigma^i \otimes \sigma^j \right], \end{aligned} \quad (\text{A9a})$$

$$\begin{aligned} \text{Im } \mathcal{M}_{7(b)} = & \frac{\pi\alpha_s^2}{2M^2} (T^a T^b \otimes T^a T^b) \left[\left(1 - \frac{4}{3}v^2 - \frac{1}{3}\mathbf{v} \cdot \mathbf{v}'\right) 1 \otimes 1 \right. \\ & - \left(\frac{1}{3} - \frac{1}{5}v^2 - \frac{2}{5}\mathbf{v} \cdot \mathbf{v}'\right) \sigma^i \otimes \sigma^i \\ & \left. + \left(\frac{2}{5}v^i v'^j + \frac{11}{15}v^i v^j + \frac{11}{30}(v^i v^j + v'^i v'^j)\right) \sigma^i \otimes \sigma^j \right]. \end{aligned} \quad (\text{A9b})$$

The color matrices can be simplified as follows:

$$T^a T^b \otimes T^b T^a = \frac{C_F}{2N_c} 1 \otimes 1 + \frac{N_c^2 - 2}{2N_c} T^a \otimes T^a, \quad (\text{A10a})$$

$$T^a T^b \otimes T^a T^b = \frac{C_F}{2N_c} 1 \otimes 1 - \frac{1}{N_c} T^a \otimes T^a, \quad (\text{A10b})$$

where $C_F = (N_c^2 - 1)/(2N_c)$ is the Casimir for the fundamental representation. The diagrams in Fig. 7(c) and 7(d), which involve the triple-gluon vertex, yield

$$\text{Im } \mathcal{M}_{7(c)} = \frac{N_c \pi \alpha_s^2}{6M^2} (T^a \otimes T^a) \left[\left(1 - \frac{11}{10}v^2\right) \sigma^i \otimes \sigma^i - \left(\frac{1}{5}v^i v'^j + \frac{1}{2}v'^i v'^j\right) \sigma^i \otimes \sigma^j \right], \quad (\text{A11a})$$

$$\text{Im } \mathcal{M}_{7(d)} = \frac{N_c \pi \alpha_s^2}{6M^2} (T^a \otimes T^a) \left[\left(1 - \frac{11}{10}v^2\right) \sigma^i \otimes \sigma^i - \left(\frac{1}{2}v^i v'^j + \frac{1}{5}v'^i v'^j\right) \sigma^i \otimes \sigma^j \right]. \quad (\text{A11b})$$

From the gluon-loop diagram in Fig. 7(e) combined with the associated ghost loop diagram in Fig. 7(f), we obtain

$$\text{Im} \left(\mathcal{M}_{7(e)} + \mathcal{M}_{7(f)} \right) = -\frac{5N_c\pi\alpha_s^2}{12M^2} (T^a \otimes T^a) \left[(1-v^2)\sigma^i \otimes \sigma^i - \frac{1}{2}(v^i v^j + v^i v'^j)\sigma^i \otimes \sigma^j \right]. \quad (\text{A12})$$

The quark loop diagram in Fig. 7(g) gives

$$\text{Im} \mathcal{M}_{7(g)} = \frac{n_f\pi\alpha_s^2}{6M^2} (T^a \otimes T^a) \left[(1-v^2)\sigma^i \otimes \sigma^i - \frac{1}{2}(v^i v^j + v^i v'^j)\sigma^i \otimes \sigma^j \right]. \quad (\text{A13})$$

Adding the amplitudes (A9), and (A11)–(A13) and comparing with (A5), we can read off the imaginary parts of the coefficients of the dimension-6 operators:

$$\text{Im} f_1(^1S_0) = \frac{\pi C_F}{2N_c} \alpha_s^2(M), \quad (\text{A14a})$$

$$\text{Im} f_8(^1S_0) = \frac{\pi(N_c^2 - 4)}{4N_c} \alpha_s^2(M), \quad (\text{A14b})$$

$$\text{Im} f_8(^3S_1) = \frac{\pi n_f}{6} \alpha_s^2(M). \quad (\text{A14c})$$

The imaginary part of the coefficient $f_1(^3S_1)$ vanishes at order α_s^2 . Comparing with (A7), we see that the coefficients of the color-singlet dimension-8 operators are

$$\text{Im} f_1(^3P_0) = \frac{3\pi C_F}{2N_c} \alpha_s^2(M), \quad (\text{A15a})$$

$$\text{Im} f_1(^3P_2) = \frac{2\pi C_F}{5N_c} \alpha_s^2(M), \quad (\text{A15b})$$

$$\text{Im} g_1(^1S_0) = -\frac{2\pi C_F}{3N_c} \alpha_s^2(M). \quad (\text{A15c})$$

The imaginary parts of the coefficients $f_1(^1P_1)$, $f_1(^3P_1)$, $g_1(^3S_1)$ and $g_1(^3S_1, ^3D_1)$ vanish at order α_s^2 .

3. Imaginary Parts at Higher Order in α_s

According to the matching condition (2.18), the coefficients of the 4-fermion operators can be computed at next-to-leading order in α_s by calculating scattering amplitudes at next-to-leading order in full QCD and equating them to the scattering amplitudes in NRQCD,

calculated to next-to-leading order in α_s . For some of the 4-fermion operators, the imaginary parts of the coefficients can be extracted at next-to-leading order in α_s from calculations of heavy-quarkonium annihilation rates that already exist in the literature.

As an illustration of our factorization approach, we discuss in detail the calculation of $\text{Im } f_1(^1S_0)$ at next-to-leading order in α_s . In order to determine $\text{Im } f_1(^1S_0)$, we consider the matrix element \mathcal{M} for the forward scattering of a $Q\bar{Q}$ pair above threshold in a color-singlet spin-singlet state with relative velocity $2v$. The imaginary part of \mathcal{M} can be expressed as a sum over cuts through the Feynman diagrams for forward scattering. The annihilation contribution to $\text{Im } \mathcal{M}$ is the sum over cuts through gluon and light quark lines only. It has been calculated in full QCD at next-to-leading order in α_s and in the limit $v \rightarrow 0$ by Barbieri *et al.* [5]:

$$\text{Im } \mathcal{M} = \frac{\pi C_F \alpha_s^2(2M)}{M^2} \left\{ 1 + \left[\left(\frac{\pi^2}{2v} + \frac{\pi^2}{4} - 5 \right) C_F + \left(\frac{199}{18} - \frac{13\pi^2}{24} \right) C_A - \frac{8}{9} n_f \right] \frac{\alpha_s}{\pi} \right\}, \quad (\text{A16})$$

where $C_A = N_c$ is the Casimir for the adjoint representation, $\alpha_s(M)$ is the QCD coupling constant in the modified minimal subtraction ($\overline{\text{MS}}$) renormalization scheme for QCD with n_f flavors of light quarks, and M is the perturbative pole mass of the heavy quark. We have corrected apparent errors in Ref. [5] of $2/3$ in the overall coefficient and $1/2$ in the coefficient of the π^2/v term. The next-to-leading order correction contains a Coulomb singularity proportional to $1/v$, which gives an infrared divergence in the limit $v \rightarrow 0$.

In order to determine $\text{Im } f_1(^1S_0)$, we must calculate the corresponding contribution to $\text{Im } \mathcal{M}$ in NRQCD at next-to-leading order in α_s . The relevant Feynman diagrams are shown in Fig. 8. They contain a 4-fermion vertex that corresponds to the term $\psi^\dagger \chi \chi^\dagger \psi$ in the effective lagrangian. The annihilation contribution is the sum over all cuts that pass through that vertex. The Cutkosky rules specify that a cut passing through the 4-fermion vertex is computed by taking the imaginary part of the coefficient $f_1(^1S_0)$ and complex-conjugating the part of the diagram to the right of the cut. The incoming and outgoing states consist of a $Q\bar{Q}$ pair in a color-singlet spin-singlet state with relative velocity $\mathbf{v} \rightarrow 0$.

Explicitly, the in state is

$$|Q\bar{Q}\rangle = \sum_{ij} \frac{1}{\sqrt{N_c}} \delta^{ij} \sum_{mm'} \frac{1}{\sqrt{2}} (i\sigma_2)_{mm'} |Q(\mathbf{p}, m, i)\bar{Q}(-\mathbf{p}, m', j)\rangle, \quad (\text{A17})$$

where $\mathbf{p} = M\mathbf{v}$ is the momentum of the quark in the center of momentum frame. The quark states $|Q(\mathbf{p}, m, i)\rangle$ with momentum \mathbf{p} , spin quantum number $m = \pm 1/2$, and color i have the standard nonrelativistic normalization:

$$\langle Q(\mathbf{p}', m', j) | Q(\mathbf{p}, m, i) \rangle = \delta^{ij} \delta^{mm'} (2\pi)^3 \delta^3(\mathbf{p}' - \mathbf{p}). \quad (\text{A18})$$

For the leading-order diagram in Fig. 8(a), the cut through the 4-fermion vertex gives simply the imaginary part of the coefficient $f_1(^1S_0)/M^2$:

$$\text{Im } \mathcal{M}_{8(a)} = \frac{2N_c \text{Im } f_1(^1S_0)}{M^2}. \quad (\text{A19})$$

It is convenient to calculate the next-to-leading order diagrams in Figs. 8(b) and 8(c) by using Coulomb gauge, since then only Coulomb exchange contributes in the limit $v \rightarrow 0$.

For the diagram in Fig. 8(b), we obtain

$$\left(\text{Im } \mathcal{M} \right)_{8(b)} = \frac{2N_c \text{Im } f_1(^1S_0)}{M^2} (-i4\pi C_F \alpha_s) \int \frac{d^4q}{(2\pi)^4} \frac{1}{\mathbf{q}^2} \frac{1}{E + q_0 - (\mathbf{p} + \mathbf{q})^2/2M + i\epsilon} \frac{1}{E - q_0 - (\mathbf{p} + \mathbf{q})^2/2M + i\epsilon}, \quad (\text{A20})$$

where $E = p^2/2M$. After using contour integration to integrate over the energy q_0 of the exchanged gluon, we find that the contribution reduces to an integral over the gluon's 3-momentum:

$$\left(\text{Im } \mathcal{M} \right)_{8(b)} = \frac{2N_c \text{Im } f_1(^1S_0)}{M^2} 4\pi C_F \alpha_s M \int \frac{d^3q}{(2\pi)^3} \frac{1}{\mathbf{q}^2} \frac{1}{\mathbf{q}^2 + 2\mathbf{p} \cdot \mathbf{q} - i\epsilon}. \quad (\text{A21})$$

The integral is infrared divergent, and can be regularized by using dimensional regularization. The integral over \mathbf{q} is analytically continued to $D = 3 - 2\epsilon_{\text{IR}}$ spatial dimensions. Evaluating the regularized integral in (A21), we obtain

$$\left(\text{Im } \mathcal{M} \right)_{8(b)} = \frac{2N_c \text{Im } f_1(^1S_0)}{M^2} \frac{\pi C_F \alpha_s}{4v} \left[1 - \frac{i}{\pi} \left(\frac{1}{\epsilon_{\text{IR}}} + \log(4\pi) - \gamma - 2 \log \frac{2Mv}{\mu_{\text{IR}}} \right) \right], \quad (\text{A22})$$

where γ is Euler's constant and μ_{IR} is the arbitrary regularization scale introduced with dimensional regularization. The logarithmic infrared divergence appears as a pole in ϵ_{IR} . The subscripts IR on ϵ and μ serve as a reminder that they are associated with infrared divergences. Note that (A22) is complex valued. The imaginary part of (A22) arises because it is possible for the incoming quark and antiquark to scatter on-shell before annihilating at the 4-fermion vertex. After summing over all diagrams, one must, of course, obtain a real result for $\text{Im } \mathcal{M}$. The diagram in Fig. 8(c) is evaluated in the same way as Fig. 8(b), except that the Cutkosky cutting rules require the complex-conjugation of the part of the diagram that involves the Coulomb-gluon exchange. The result is

$$\left(\text{Im } \mathcal{M}\right)_{8(c)} = \frac{2N_c \text{Im } f_1(^1S_0)}{M^2} \frac{\pi C_F \alpha_s}{4v} \left[1 + \frac{i}{\pi} \left(\frac{1}{\epsilon_{\text{IR}}} + \log(4\pi) - \gamma - 2 \log \frac{2Mv}{\mu_{\text{IR}}} \right) \right]. \quad (\text{A23})$$

Note that the imaginary part of (A23) cancels that of (A22). Adding (A19), (A22), and (A23), we obtain the complete result for $\text{Im } \mathcal{M}$ through next-to-leading order in α_s :

$$\text{Im } \mathcal{M} = \frac{2N_c \text{Im } f_1(^1S_0)}{M^2} \left[1 + \frac{\pi^2}{2v} C_F \frac{\alpha_s}{\pi} \right]. \quad (\text{A24})$$

Comparing (A16) and (A24), we can read off the imaginary part of $f_1(^1S_0)$ through next-to-leading order in α_s :

$$\text{Im } f_1(^1S_0) = \frac{\pi C_F}{2N_c} \alpha_s^2 (2M) \left\{ 1 + \left[\left(\frac{\pi^2}{4} - 5 \right) C_F + \left(\frac{199}{18} - \frac{13\pi^2}{24} \right) C_A - \frac{8}{9} n_f \right] \frac{\alpha_s}{\pi} \right\}. \quad (\text{A25})$$

Note that the factorization approach reproduces the standard prescription of simply dropping the $1/v$ terms in the perturbatively calculated annihilation rate [54]. The factorization approach puts this prescription on a rigorous footing, and makes it clear how to extend the calculation systematically to higher orders in α_s and in v .

In (A25), $\alpha_s(M)$ is the $\overline{\text{MS}}$ coupling constant with renormalization scale M . If we make a different choice for the renormalization scale μ of $\alpha_s(\mu)$, then we must differentiate between the $\overline{\text{MS}}$ coupling constant $\alpha_s^{(n_f+1)}(\mu)$ for full QCD with n_f flavors of light quarks and a heavy

quark and the corresponding coupling constant $\alpha_s^{(n_f)}(\mu)$ for only n_f flavors of light quarks, which is the appropriate running coupling constant below the heavy-quark threshold. These coupling constants satisfy the matching condition [55] $\alpha_s^{(n_f)}(M) = \alpha_s^{(n_f+1)}(M) + O(\alpha_s^3)$. If we wish to use a different renormalization scale $\mu \neq M$ for α_s in (A25), then we must make one of the following substitutions:

$$\alpha_s(M) = \alpha_s^{(n_f)}(\mu) \left[1 + \beta_0 \log \frac{\mu}{M} \frac{\alpha_s}{\pi} + O(\alpha_s^2) \right], \quad (\text{A26a})$$

$$\alpha_s(M) = \alpha_s^{(n_f+1)}(\mu) \left[1 + \left(\beta_0 - \frac{1}{3} \right) \log \frac{\mu}{M} \frac{\alpha_s}{\pi} + O(\alpha_s^2) \right], \quad (\text{A26b})$$

where $\beta_0 = (33 - 2n_f)/6$ is the first coefficient in the beta function for QCD with n_f flavors of light quarks: $\mu(d/d\mu)\alpha_s(\mu) = -\beta_0\alpha_s^2/\pi + \dots$

The coefficient of the operator $\mathcal{O}_1(^1S_0)$ in the NRQCD lagrangian is $f_1(^1S_0)/M^2$, and the perturbation series for $f_1(^1S_0)$ depends on the definition of the heavy quark mass M . The order- α_s^3 correction in (A25) corresponds to the choice $M = M_{\text{pole}}$, where M_{pole} is the perturbative pole mass, i.e., the location of the pole in the heavy-quark propagator in perturbation theory. An alternative choice is the running mass $M(\mu)$ in the $\overline{\text{MS}}$ renormalization scheme. Its relation to the pole mass through order α_s is [56]

$$M_{\text{pole}} = M(\mu) \left[1 + \left(1 + \frac{3}{2} \log \frac{\mu}{M} \right) C_F \frac{\alpha_s}{\pi} + O(\alpha_s^2) \right]. \quad (\text{A27})$$

Throughout this paper, we will adopt the choice $M = M_{\text{pole}}$ for the heavy quark mass in the coefficient f_n/M^{d_n-4} of a 4-fermion operator with naive scaling dimension d_n .

We can obtain the imaginary part of the coefficient $f_1(^3S_1)$ through next-to-leading order in α_s from a calculation by MacKenzie and Lepage of the annihilation decay rate of the J/ψ or Υ [6]. Their published result is given explicitly only for $N_c = 3$, but one can insert the appropriate color factors in the various classes of diagrams and obtain the result

$$\begin{aligned} & \text{Im } f_1(^3S_1) \\ &= \frac{(\pi^2 - 9)(N_c^2 - 4)C_F}{54N_c} \alpha_s^3(M) \left[1 + (-9.46(2)C_F + 4.13(17)C_A - 1.161(2)n_f) \frac{\alpha_s}{\pi} \right] \\ & \quad + \pi Q^2 \left(\sum_i Q_i^2 \right) \alpha^2 \left[1 - \frac{13}{4} C_F \frac{\alpha_s}{\pi} \right], \end{aligned} \quad (\text{A28})$$

where Q is the electric charge of the heavy quark ($Q = +2/3$ for the charmed quark and $Q = -1/3$ for the bottom quark) and the Q_i , $i = 1, \dots, n_f$, are the electric charges of the light quarks. The perturbative correction in the first term on the right side of (A28) was calculated by Mackenzie and Lepage [6]. The term proportional to α^2 is due to annihilation of the $Q\bar{Q}$ pair into a virtual photon, which then decays into light hadrons. The order- α_s correction can be calculated as the sum of two terms: $-4C_F\alpha_s/\pi$, which is the order- α_s correction to the rate for $\psi \rightarrow e^+e^-$, and $3C_F\alpha_s/(4\pi)$, which is the order- α_s correction to the rate for $\gamma^* \rightarrow q\bar{q}$. For completeness, we also give the coefficient analogous to (A28) for the decay of the ψ into a photon plus light hadrons:

$$\begin{aligned} & \text{Im } f_{\gamma 1}(^3S_1) \\ &= \frac{2(\pi^2 - 9)C_F Q^2 \alpha}{3N_c} \alpha_s^2(M) \left[1 + (-9.46(2)C_F + 2.75(11)C_A - 0.774(1)n_f) \frac{\alpha_s}{\pi} \right]. \end{aligned} \quad (\text{A29})$$

Calculations of the annihilation rates of P-wave states were carried out through order α_s^3 by Barbieri and collaborators [7,8,21]. They calculated only the coefficients of $|\overline{R}_P|^2$ in (4.7). These coefficients contain logarithmic infrared divergences that should be factored into the color-octet matrix elements, along with associated constants that can be determined from calculations in NRQCD. In Ref. [7], the logarithmic infrared divergences in $\text{Im } f_1(^3P_0)$ and $\text{Im } f_1(^3P_2)$ were cut off by taking the heavy quark and antiquark off their mass-shells and below threshold, in which case the infrared divergence manifests itself as a logarithm of the binding energy. In order to extract NRQCD coefficients, it might be necessary to repeat the next-to-leading order calculations in Ref. [7] using on-shell scattering amplitudes and dimensional regularization of the infrared divergences in order to maintain gauge invariance.

4. Coefficients of Electromagnetic Operators

The calculation in Section A 2 can be easily modified to give the imaginary parts of the coefficients of the electromagnetic 4-fermion operators at order α^2 and at leading order in α_s . The Feynman diagrams in Figs. 9(a) and 9(b) yield imaginary parts that correspond

to annihilation into two photons. These imaginary parts can be obtained from (A9) by replacing the color matrices T^a by the unit color matrix and by substituting $\alpha_s \rightarrow Q^2\alpha$, where Q is the electric charge of the heavy quark: $Q = +2/3$ for the charmed quark, and $Q = -1/3$ for the bottom quark. The sum of the 2 diagrams yields

$$\begin{aligned} \text{Im} \left(\mathcal{M}_{9(a)} + \mathcal{M}_{9(b)} \right) &= \frac{\pi Q^4 \alpha^2}{M^2} (1 \otimes 1) \left[\left(1 - \frac{4}{3} v^2 \right) 1 \otimes 1 + \frac{2}{5} \mathbf{v} \cdot \mathbf{v}' \sigma^i \otimes \sigma^i \right. \\ &\quad \left. + \left(\frac{2}{5} v^i v'^j + \frac{11}{15} v'^i v^j \right) \sigma^i \otimes \sigma^j \right]. \end{aligned} \quad (\text{A30})$$

Comparing to the NRQCD scattering amplitudes analogous to (A5), we find that the only nonzero coefficient for the dimension-6 operators is

$$\text{Im} f_{\gamma\gamma}(^1S_0) = \pi Q^4 \alpha^2. \quad (\text{A31})$$

Comparing to the NRQCD scattering amplitudes analogous to (A7), we can read off the nonzero coefficients of the dimension-8 operators:

$$\text{Im} f_{\gamma\gamma}(^3P_0) = 3\pi Q^4 \alpha^2, \quad (\text{A32a})$$

$$\text{Im} f_{\gamma\gamma}(^3P_2) = \frac{4\pi Q^4 \alpha^2}{5}, \quad (\text{A32b})$$

$$\text{Im} g_{\gamma\gamma}(^1S_0) = -\frac{4\pi Q^4 \alpha^2}{3}. \quad (\text{A32c})$$

The diagram in Fig. 9(c) yields an imaginary part that corresponds to the annihilation into lepton pairs. The imaginary part can be obtained from (A13) by replacing T^a by the unit color matrix, and by substituting $(n_f/2)\alpha_s \rightarrow -Q\alpha$. The resulting matrix element is

$$\text{Im} \mathcal{M}_{9(c)} = \frac{\pi Q^2 \alpha^2}{3M^2} (1 \otimes 1) \left[(1 - v^2) \sigma^i \otimes \sigma^i - \frac{1}{2} (v^i v^j + v'^i v'^j) \sigma^i \otimes \sigma^j \right]. \quad (\text{A33})$$

Comparing to the NRQCD scattering amplitudes analogous to (A5), we find that the only nonzero coefficient of the dimension-6 operators is

$$\text{Im} f_{ee}(^3S_1) = \frac{\pi Q^2 \alpha^2}{3}. \quad (\text{A34})$$

Comparing to the NRQCD scattering amplitudes analogous to (A7), we can read off the nonzero coefficients of the dimension-8 operators:

$$\text{Im } g_{ee}(^3S_1) = -\frac{4\pi Q^2 \alpha^2}{9}, \quad (\text{A35a})$$

$$\text{Im } g_{ee}(^3S_1, ^3D_1) = -\frac{\pi Q^2 \alpha^2}{3}. \quad (\text{A35b})$$

Several of the electromagnetic coefficients can be determined through next-to-leading order in α_s from calculations that are available in the literature. The annihilation rates for η_c , χ_{c0} , and χ_{c2} into two photons have been calculated through next-to-leading order in α_s by Barbieri *et al.* [5,7]. The corresponding coefficients are

$$\text{Im } f_{\gamma\gamma}(^1S_0) = \pi Q^4 \alpha^2 \left[1 + \left(\frac{\pi^2}{4} - 5 \right) C_F \frac{\alpha_s}{\pi} \right], \quad (\text{A36a})$$

$$\text{Im } f_{\gamma\gamma}(^3P_0) = 3\pi Q^4 \alpha^2 \left[1 + \left(\frac{\pi^2}{4} - \frac{7}{3} \right) C_F \frac{\alpha_s}{\pi} \right], \quad (\text{A36b})$$

$$\text{Im } f_{\gamma\gamma}(^3P_2) = \frac{4\pi Q^4 \alpha^2}{5} \left[1 - 4C_F \frac{\alpha_s}{\pi} \right]. \quad (\text{A36c})$$

The rate for $\psi \rightarrow e^+e^-$ is known through next-to-leading order in α_s [57]:

$$\text{Im } f_{ee}(^3S_1) = \frac{\pi Q^2 \alpha^2}{3} \left[1 - 4C_F \frac{\alpha_s}{\pi} \right]. \quad (\text{A37})$$

Finally, Mackenzie and Lepage [6] have calculated the rate for $\psi \rightarrow \gamma\gamma\gamma$ to next-to-leading order in α_s . The corresponding coefficient is

$$\text{Im } f_{3\gamma}(^3S_1) = \frac{4(\pi^2 - 9)Q^6 \alpha^3}{9} \left[1 - 9.46(2)C_F \frac{\alpha_s}{\pi} \right]. \quad (\text{A38})$$

APPENDIX B: EVOLUTION OF 4-FERMION OPERATORS

As we mentioned in Section III E, loop corrections to the 4-fermion operators in the NRQCD lagrangian are, in general, ultraviolet divergent, and, therefore, must be regularized. One can remove power divergences, either by employing a mass-independent regularization scheme, such as dimensional regularization, or by making explicit subtractions. Once this has been done, the 4-fermion operators satisfy simple evolution equations of the form (3.22). The evolution equation for an operator \mathcal{O}_n with naive scaling dimension d_n involves only operators \mathcal{O}_k with dimensions $d_k \geq d_n$. The coefficients γ_{nk} in the evolution equation can be computed as power series in α_s . For $d_k = d_n$, the coefficients γ_{nk} are at most of order α_s^2 , because the logarithmic ultraviolet divergences at order α_s come only from corrections of relative order v^2 , which correspond to operators \mathcal{O}_k of dimension $d_n + 2$ or larger. In this Appendix, we compute at order α_s the coefficients of the dimension-8 operators that appear in the evolution of the dimension-6 4-fermion operators.

1. Heavy Quark Self-energy

In order to illustrate the methods that are used to calculate the coefficients in the evolution equations, we first calculate the self-energy of the heavy quark in NRQCD through order α_s . From this calculation, we determine the relation between the perturbative pole mass M_{pole} and the mass parameter M in the NRQCD lagrangian, and we extract the residue $Z(p)$ of the pole in the heavy-quark propagator through order $\alpha_s v^2$. The residue is given by

$$Z(p)^{-1} = 1 - \frac{\partial \Sigma}{\partial E}(E = p^2/2M_{\text{pole}}, p), \quad (\text{B1})$$

where $\Sigma(E, p)$ is the self-energy correction. To determine $Z(p)$ to order α_s and to order v^2 , we must calculate the self-energy correction Σ that arises from the one-loop diagrams in Fig. 10. We calculate these diagrams in Coulomb gauge, because it facilitates the extraction of the dependence on v . The seagull diagram in Fig. 10(b) gives only power ultraviolet divergences, which are subtracted as part of the regularization scheme. Interactions from

$\mathcal{L}_{\text{bilinear}}$ also need not be included, because the terms of order $\alpha_s v^2$ that they produce are all proportional to power ultraviolet divergences.

The contribution to the self-energy from the diagram in Fig. 10(a) is

$$\Sigma(E, p) = i4\pi C_F \alpha_s \int \frac{d^4 q}{(2\pi)^4} \frac{1}{E - q_0 - (\mathbf{p} - \mathbf{q})^2/2M + i\epsilon} \left(\frac{1}{\mathbf{q}^2} + \frac{p^2 - (\mathbf{p} \cdot \hat{\mathbf{q}})^2}{M^2(q_0^2 - \mathbf{q}^2 + i\epsilon)} \right). \quad (\text{B2})$$

The integral of the term containing $1/\mathbf{q}^2$, which comes from Coulomb exchange, gives rise to an ill-defined power divergence, which can be dropped. After using contour integration to integrate over the energy q_0 of the gluon, we find that the contribution reduces to

$$\Sigma(E, p) = \frac{2\pi C_F \alpha_s}{M^2} \int \frac{d^3 q}{(2\pi)^3} \frac{1}{q} \frac{p^2 - (\mathbf{p} \cdot \hat{\mathbf{q}})^2}{E - q - (\mathbf{p} - \mathbf{q})^2/2M + i\epsilon}. \quad (\text{B3})$$

In order to identify the power divergences in (B3), we expand the denominator in a Taylor series in $1/M$:

$$\Sigma(E, p) = -\frac{2\pi C_F \alpha_s}{M^2} \int \frac{d^3 q}{(2\pi)^3} \frac{p^2 - (\mathbf{p} \cdot \hat{\mathbf{q}})^2}{q^2} \left(1 + \frac{E - p^2/2M + (2\mathbf{p} \cdot \mathbf{q} - q^2)/2M}{q} + \dots \right). \quad (\text{B4})$$

Setting $E = p^2/2M$, we find that every remaining term in the integrand in (B4) yields a power divergence, which is subtracted in our regularization scheme. Thus, after regularization, the self-energy vanishes on the energy shell, and there is no correction to the energy-momentum relation $E = p^2/2M$. In full QCD, the energy-momentum relation defined by the pole in the perturbative heavy-quark propagator is $E^2 = p^2 + M_{\text{pole}}^2$. Matching the coefficients of p^2 in these energy-momentum relations, we obtain

$$M = M_{\text{pole}} \left(1 + O(\alpha_s^2) \right). \quad (\text{B5})$$

Thus, through order α_s , the mass parameter M in the lagrangian for NRQCD can be identified with the perturbative pole mass.

We proceed to compute the residue of the pole in the heavy-quark propagator, which is given by (B1). After we subtract the power divergences, the only term remaining in (B4)

that contributes at order $\alpha_s v^2$ is the term proportional to $E - p^2/2M$. Consequently, the expression for the residue is

$$Z(p) = 1 - \frac{2\pi C_F \alpha_s}{M^2} \int \frac{d^3 q}{(2\pi)^3} \frac{p^2 - (\mathbf{p} \cdot \hat{\mathbf{q}})^2}{q^3}. \quad (\text{B6})$$

Imposing a momentum cutoff $|\mathbf{q}| < \Lambda$ on the magnitude of the gluon momentum and keeping only the logarithmic ultraviolet divergence at order α_s , we find that the residue $Z(p)$ is

$$Z(p) \approx 1 - \frac{2C_F \alpha_s \log \Lambda}{3\pi} v^2, \quad (\text{B7})$$

where $v^2 = p^2/M^2$.

2. One-loop Ultraviolet Divergences

The coefficients in the evolution equation for the operator $\mathcal{O}_8(^1S_0) = \psi^\dagger T^a \chi \chi^\dagger T^a \psi$ can be determined at order α_s by computing one-loop corrections to scattering amplitudes in NRQCD that involve this operator. We consider the amplitude for the scattering of a $Q\bar{Q}$ pair with momenta \mathbf{p} and $-\mathbf{p}$ into a $Q\bar{Q}$ pair with momenta \mathbf{p}' and $-\mathbf{p}'$. We use the compact notation with suppressed Pauli spinors that was introduced in Eq. (A4). The matrix element corresponding to the leading-order diagram in Fig. 8(a) is then written

$$\mathcal{M} = (T^a \otimes T^a) (1 \otimes 1), \quad (\text{B8})$$

where the first factor gives the color structure and the second factor gives the spin structure. The one-loop correction to the matrix element is given by the sum of the contributions of the 10 diagrams in Figs. 11(a)–11(j). We wish to calculate the terms in these contributions that are proportional to $\log \Lambda$, where Λ is an ultraviolet cutoff. For higher-order calculations, it might be wise to impose the cutoff by using dimensional regularization, in order to maintain gauge invariance, but for our purposes it is sufficient to impose a cutoff on the magnitude of the gluon 3-momentum: $|\mathbf{q}| > \Lambda$.

The 4 diagrams in Fig. 11(a)–11(d) are self-energy corrections to the external quark lines. Each diagram contributes $\sqrt{Z} - 1$ times the leading order amplitude in (B8). Using the

expression (B7) for the renormalization constant Z , we find that the sum of the contributions of the 4 diagrams is

$$\mathcal{M}_{11(\text{a-d})} \approx -\frac{4C_F\alpha_s \log \Lambda}{3\pi} v^2 (T^a \otimes T^a) (1 \otimes 1). \quad (\text{B9})$$

The diagram in Fig. 11(e) represents the exchange of a transverse gluon between the incoming quark and antiquark. (The exchange of a Coulomb gluon does not lead to an ultraviolet divergence.) This diagram yields the contribution

$$\mathcal{M}_{11(\text{e})} = i \frac{4\pi\alpha_s}{M^2} (T^a \otimes T^b T^a T^b) (1 \otimes 1) \int \frac{d^4 q}{(2\pi)^4} \frac{p^2 - (\mathbf{p} \cdot \hat{\mathbf{q}})^2}{q_0^2 - \mathbf{q}^2 + i\epsilon} \frac{1}{E + q_0 - (\mathbf{p} + \mathbf{q})^2/2M + i\epsilon} \frac{1}{E - q_0 - (\mathbf{p} + \mathbf{q})^2/2M + i\epsilon}, \quad (\text{B10})$$

where $E = p^2/2M$. We integrate over the energy q_0 of the exchanged gluon and identify the power divergences by expanding the denominators in a Taylor series in $1/M$. Keeping only the term that gives a logarithmic ultraviolet divergence, we find that the contribution reduces to

$$\mathcal{M}_{11(\text{e})} = -\frac{2\pi\alpha_s}{M^2} (T^a \otimes T^b T^a T^b) (1 \otimes 1) \int \frac{d^3 q}{(2\pi)^3} \frac{p^2 - (\mathbf{p} \cdot \hat{\mathbf{q}})^2}{q^3}. \quad (\text{B11})$$

The integral is the same as in (B6). The diagram in Fig. 11(f) gives an identical contribution:

$$\mathcal{M}_{11(\text{e})} \approx \mathcal{M}_{11(\text{f})} \approx -\frac{2\alpha_s \log \Lambda}{3\pi} v^2 (T^a \otimes T^b T^a T^b) (1 \otimes 1). \quad (\text{B12})$$

The diagrams in Figs. 11(g)–11(j) involve the exchange of a transverse gluon between initial and final quark or antiquark lines. (The exchange of a Coulomb gluon leads to a vanishing contribution.) These diagrams are evaluated in the same way as those in Fig. 11(e).

The results are

$$\mathcal{M}_{11(\text{g})} \approx \mathcal{M}_{11(\text{h})} \approx \frac{2\alpha_s \log \Lambda}{3\pi} \mathbf{v} \cdot \mathbf{v}' (T^a T^b \otimes T^a T^b) (1 \otimes 1), \quad (\text{B13a})$$

$$\mathcal{M}_{11(\text{i})} \approx \mathcal{M}_{11(\text{j})} \approx \frac{2\alpha_s \log \Lambda}{3\pi} \mathbf{v} \cdot \mathbf{v}' (T^a T^b \otimes T^b T^a) (1 \otimes 1). \quad (\text{B13b})$$

The color factors in (B13) can be simplified by using the identities in (A10). Adding up the results for the diagrams in (B9) and (B12)–(B13), we find that the sum of the logarithmically divergent terms of order $\alpha_s v^2$ is

$$\begin{aligned} \mathcal{M}_8(^1S_0) \approx & \frac{2\alpha_s \log \Lambda}{3\pi N_c} \left(2C_F \mathbf{v} \cdot \mathbf{v}' (1 \otimes 1) \right. \\ & \left. + \left[(N_c^2 - 4) \mathbf{v} \cdot \mathbf{v}' - (N_c^2 - 2) v^2 \right] (T^a \otimes T^a) \right) (1 \otimes 1). \end{aligned} \quad (\text{B14})$$

The logarithmically divergent part of the diagrams for scattering through the color-singlet operator $\mathcal{O}_1(^1S_0) = \psi^\dagger \chi \chi^\dagger \psi$ can be obtained from the expressions (B9) and (B12)–(B13b) simply by replacing the color matrix T^a by the unit matrix 1. Adding up these contributions, we obtain

$$\mathcal{M}_1(^1S_0) \approx \frac{8\alpha_s \log \Lambda}{3\pi} \left(\mathbf{v} \cdot \mathbf{v}' (T^a \otimes T^a) - C_F v^2 (1 \otimes 1) \right) (1 \otimes 1). \quad (\text{B15})$$

The ultraviolet divergent parts of the matrix elements $\mathcal{M}_8(^3S_1)$ and $\mathcal{M}_1(^3S_1)$, which correspond to scattering through the spin-triplet operators $\mathcal{O}_8(^3S_1)$ and $\mathcal{O}_1(^3S_1)$, can be obtained by replacing the spin factor $1 \otimes 1$ by $\sigma^i \otimes \sigma^i$ in (B14) and (B15), respectively.

3. Evolution Equations

The logarithmically divergent contributions to the scattering amplitudes in Section B2 can be expressed to leading order in v as the matrix elements of dimension-8 operators. Differentiating the operator equation corresponding to (B15) with respect to Λ , we obtain the evolution equation for the operator $\mathcal{O}_1(^1S_0)$:

$$\Lambda \frac{d}{d\Lambda} \mathcal{O}_1(^1S_0) = \frac{8\alpha_s}{3\pi M^2} \mathcal{O}_8(^1P_1) - \frac{8C_F \alpha_s}{3\pi M^2} \mathcal{P}_1(^1S_0). \quad (\text{B16})$$

By differentiating the operator equation corresponding to (B14) with respect to Λ , we obtain the evolution equation for the operator $\mathcal{O}_8(^1S_0)$:

$$\Lambda \frac{d}{d\Lambda} \mathcal{O}_8(^1S_0) = \frac{4C_F \alpha_s}{3\pi N_c M^2} \mathcal{O}_1(^1P_1) + \frac{2(N_c^2 - 4)\alpha_s}{3\pi N_c M^2} \mathcal{O}_8(^1P_1) - \frac{2(N_c^2 - 2)\alpha_s}{3\pi N_c M^2} \mathcal{P}_8(^1S_0). \quad (\text{B17})$$

The evolution equations for the corresponding spin-triplet operators can be obtained from (B17) and (B16) simply by inserting σ^i between ψ^\dagger and χ and also between χ^\dagger and ψ . It is convenient to express the resulting operators in terms of the combinations that appear in (2.11) by using the identity

$$D^i \sigma^j \otimes D^i \sigma^j = \frac{1}{3} \mathbf{D} \cdot \boldsymbol{\sigma} \otimes \mathbf{D} \cdot \boldsymbol{\sigma} + \frac{1}{2} (\mathbf{D} \times \boldsymbol{\sigma})^i \otimes (\mathbf{D} \times \boldsymbol{\sigma})^i + D^{(i} \sigma^{j)} \otimes D^{(i} \sigma^{j)}. \quad (\text{B18})$$

The resulting evolution equations are

$$\Lambda \frac{d}{d\Lambda} \mathcal{O}_1(^3S_1) = \frac{8\alpha_s}{3\pi M^2} \left(\mathcal{O}_8(^3P_0) + \mathcal{O}_8(^3P_1) + \mathcal{O}_8(^3P_2) \right) - \frac{8C_F\alpha_s}{3\pi M^2} \mathcal{P}_1(^3S_1), \quad (\text{B19a})$$

$$\begin{aligned} \Lambda \frac{d}{d\Lambda} \mathcal{O}_8(^3S_1) &= \frac{4C_F\alpha_s}{3\pi N_c M^2} \left(\mathcal{O}_1(^3P_0) + \mathcal{O}_1(^3P_1) + \mathcal{O}_1(^3P_2) \right) \\ &+ \frac{2(N_c^2 - 4)\alpha_s}{3\pi N_c M^2} \left(\mathcal{O}_8(^3P_0) + \mathcal{O}_8(^3P_1) + \mathcal{O}_8(^3P_2) \right) - \frac{2(N_c^2 - 2)\alpha_s}{3\pi N_c M^2} \mathcal{P}_8(^3S_1). \end{aligned} \quad (\text{B19b})$$

The evolution equations for electromagnetic operators can be calculated in the same way, except that there are no contributions from diagrams such as those in Figs. 11(g)-11(j), which involve exchange of gluons between initial and final quark lines. The evolution equations for the dimension-6 electromagnetic operators can be obtained from (B16) and (B19a) by dropping the color-octet terms on the right sides and inserting vacuum projections:

$$\Lambda \frac{d}{d\Lambda} \left(\psi^\dagger \chi |0\rangle \langle 0| \chi^\dagger \psi \right) = - \frac{4C_F\alpha_s}{3\pi M^2} \left[\psi^\dagger \chi |0\rangle \langle 0| \chi^\dagger \left(-\frac{i}{2} \vec{\mathbf{D}} \right)^2 \psi + \text{h.c.} \right], \quad (\text{B20a})$$

$$\Lambda \frac{d}{d\Lambda} \left[\psi^\dagger \boldsymbol{\sigma} \chi |0\rangle \cdot \langle 0| \chi^\dagger \boldsymbol{\sigma} \psi \right] = - \frac{4C_F\alpha_s}{3\pi M^2} \left[\psi^\dagger \boldsymbol{\sigma} \chi |0\rangle \cdot \langle 0| \chi^\dagger \boldsymbol{\sigma} \left(-\frac{i}{2} \vec{\mathbf{D}} \right)^2 \psi + \text{h.c.} \right]. \quad (\text{B20b})$$

REFERENCES

- [1] T. Appelquist and H.D. Politzer, Phys. Rev. Lett. **34**, 43 (1975); A. de Rujula and S.L. Glashow, Phys. Rev. Lett. **34**, 46 (1975).
- [2] R. Barbieri, R. Gatto, and R. Kögerler, Phys. Lett. **60B**, 183 (1976).
- [3] V.A. Novikov, L.B. Okun, M.A. Shifman, A.I. Vainshtein, M.B. Voloshin, and V.I. Zakharov, Phys. Rep. **41C**, 1 (1978).
- [4] E. Remiddi, in *Int. School of Physics E. Fermi*, edited by N. Costa and R. Gatto (North Holland, Amsterdam, 1982).
- [5] R. Barbieri, G. Curci, E. d'Emilio, and E. Remiddi, Nucl. Phys. **B154**, 535 (1979); K. Hagiwara, C.B. Kim, and T. Yoshino, Nucl. Phys. **B177**, 461 (1981).
- [6] P. Mackenzie and G.P. Lepage, Phys. Rev. Lett. **47**, 1244 (1981); P. Mackenzie and G.P. Lepage, in *Perturbative Quantum Chromodynamics*, edited by D.W. Duke and J.F. Owens (American Institute of Physics, New York, 1981).
- [7] R. Barbieri, M. Caffo, R. Gatto, and E. Remiddi, Phys. Lett. **95B**, 93 (1980); Nucl. Phys. **B192**, 61 (1981).
- [8] R. Barbieri, R. Gatto, and E. Remiddi, Phys. Lett. **61B**, 465 (1976).
- [9] W.E. Caswell and G.P. Lepage, Phys. Lett. **167B**, 437 (1986).
- [10] G.T. Bodwin, E. Braaten, and G.P. Lepage, Phys. Rev. **D46**, R1914 (1992).
- [11] See, for example, C. Quigg and J.L. Rosner, Phys. Reports **56**, 167 (1979).
- [12] S. Tani, Prog. Theor. Phys. **6**, 267 (1951); L.L. Foldy and S.A. Wouthuysen, Phys. Rev. **78**, 29 (1950).
- [13] G.P. Lepage, in *From Actions to Answers*, edited by T. DeGrand and D. Toussaint (World Scientific, Singapore, 1989).

- [14] G.P. Lepage, L. Magnea, C. Nakhleh, U. Magnea, and K. Hornbostel, Cornell preprint CLNS 92/1136 (February 1992).
- [15] C.J. Morningstar, Phys. Rev. **D48**, 2265 (1993); Edinburgh preprint 94/1.
- [16] S. Love, Ann. Phys. (N.Y.) **113**, 153 (1978); G.T. Bodwin, D.R. Yennie and M.A. Gregorio, Rev. Mod. Phys. **57**, 723 (1985).
- [17] G.P. Lepage (unpublished).
- [18] See, for example, B. Grinstein, Ann. Rev. Nucl. Part. Sci. **42**, 101 (1992); M. Neubert, SLAC preprint SLAC-PUB-6263 (June 1993).
- [19] T. Kinoshita, J. Math. Phys. **3**, 650 (1962); T.D. Lee and M. Nauenberg, Phys. Rev. **B133**, 1549 (1964).
- [20] E. Poggio, H. Quinn, and S. Weinberg, Phys. Rev. **D13**, 1958 (1976).
- [21] R. Barbieri, M. Caffo, and E. Remiddi, Nucl. Phys. **B162**, 220 (1980).
- [22] G. Grammer, Jr. and D.R. Yennie, Phys. Rev. **D8**, 4332 (1973).
- [23] G.A. Schuler, CERN preprint CERN-TH.7170/94, and references therein.
- [24] G.T. Bodwin, E. Braaten, T.C. Yuan, and G.P. Lepage, Phys. Rev. **D46**, R3703 (1992).
- [25] G.T. Bodwin, Phys. Rev. **D31**, 2616 (1985); *erratum, ibid.* Phys. Rev. **D34**, 3932 (1986): J.C. Collins, D.E. Soper, and G. Sterman, Nucl. Phys. **B261**, 104 (1985); *ibid.* **B308**, 833 (1988); in *Perturbative Quantum Chromodynamics*, edited by A. H. Mueller (World Scientific, Singapore, 1989). An outline of the factorization program is given in J.C. Collins, D.E. Soper, and G. Sterman, Phys. Rev. Lett. **134B**, 263 (1984).
- [26] J.-W. Qiu and G. Sterman, Nucl. Phys. **B353**, 137 (1991); *ibid.* **B353**, 105 (1991).
- [27] R. Doria, J. Frenkel, and J.C. Taylor, Nucl. Phys. **B168**, 93 (1980).
- [28] G. Curci, W. Furmanski, and R. Petronzio, Nucl. Phys. **B194**, 445 (1980); J.C. Collins

- and D.E. Soper, Nucl. Phys. **B194**, 445 (1982).
- [29] J.H. Kühn, J. Kaplan, and E.G.O. Safiani, Nucl. Phys. **B157**, 125 (1979); B. Guberina, J.H. Kühn, R.D. Peccei, and R. Rückl, Nucl. Phys. **B174**, 317 (1980); R.W. Robinett and L. Weinkauff, Phys. Rev. **D46**, 3832 (1992).
- [30] M.B. Einhorn and S.D. Ellis, Phys. Rev. **D12**, 2007 (1975); S.D. Ellis, M.B. Einhorn, and C. Quigg, Phys. Rev. Lett. **36**, 1263 (1976); C.E. Carlson and R. Suaya, Phys. Rev. **D14**, 3115 (1976); J.H. Kühn, Phys. Lett. **B89**, 385 (1980).
- [31] T.A. DeGrand and D. Toussaint, Phys. Lett. **89B**, 256 (1980); J.H. Kühn, S. Nussinov, and R. Rückl, Z. Phys. **C5**, 117 (1980); M.B. Wise, Phys. Lett. **89B**, 229 (1980).
- [32] C.-H. Chang, Nucl. Phys. **B172**, 425 (1980); R. Baier and R. Rückl, Phys. Lett. **102B**, 364 (1981).
- [33] E.L. Berger and D. Jones, Phys. Rev. **D23**, 1521 (1981); W.-Y. Keung, in *Proceedings of the Cornell Z^0 Theory Workshop*, edited by M.E. Peskin and S.-H. Tye (Cornell University, Ithaca, 1981).
- [34] W.-Y. Keung and I.J. Muzinich, Phys. Rev. **D27**, 1518 (1983).
- [35] M.A. Shifman and M.B. Voloshin, Sov. J. Nucl. Phys. **41**, 120 (1985); I.I. Bigi, M.G. Uraltsev, and A.I. Vainshtein, Phys. Lett. **B293**, 430 (1992); *erratum, ibid.* **B297**, 477 (1993); B. Blok and M.A. Shifman, Nucl. Phys. **B399**, 441 (1993); Nucl. Phys. **B399**, 459 (1993).
- [36] A. Duncan and A. Mueller, Phys. Lett. **93B**, 119 (1980).
- [37] M.E. Peskin, Nucl. Phys. **B156**, 365 (1979); G. Bhanot and M.E. Peskin, Nucl. Phys. **B156**, 391 (1979).
- [38] M.B. Voloshin, Sov. J. Nucl. Phys. **36**, 143 (1982); *ibid.* **40**, 662 (1984).
- [39] H. Fritzsch, Phys. Lett. **67B**, 217 (1977).

- [40] G.T. Bodwin, E. Braaten, and G.P. Lepage, in preparation.
- [41] G. Bélanger and P. Moxhay, Phys. Lett. **199**, 575 (1987).
- [42] L. Bergström and P. Ernström, Stockholm preprint USITP-94-02.
- [43] J.H. Kühn and E. Mirkes, Phys. Lett. **B296**, 425 (1992); Phys. Rev. **D48**, 179 (1993).
- [44] H. Jung, D. Krücker, C. Greub, and D. Wyler, DESY preprint DESY 93-072.
- [45] E. Braaten and T.C. Yuan, Phys. Rev. Lett. **71**, 1673 (1993).
- [46] E. Braaten, K. Cheung, and T.C. Yuan, Phys. Rev. **D48**, 4230 (1993); *ibid.* **D48**, R5049 (1993); C.-H. Chang and Y.-Q. Chen, Phys. Lett. **B284**, 127 (1992); Phys. Rev. **D46**, 3845 (1992); A.F. Falk, M. Luke, M.J. Savage, and M.B. Wise, Phys. Lett. **B312**, 486 (1993).
- [47] H. Trottier, Phys. Lett. **B320**, 145 (1994).
- [48] E. Braaten and T.C. Yuan, Fermilab preprint FERMILAB-PUB-94/040-T; J.P. Ma, Melbourne preprint UM-P-94-01 (1994).
- [49] T.C. Yuan, U.C. Davis preprint UCD-94-2 (1994); Y.-Q. Chen, Phys. Rev. **D48**, 5158 (1993).
- [50] L. Bergström, H. Grotch, and R.W. Robinett, Phys. Rev. **D43**, 2157 (1991).
- [51] B.A. Thacker and G.P. Lepage, Phys. Rev. **D43**, 196 (1991); C.T.H. Davies and B.A. Thacker, Nucl. Phys. **B405**, 593 (1993).
- [52] G.T. Bodwin, S. Kim, and D.K. Sinclair, Nucl. Phys. (Proc. Suppl.) **B34**, 434 (1994).
- [53] See, for example, A.X. El-Khadra, G. Hockney, A.S. Kronfeld, and P.B. Mackenzie, Phys. Rev. Lett. **69**, 729 (1992); C. Davies *et al.*, Ohio State preprints OHSTPY-HEP-T-94-004 (1994) and OHSTPY-HEP-T-94-005 (1994).
- [54] I. Harris and L.M. Brown, Phys. Rev. **105**, 1656 (1957).

- [55] S. Weinberg, Phys. Lett. **91B**, 51 (1980); G. Rodrigo and A. Santamaria, Phys. Lett. **B313**, 441 (1993).
- [56] N. Gray, D.J. Broadhurst, W. Grafe, and K. Schilcher, Z. Phys. **C48**, 673 (1990).
- [57] R. Barbieri, R. Gatto, R. Kögerler, and Z. Kunszt, Phys. Lett. **57B**, 455 (1975); W. Celmaster, Phys. Rev. **D19**, 1517 (1979).

FIGURES

FIG. 1. Example of a diagram that contributes to the quarkonium annihilation rate at order α_s^3 . The three cuts of the diagram participate in a KLN cancellation.

FIG. 2. Schematic representation of the topological factorization of the rate for quarkonium annihilation. The short distance part is represented by the circle labelled **H**. The quarkonium wavefunctions are represented by the shaded ovals. The wavefunctions can be connected by light partons, such as the two gluons that are shown explicitly. Soft gluon interactions between the light partons are represented by the circle labelled **S**.

FIG. 3. Example of a Feynman diagram for quarkonium annihilation at order α_s^2 . The shaded ovals represent the quarkonium wavefunctions.

FIG. 4. Examples of real-gluon emission in quarkonium decay at order α_s^3 . The shaded ovals represent the quarkonium wavefunctions.

FIG. 5. Examples of virtual-gluon emission in quarkonium decay at order α_s^3 . The shaded ovals represent the quarkonium wavefunctions.

FIG. 6. Feynman diagrams for $Q\bar{Q}$ scattering at leading order in α_s .

FIG. 7. Feynman diagrams that contribute to the imaginary part of the amplitude for $Q\bar{Q}$ scattering at order α_s^2 .

FIG. 8. Feynman diagrams in NRQCD for the scattering of a $Q\bar{Q}$ pair in a color-singlet 1S_0 state through the operator $\psi^\dagger\chi\chi^\dagger\psi$.

FIG. 9. Feynman diagrams that contribute to the imaginary part of the amplitude for electromagnetic $Q\bar{Q}$ scattering at order α^2 .

FIG. 10. Feynman diagrams in NRQCD for the self-energy of a heavy quark at order α_s .

FIG. 11. Feynman diagrams in NRQCD that contribute to the evolution of an S-wave 4-fermion operator, such as $\psi^\dagger T^a \chi \chi^\dagger T^a \psi$ or $\psi^\dagger \chi \chi^\dagger \psi$.

TABLES

Operator	Estimate	Description
α_s	v	effective quark-gluon coupling constant
ψ	$(Mv)^{3/2}$	heavy-quark (annihilation) field
χ	$(Mv)^{3/2}$	heavy-antiquark (creation) field
D_t (acting on ψ or χ)	Mv^2	gauge-covariant time derivative
\mathbf{D} (acting on ψ or χ)	Mv	gauge-covariant spatial derivative
$g\mathbf{E}$	M^2v^3	chromoelectric field
$g\mathbf{B}$	M^2v^4	chromomagnetic field
$g\phi$ (in Coulomb gauge)	Mv^2	scalar potential
$g\mathbf{A}$ (in Coulomb gauge)	Mv^3	vector potential

TABLE I. Estimates of the magnitudes of NRQCD operators for matrix elements between heavy-quarkonium states in terms of the heavy-quark mass M and the typical heavy-quark velocity v . The estimates shown apply to matrix elements in a quarkonium state $|H\rangle$ whose position is localized to a region of size $1/Mv$ or less. If the states are normalized to $\langle H|H\rangle = 1$, then the product of the magnitudes of the operators gives the magnitude of the matrix element. (In order to obtain estimates for matrix elements between momentum eigenstates that are normalized to $\langle H|H\rangle = V$, where V is the volume of space, one should multiply the estimates for localized states of unit norm by $(Mv)^{-3}$.)

**Erratum: Rigorous QCD Analysis of Inclusive Annihilation
and Production of Heavy Quarkonium**

[Phys. Rev. D 51, 1125 (1995)]

[hep-ph/9407339]

Geoffrey T. Bodwin, Eric Braaten, and G. Peter Lepage

In this erratum, we clarify the velocity-scaling rules for those NRQCD matrix elements whose leading contributions come from $|Q\bar{Q}g\rangle$ Fock states that can be reached through a spin-flip transition from the dominant Fock state. A correct accounting of these spin-flip Fock states leads to revisions of the error estimates in several equations in the paper. In addition, we emphasize that the velocity-scaling rules should be used to estimate the probabilities of higher Fock states, rather than their amplitudes. We also correct some typographical errors.

- Throughout the paper, phrases of the type “amplitude of order v^n ” should be replaced with “probability of order v^{2n} ”. The reason is that the probability of a $|Q\bar{Q}g\rangle$ Fock state is the square of the amplitude integrated over the phase space of the particles. Some of the dependence on v arises from the integration over the phase space of the gluon.
- Throughout the paper, one should keep in mind that the velocity expansion may contain odd, as well as even, powers of v . Thus, for example, v^2 should be replaced with v in phrases such as “expansion in powers of v^2 ”.
- The following paragraph should be inserted after the paragraph that includes Eq. (2.6):

“The above estimates for the probabilities of $|Q\bar{Q}g\rangle$ Fock states apply if the spin state of the $Q\bar{Q}$ pair is the same as in the dominant $|Q\bar{Q}\rangle$ Fock state. If the spin state is

different, we must replace $g\mathbf{A}\cdot\nabla$ in (2.6) with $g\mathbf{B}\cdot\boldsymbol{\sigma}$ to obtain a nonzero matrix element. Using the velocity-scaling rules of Table I, we again obtain an estimate $\Delta E \sim Mv^4$ for the energy shift, implying that the probability for a $|Q\bar{Q}g\rangle$ state containing a gluon with momentum on the order of Mv is $P_{Q\bar{Q}g} \sim v^3$. However, in the derivation of the velocity-scaling rules in Ref. [14], it was assumed that dynamical gluons have momenta of order Mv . If the gluon has a much smaller momentum k , then the estimate M^2v^4 for the operator $g\mathbf{B}$ in Table I should be replaced with k^2v^2 . Using this to estimate the energy shift from a $|Q\bar{Q}g\rangle$ Fock state containing a gluon with momentum of order Mv^2 , we obtain $\Delta E \sim Mv^6$ and $P_{Q\bar{Q}g} \sim v^4$. Thus, gluons with very low momenta exhibit the suppression that is characteristic of the multipole expansion. We conclude that a $|Q\bar{Q}g\rangle$ Fock state that can be reached from the dominant $|Q\bar{Q}\rangle$ Fock state by a spin-flip transition is dominated by dynamical gluons with momenta of order Mv and that the probability of such a Fock state is $P_{Q\bar{Q}g} \sim v^3$.”

- The following paragraph should be added at the end of Sec. IID:

“The above discussion applies to Fock states $|Q\bar{Q}g\rangle$ in which the $Q\bar{Q}$ pair has the same total spin quantum number S as in the dominant $|Q\bar{Q}\rangle$ state. The probabilities for Fock states $|Q\bar{Q}g\rangle$ that can be reached from the dominant Fock state by a spin-flip transition also scale in a definite way with v . The probability for such a Fock state to contain a dynamical gluon with momentum of order Mv is of order v^3 , just as in the case of a non-spin-flip transition. However, in the case of a spin-flip transition, this momentum region dominates because, as we have seen, gluons with softer momenta, on the order of Mv^2 , are suppressed by the multipole expansion. Thus, if the $Q\bar{Q}$ pair in the dominant Fock state has angular-momentum quantum numbers $^{2S+1}L_J$, then the Fock state $|Q\bar{Q}g\rangle$, with the $Q\bar{Q}$ pair in a color-octet state with the same value of L but different total spin quantum number, has a probability of order v^3 . For example, if the dominant Fock state consists of a $Q\bar{Q}$ pair in a 3S_1 state, then the Fock state $|Q\bar{Q}g\rangle$ with the $Q\bar{Q}$ pair in a color-octet 1S_0 state has a probability of order v^3 . If the

dominant Fock state consists of a $Q\bar{Q}$ pair in a 1P_1 state, then the Fock state $|Q\bar{Q}g\rangle$ with the $Q\bar{Q}$ pair in a color-octet 3P_J state has probability of order v^3 .”

- In the first paragraph of Sec. IIIA, the following two sentences should be inserted just before the last sentence of the paragraph:

“The matrix element is suppressed by v^3 relative to the velocity-scaling rules in Table I if \mathcal{O}_n annihilates and creates $Q\bar{Q}$ pairs in the same color-spin-orbital state as appears in one of the Fock states $|Q\bar{Q}g\rangle$ that can be obtained from the dominant Fock state by a spin-flip transition. In such a Fock state, the $Q\bar{Q}$ pair must be in a color-octet state with the same orbital-angular-momentum quantum number L as in the dominant $|Q\bar{Q}\rangle$ state, but with different total spin quantum number.”

- After the first paragraph of Sec. IIIA, the following new paragraph should be inserted:

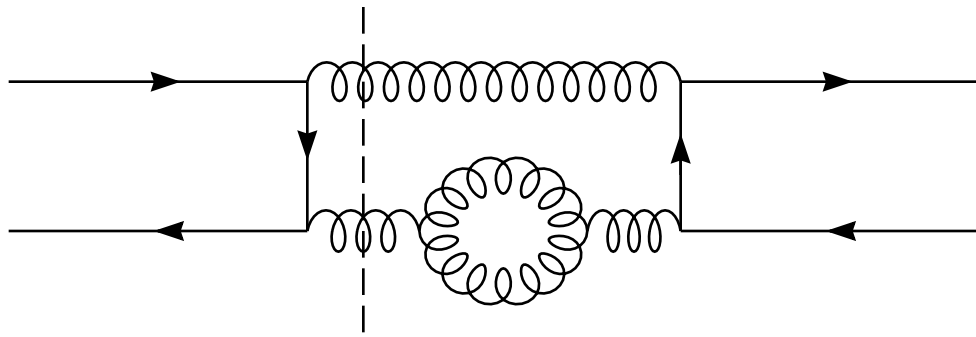
“If perturbation theory remained accurate down to the scale Mv , then the spin-flip matrix elements would be suppressed by an additional power of v . The reason for this is that the contribution to a spin-flip matrix element that is suppressed by only v^3 relative to the velocity-scaling rules is power ultraviolet divergent. Therefore, one could carry out a renormalization of the matrix element in which this contribution is subtracted. The corresponding contribution to the decay rate would then reside in the short-distance coefficient of the matrix element that is associated with the dominant Fock state. (Such a subtraction is carried out automatically if dimensional regularization is used to cut off the ultraviolet divergences in the matrix element.) Once the subtraction has been made, the leading contribution to the spin-flip matrix element comes from the scale Mv^2 . It is subject to the usual multipole suppression and scales as v^4 relative to the velocity-scaling rules. In practice, one usually makes such subtractions perturbatively. It is not clear, in the charmonium and bottomonium systems, that perturbation theory is sufficiently accurate at the scale Mv to remove the v^3 contribution completely. Therefore, we assume in the error estimates below

that the spin-flip matrix elements scale as v^3 relative to the velocity-scaling rules.”

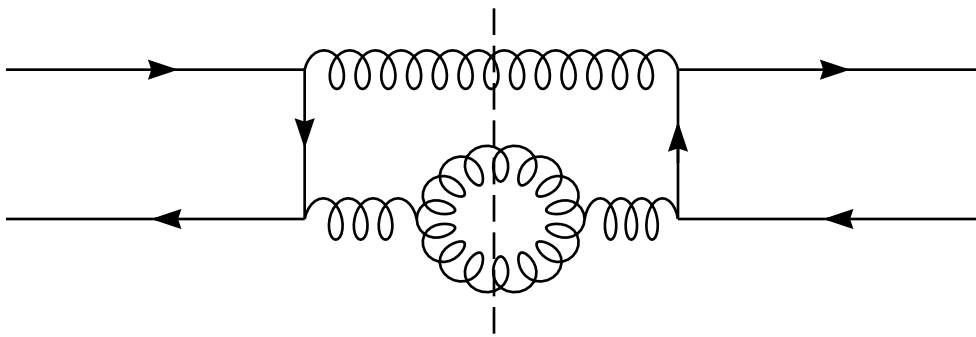
- In the second paragraph of Sec. IIIA, v^4 should be replaced with v^3 in the phrase “suppressed by v^4 or more”. In Eq. (3.1), the error estimate $O(v^4\Gamma)$ should be replaced with $O(v^3\Gamma)$. In the third paragraph of Sec. IIIA, v^4 should be replaced with v^3 in the phrase “are of order $v^4\Gamma$ or higher”.
- In Eqs. (4.1a), (4.1b), (4.3a), and (4.3b), the error estimates should be $O(v^3\Gamma)$. At the end of the paragraph containing Eq. (4.2), “relative order v^4 ” should be replaced with “relative order v^3 ”.
- In Eqs. (6.8a), (6.8b), (6.9a), and (6.9b), the error estimates should be $O(v^3\sigma)$.
- There is a typesetting error in Eqs. (3.19a) and (3.19b). The first factor on the right side should be $\sqrt{3N_c/2\pi}$, just as in Eqs. (3.19c) and (3.19d). In the subsequent sentence, “order v^2 ” should be replaced with “relative order v^2 ”.
- In Eq. (5.4), the last color matrix should be $T_{i'j'}^a$. In Eq. (5.5), the coefficient of the second term on the right-hand side should be $4/(N_c^2 - 1)$, rather than $2/(N_c^2 - 1)$.
- In Eqs. (A16) and (A25), the running coupling constant should be $\alpha_s(2M)$ rather than $\alpha_s(M)$.

This figure "fig1-1.png" is available in "png" format from:

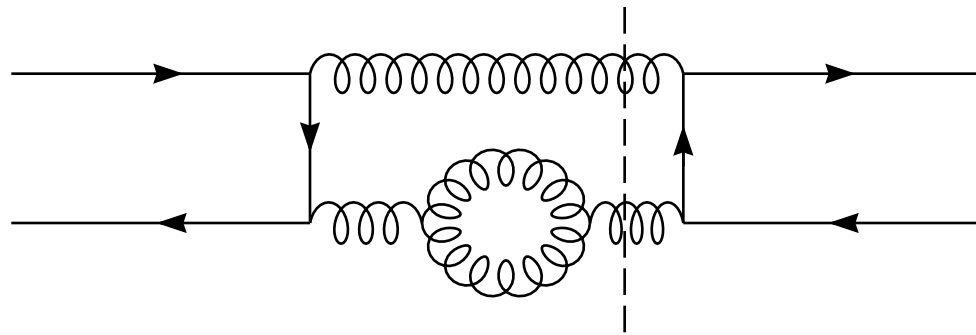
<http://arXiv.org/ps/hep-ph/9407339v2>



(a)



(b)



(c)

Figure 1

This figure "fig2-1.png" is available in "png" format from:

<http://arXiv.org/ps/hep-ph/9407339v2>

This figure "fig1-2.png" is available in "png" format from:

<http://arXiv.org/ps/hep-ph/9407339v2>

This figure "fig2-2.png" is available in "png" format from:

<http://arXiv.org/ps/hep-ph/9407339v2>

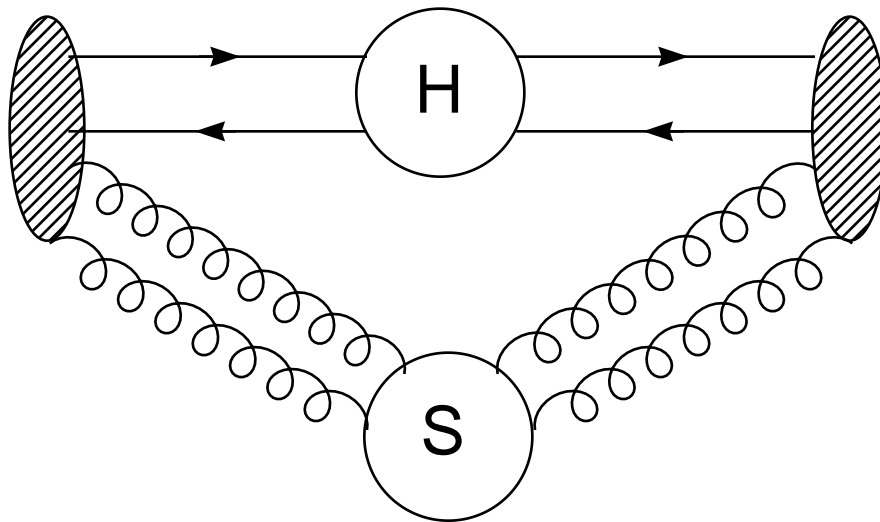


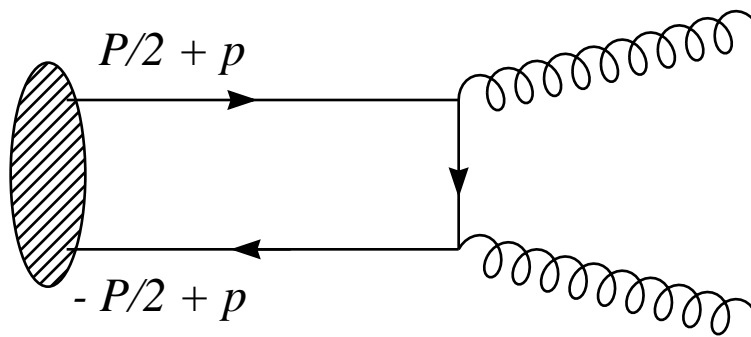
Figure 2

This figure "fig1-3.png" is available in "png" format from:

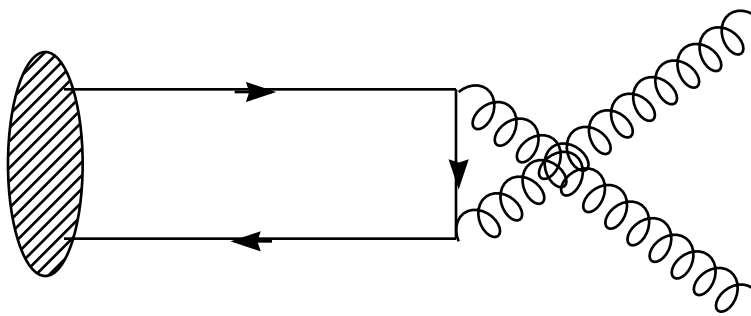
<http://arXiv.org/ps/hep-ph/9407339v2>

This figure "fig2-3.png" is available in "png" format from:

<http://arXiv.org/ps/hep-ph/9407339v2>



(a)



(b)

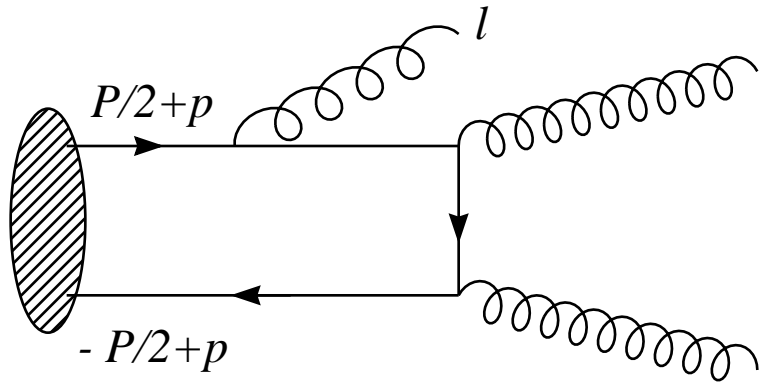
Figure 3

This figure "fig1-4.png" is available in "png" format from:

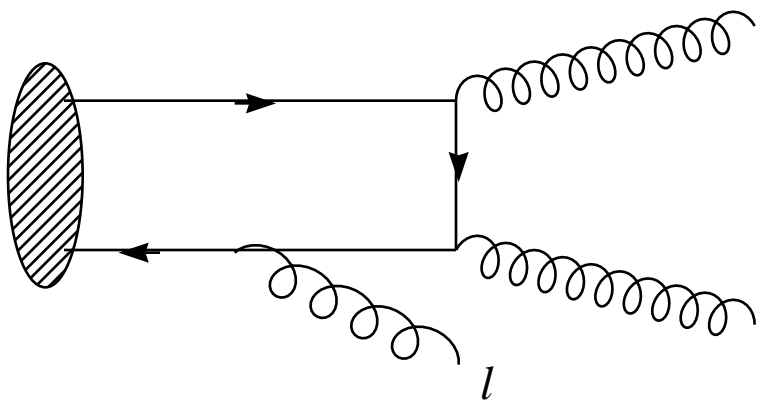
<http://arXiv.org/ps/hep-ph/9407339v2>

This figure "fig2-4.png" is available in "png" format from:

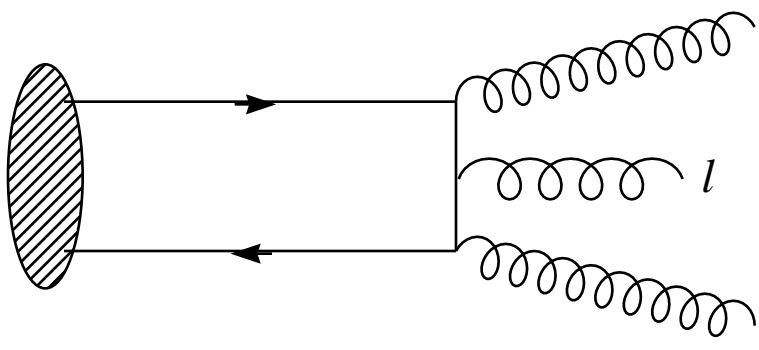
<http://arXiv.org/ps/hep-ph/9407339v2>



(a)



(b)



(c)

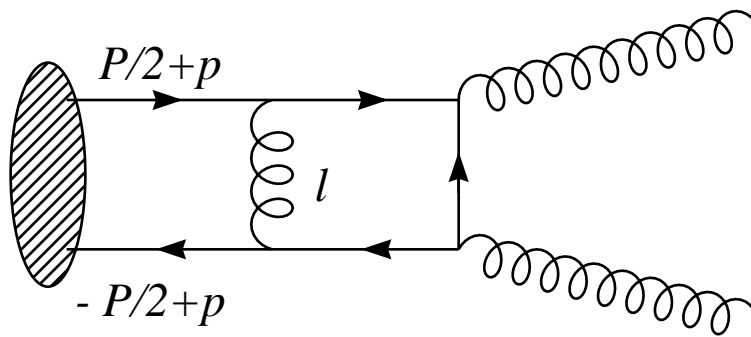
Figure 4

This figure "fig1-5.png" is available in "png" format from:

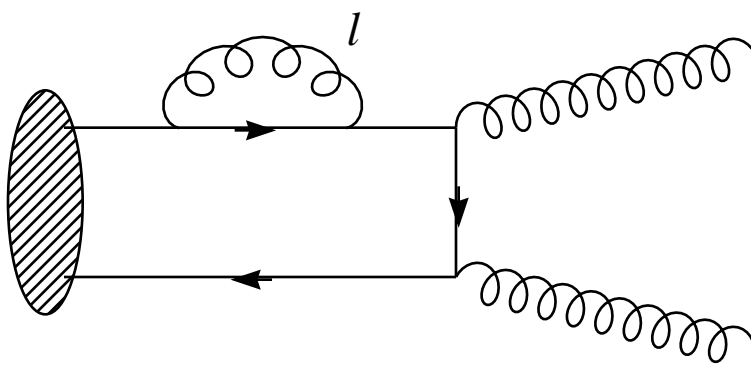
<http://arXiv.org/ps/hep-ph/9407339v2>

This figure "fig2-5.png" is available in "png" format from:

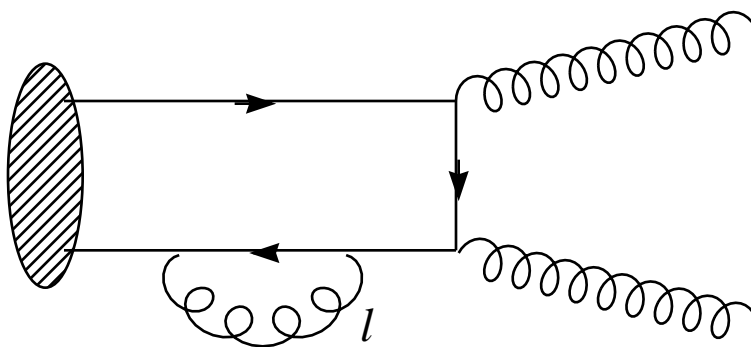
<http://arXiv.org/ps/hep-ph/9407339v2>



(a)



(b)

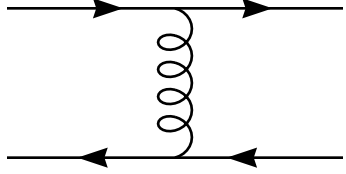


(c)

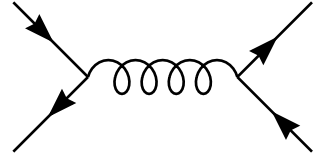
Figure 5

This figure "fig2-6.png" is available in "png" format from:

<http://arXiv.org/ps/hep-ph/9407339v2>

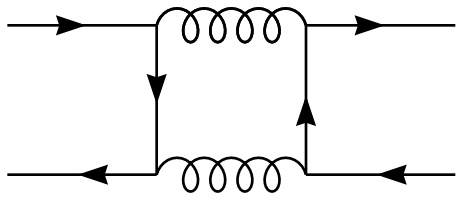


(a)

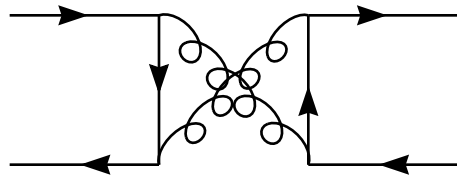


(b)

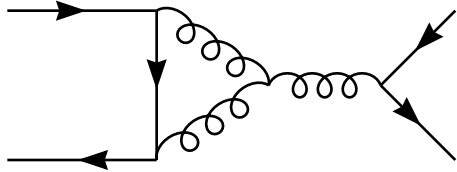
Figure 6



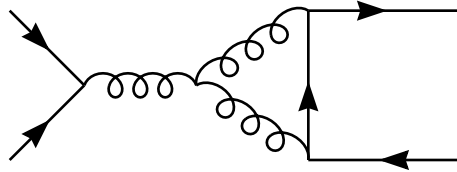
(a)



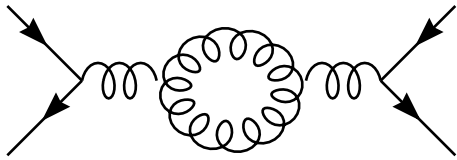
(b)



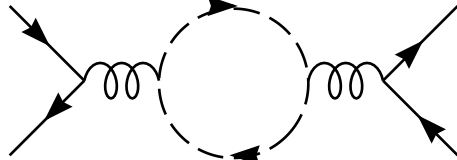
(c)



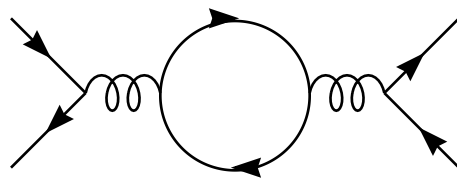
(d)



(e)

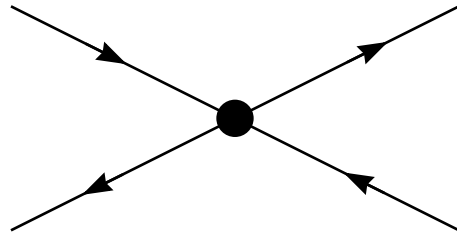


(f)

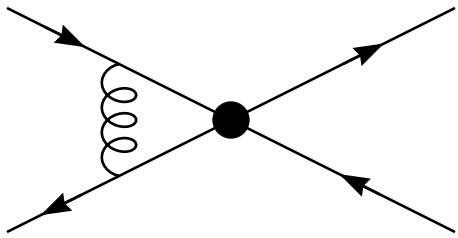


(g)

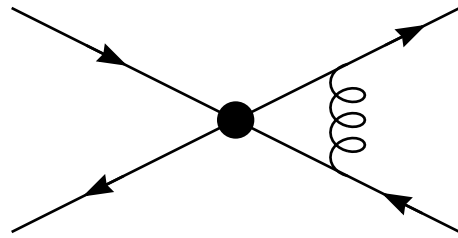
Figure 7



(a)

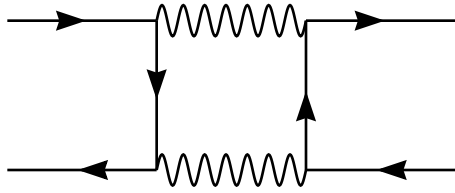


(b)

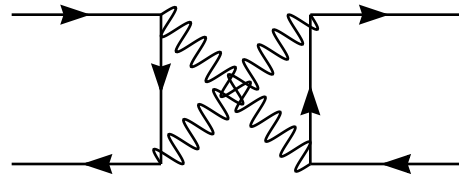


(c)

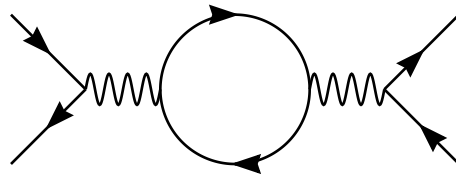
Figure 8



(a)

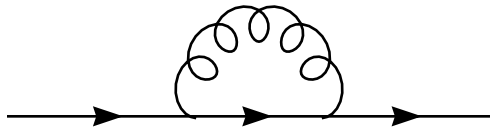


(b)

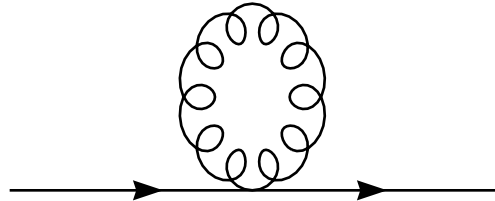


(c)

Figure 9



(a)



(b)

Figure 10

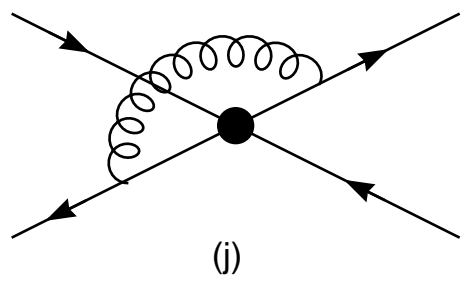
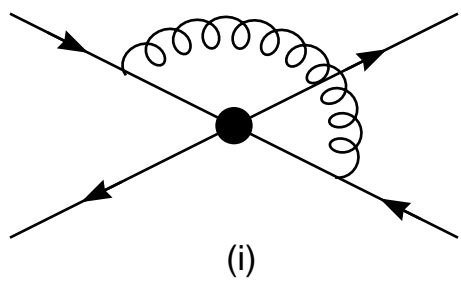
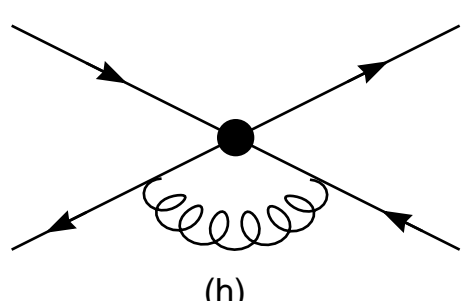
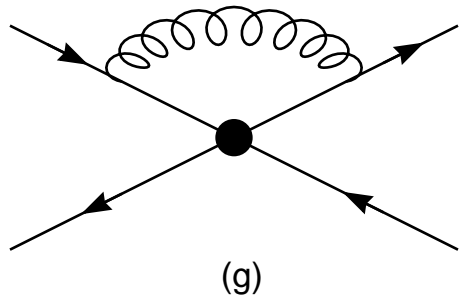
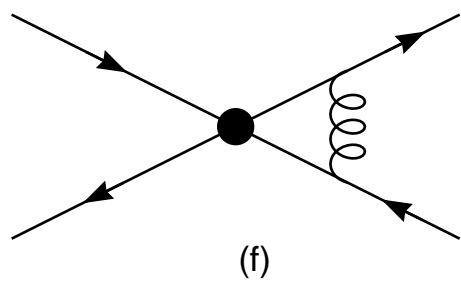
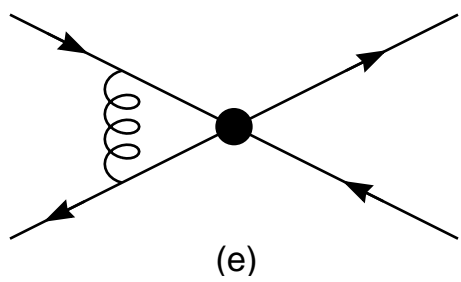
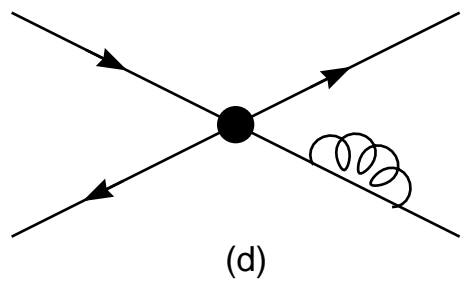
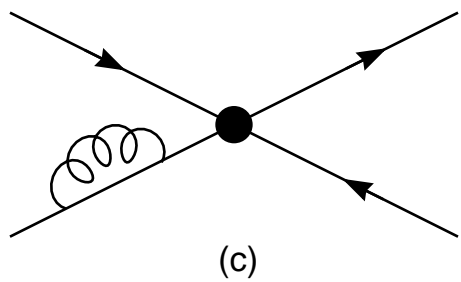
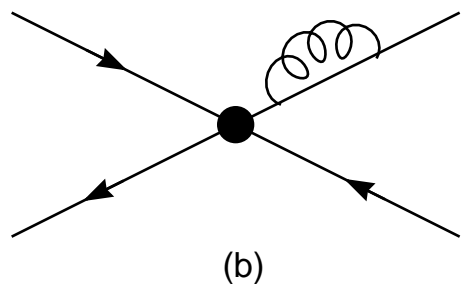
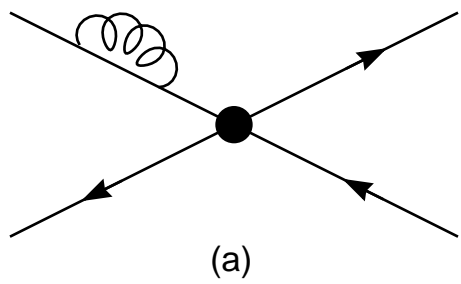


Figure 11